Stony Brook University

Exploring a Role for PLD3 during *in vitro* myogenesis

A Dissertation Presented

by

Mary O. Osisami

to

The Graduate School

in Partial Fulfillment of the

Requirements

for the Degree of

Doctor of Philosophy

in

Genetics

Stony Brook University

August 2010

Stony Brook University

The Graduate School

Mary O. Osisami

We, the dissertation committee for the above candidate for the Doctor of Philosophy degree, hereby recommend acceptance of this dissertation.

Michael A. Frohman, M.D., Ph.D. Dissertation Advisor
Professor, Department of Pharmacological Sciences

Michael Hadjiagyrou PhD. Chairperson of Defense
Associate Professor, Department of Biomedical Engineering

Aaron Neiman, Ph.D.
Associate Professor, Department of Biochemistry

Joav Prives, Ph.D.
Professor, Department of Pharmacological Sciences

Hal Skopicki, M.D., Ph.D.
Assistant Professor, Department of Medicine

This dissertation is accepted by The Graduate School

Lawrence Martin

Dean of The Graduate School

Abstract of the Dissertation

Exploring a Role for PLD3 during in vitro myogenesis

by

Mary O. Osisami

Doctor of Philosophy

in

Genetics

Stony Brook University

2010

Phospholipase D 3 (PLD3) is an atypical and uncharacterized member of the phospholipase D (PLD) superfamily. First discovered as the mammalian homologue of the vaccinia virus K4L protein, PLD3 is a type II glycoprotein associated with the endoplasmic reticulum. PLD3 is expressed in a wide range of tissues and cells, including neural and skeletal especially during differentiation events. To date, there are no published reports describing a cellular function or biochemical activity for PLD3. Very little information can be deciphered from vK4L because it is not essential to the viral life cycle. The closest homologue of mammalian PLD3 with a known function is the vaccinina virus F13L protein. Like other members of the PLD superfamily, F13L is involved in membrane trafficking and fusion events. Specifically, F13L is involved in wrapping viral particle is post –Golgi vesicles, presumptively, through broad spectrum lipase activity.

Using an *in vitro* skeletal muscle differentiation system, I have demonstrated that overexpressed PLD3 enhances myotube formation in differentiating myoblasts, a phenotype that may be associated with the ER-stress response. Knockdown of PLD3 expression via RNAi, lead to decreased cell fusion, increased cell death and, paradoxically, a significant increase in PLD3 expression over time. Using indirect immunofluorescence and exhaustive colocalization studies, I observed that PLD3 protein localizes to unknown intracellular vesicles, which may be derived from the endoplasmic reticulum. These findings suggest that PLD3 plays a role in myogenesis and may be involved in cell viability and myotube formation.

This work is dedicated to all those who were lost during this journey.

Table of Contents

Figure List

CHAPTER 1

CHAPTER 3

CHAPTER 4

List of Abbreviations

DAPI	4',6-diamidino-2-phenylindole
amph B	amphotericin b
β-gal	Betagalactosidase
BSA	bovine serum albumin
BFA	Brefeldin A
CSQ	calsquestrin
co-IP	co-immunoprecipitation
cyto-c	cytochrome-C
DM	differentiation media
DMSO	Dimethyl sulfoxide
DTT	Dithiothreitol
EndoH	Endoglycosidase H
ER	endoplasmic reticulum
FBS	fetal bovine serum
GAPDH	Glyceraldehyde 3-phosphate dehydrogenase
GFP	green fluorescent protein
HS	horse serum
iNOS	inducible nitric oxide synthase
KDEL	lysine aspartic acid
mRNA	messenger RNA
μm	micro meter
μg	micro gram

µl	micro liter
µM	micro molar
miR	micro RNA
miRNA	micro RNA
mg	milli gram
mM	milli molar
ml	milliliter
MHC	myosin heavy chain
nM	nano molar
NGF	neural growth factor
NP-40	Nonidet P40
NLS	nuclear localization signal
PNGase F	Peptide N-Glycosidase F
PC	phosphatidylcholine
PBS	phosphate buffered saline
PA	phosphatidic acid
PLA	phospholipase A
PLC	phospholipase C
PLD	phospholipase D
PCR	polymerase chain reaction
PM	proliferation media
PCA	protein complementation assay
qPCR	quantitative polymerase chain reaction
RPM	revolutions per minute
RNA	ribonucleic acid

RNAi	RNA interference
SR	sarcoplasmic reticulum
shRNA	short hairpin RNA
siRNA	short interfering RNA
SDS	sodium dodecyl sulfate
SDS-PAGE	sodium dodecyl sulfate polyacrylamide gel electrophoresis
SPB	spindle pole bodies
TG	Tharpsigargin
TBST	tris buffered saline plus tween
TBS	tris buffered saline
TN	tunicamycin
UPR	unfolded protein response
WT	wild type
YFP	yellow fluorescent protein

Acknowledgements

First I would like to thank God for giving me the strength to finish this arduous journey. Lai si agbara re Emi o bati sonu.

I would like to give a big thank you to my family. All of you have been a constant source of strength and support throughout the years. No matter what was going on, I always knew that I could come home and let my hair down and enjoy life. All of you were the blessing I never truly realized until now, thank you for it all.

I would also like to give a cordial thank you to my Advisor Michael Frohman, who has encouraged me to be very independent. He has always given me the space to work independently, making me a stronger scientist in the end.

A large thank you to my committee members: Dr. Michael Hadjiargyrou, Dr. Aaron Neiman, Dr. Joav Prives and Dr. Hal Skopicki. They always gave invaluable advice and help that was always greatly appreciated.

I am very thankful to Kate Bell the Genetics program secretary. She has been a wonderful person to know. Kate has always had an open door, free shoulder and full candy jar policy that has gotten me through some of the toughest times in my graduate career.

Finally I would like to thank all of the many friends I have made along the way. Knowing you guys have made life here more pleasant. From karaoke, to turducken to divas night out, it has been a blast. Through it all I have always felt your love. Thank you for allowing me to be a part of your life, but more importantly, thank you for being a part of mine.

Chapter 1
Introduction

1.1 Initiative and specific aims

The objective of this thesis was to identify a functional role for phospholipase D 3 (PLD3) during *in vitro* skeletal myogenesis. Unlike other mammalian phospholipase D (PLD) superfamily members, very little is known about PLD3. At the start of this thesis, all that was known of this uncharacterized PLD was that it is a transmembrane protein associated with the endoplasmic reticulum, with a luminal catalytic domain. There was no assigned cellular function or biochemical activity to PLD3.

In recent years, published as well as non-published data have shown that the two main mammalian PLDs, PLD1 and PLD2, are involved in myogenesis. Interestingly, an increase in PLD3 mRNA and protein expression during myoblast fusion was also found, suggesting that it may also be involved in myogenesis. Therefore using the mouse C2C12 myoblast cell line I studied the role of PLD3 during early *in vitro* myogenesis.

The specific aims of this thesis were to:

1. Characterize PLD3 expression during C2C12 myoblast differentiation.

For this, I examined the temporal and spatial expression of PLD3 in proliferating and differentiating C2C12 myoblasts via Western blot analysis, quantitative PCR and indirect immunoflourescent microscopy.

2. Examine the Role of PLD3 during C2C12 differentiation.

Since PLD3 is a member of the PLD superfamily and all of the known mammalian PLD are involved in membrane fusion or vesicle trafficking I hypothesized that PLD3 may also participate in membrane fusion and trafficking events. Specifically, I hypothesized that PLD3 would be involved in the formation of the T-tubule membrane system. I examined this using indirect immunoflourescent staining, western blot analysis, overexpression and RNAi mediated knockdown of PLD3 in C2C12 myoblasts undergong differentiation.

1.2 Overview of the Phospholipase D Superfamily

The phospholipase D (PLD) superfamily consists of multi-functional enzymes that perform a multitude of cellular activities. PLD activity was first discovered in plants as a phospholipid-specific phosphodiesterase that uses phosphatdylcholine to produce phosphatidic acid (PA) and free choline ((1) Figure 1.1 B). PLD activity can be found in many organisms from viruses to mammalian systems. In mammalian systems, there are two "classic" PLD isoforms, PLD1 and PLD2, which are 50% identical and generally active in most cell types (reviewed in (1, 2)). All members of the PLD superfamily contain at least one HxxxxKxD/E (HKD) catalytic motif ((1, 3); Figure 1.1 A), which is both required for enzymatic activity and defines a protein as a member of the superfamily (4).

The "classic" mammalian PLDs, PLD1 and PLD2 are membrane associated enzymes that play vital roles in vesicle trafficking and fusion events. PLD1 and PLD2 have been shown to localize to the plasma membrane and to perinuclear structures including the Golgi, endoplasmic reticulum (ER) and endosomes, potentially linking them to several steps of the secretory and retrieval

pathways (3). PLD1 is involved in vesicle trafficking from the ER to the Golgi (5), as well as vesicle budding and trafficking from the Golgi to the plasma membrane (6, 7). PLD1 has also been reported to promote membrane vesicle trafficking and fusion into the plasma membrane during regulated secretion (7, 8). PLD2 has been shown to be involved in cell adhesion, cell migration and receptor-mediated endocytosis (9, 10).

Other members of the PLD superfamily also play roles in membrane fusion events, including in the context of mitochondrial fusion and yeast prospore membrane formation. In yeast, Spo14, the sole classical yeast PLD, is required for formation of prospore membranes during meiosis (11). During meiosis II, spindle pole bodies (SPBs), future initiation points of prospore membrane initiation, are formed. Post-Golgi vesicles then localize to and begin to fuse at the newly formed SPBs (reviewed in (12). Nakanishi et. al. showed that the loss of Spo14p leads to an accumulation of prospore precursor membrane vesicles at SPBs that fail to fuse (11). Mitochondria are constantly fusing and dividing as part of their normal physiology to maintain normal function, and a very divergent PLD superfamily member, MitoPLD, is involved in this process (13). Loss of MitoPLD leads to mitochondrial fragmentation, while overexpression of MitoPLD causes mitochondrial aggregation through synthesizing PA on the mitochondrial surface from cardiolipin ((13), Figure 1.1 C).

A role for classical PLD activitu has been suggested during skeletal muscle myogenesis(14). Using an *in vitro* culture system, Komati et. al. reported that blocking PLD1-mediated PA production, with 1-butanol during arginine-vasopressin (AVP)-induced differentiation of L6 myoblasts resulted in decreased expression of myogenin, an early marker of the onset of myogenesis and a key factor in its progression (14). They also reported, that when overexpressed, PLD1 promotes formation of stress fiber-like actin structures, implicating its role in the cytoskeletal rearrangements that take place during myogenesis (14); however, this report PLD2 did not suggest a role for PLD2 in myogenesis. Preliminary, unpublished studies performed in in the laboratory of Michael A. Frohman by Dr. Ping Huang M.D., PhD. (Stony Brook University, unpublished results) based on an RNAi approach instead of alcohol inhibition suggested that both PLD1 and PLD2 have roles in myogenesis that are distinct and somewhat different than those reported in the literature. Analysis of differentiating L6 myoblasts stably expressing shRNA against PLD1 or PLD2 suggests that PLD activity is required at multiple stages of in vitro myogenic differentiation. PLD1 was shown to regulate of myoblast to myotube fusion Knockdown of PLD1 did not alter primary fusion events (myoblast to myoblast fusion), while secondary fusion (myoblast to myotube fusion) was reduced. PLD2 was shown to regulate the onset of myogenesis. Knockdown of PLD2 lead to the inhibition of primary fusion events. Together the above results show that PLD activity is required for early

muscle development. PLD3's activity, classical or not, may have equally important roles in myogenesis.

1.3 Myogenesis Overview

In vivo, as well as *in vitro*, mammalian myogenesis is a highly complex, multi-tiered, cell-cell fusion event. *In vivo*, the process begins in the post-gastrulation embryo when mesoderm-derived cells become committed myoblasts (15). These committed myoblasts continue to proliferate until they have received extra-cellular cues to begin the expression of basic-helix-loop-helix domain containing muscle regulatory factors, Myf5, Myf6 and MyoD and myogenin (reviewed in (*16-18*)). These above factors will then stimulate the expression of Mef2, which will in turn further stimulate the expression of myogenein in a "feed forward loop", further stimulating Mef2 expression (reviewed in (*17*)). The major factors in charge of inducing myogenesis, MEF2 and MyoD, in combination with other intracellular and extracellular cues, signal committed myoblasts to withdraw from the cell cycle, initiate muscle-specific gene expression and fuse together to form nascent myotubes (*19*). These nascent myotubes then continue to increase in size and nuclei number by fusing to more myoblasts until they eventually form mature myofibers ((*19*), Figure 1.2).

Beyond growing in size, myoblast/myotubes make significant changes to their membrane systems, cytoskeletal arrangements and protein/gene expression.

The sarcoplasmic reticulum is a specialized form of smooth endoplasmic reticulum (ER) that holds and releases calcium for muscle relaxation and contraction (reviewed in (*20*)). The SR is formed when the ER reorganizes itself and concentrates SR specific proteins in SR regions near structures called T-tubules; however, it is unclear if the ER and SR are structurally distinct from one another as several ER-chaperone proteins are found in SR designated membranes (*20*). In addition to ER reorganization, the Golgi reorganizes itself as well. The Golgi apparatus disperses into Golgi fragments that associate with myonuclei for localized export of proteins produced by different nuclei (*21-23*).The plasma membrane, now called the sarcolemma, forms specialized invaginations called Transverse (T) tubules, an extensive membrane system with lipid and protein compositions distinct from the sarcolemma (*24*). The T-tubules function to transfer action potentials from neural stimuli internally to the sarcoplasmic reticulum (SR).

All of the membrane rearrangements that occur are needed for the support and function of the myofibril. The myofibril is made up of several repeats of sarcomeres, the basic contraction unit of muscles. The sarcomere arises from several filament systems, thin (actin), thick (myosin), nebulin and titin filaments (reviewed in (*25*)). These filaments interact with each other, filament capping proteins, the plasma membrane and the extracellular matrix to not only contract, but also to participate in signal transduction events to maintain muscle homeostasis (*23, 25*).

In vitro, cultured myoblasts undergo many of the same changes that occur *in vivo*. Cultured myoblasts withdraw from the cell cycle and fuse together to form nascent myotubes, which then fuse with myoblasts and express muscle specific genes. The *in vitro* system is a reliable and a highly reproducible system to use for study of PLD3. Myogenic differentiation is easily observed and staged by the use of muscle specific markers that are expressed at set time points. The onset of myogenesis can be easily detected by the expression of myogenin, while the formation of specialized membranes and the contractile apparatus are detected by the expression of calsequestrin, caveolin 3 and sarcomeric myosin heavy chain, which marks the sarcoplasmic reticulum, early T-tubule and contractile apparatus, respectively.

1.4 PLD3

PLD3 is an atypical, non-classical member of the PLD superfamily. It was first identified in mammals as a homologue of the vaccinia virus vK4L protein (*26*). Like vK4L, PLD3 has two conserved HKD domains, which defines these proteins as members of the PLD superfamily. Structurally, the only feature in common between PLD3 and classical members of the mammalian PLD superfamily are the conserved HKD domains Except for the HKD domains, there are no other recognizable domains or motifs within the protein (Figure 1.1 A), aside from a secretory signal sequence at the amino terminus and a predicted prenylation site at the C- terminus (*27*). It should be noted that the second HKD domain of PLD3 is imperfect, containing a glutamic acid residue in place of the aspartic acid.

Like other members of the superfamily, PLD3 localizes to membranes; however, it achieves this by being a type II transmembrane protein in the endoplasmic reticulum, with both HKDs in the lumen, rather than associating via hydrophobic regions of the protein or via PX or PH domains (*1, 2, 27*). In mammals, the only other known transmembrane PLD is MitoPLD; however, MitoPLD localizes to the cytosolic surface of mitochondria with its HKD domain

facing the cytosol. To date, PLD3 is the only PLD superfamily member with a luminal catalytic domain.

Multiple studies have shown that PLD3 is expressed in a wide range of tissues, with a relatively high level of expression in brain and neural tissues, especially during the late stages of neurogenesis (*27, 28*). In addition to PLD3 induction during neurogenesis, PLD3 has been shown to be induced during myogenesis (*29*), suggesting PLD3 may be involved in the cellular differentiation events.

Currently, there is no known cellular function or biochemical activity assigned to PLD3. Very little information can be deciphered from the vaccinia virus vK4L protein because it is not critical for the viral life cycle and no in vivo function has been determined for it. However, it has been implicated in nicking and joining viral crucible DNA (*30*). The closest homolog of PLD3 and vK4L with a known function is the vaccinia virus F13L protein, which is a transmembrane protein required for efficient viral cell-cell spreading by wrapping intracellular virions in trans-Golgi or endosomal membranes (*31, 32*). Like other PLDs, F13L requires an intact HKD domain for activity (*33*), which is blocked by 1-butanol and not 2-butanol, suggesting that F13L has PLD-like activity. However, the overexpression of PLD1 does not rescue F13L deficient virions (*32*), suggesting that the role of F13L is more complex than to simply produce PA in the Golgi or other endosomal membranes. In fact, to date, there have been no

reports of F13L PLD activity; instead F13L has been reported to have phospholipase A and phospholipase C activities (*34*); suggesting F13L is a broad-spectrum lipase.

PLD3 was examined for the production of PA by Pedersen et. al. using classical PLD activity assays; however, no classical PLD activity was detected (*27, 28*). This suggests that unlike PLD1 and PLD2, PLD3 does not use phosphatidylcholine as substrate to form phosphatidic acid; however, like MitoPLD, which uses cardiolipin as a substrate (13), it is possible that PLD3 may still produce phosphatidic acid using another substrate. PLD3 may also act as a broad-spectrum lipase as its homologue F13L.

Recently, and quite interestingly, elevated levels of PLD3 expression have been suggested to increase the self-renewal properties of hematopoietic stem cells (*35*); which is in stark contrast to the idea that PLD3 aids in differentiation, since in this scenario, PLD3 would be maintaining hematopoietic stem cells in an undifferentiated state. Another interesting and novel finding for PLD3 suggests that reduced levels of PLD3 may decrease cellular sensitivity to oxidative stress (*36*), which can negatively impact differentiation events, especially myogenesis (*37*).

During skeletal muscle differentiation, there are several membrane fusion and vesicle trafficking events, as mentioned above, that may involve PLD3 regulation. Specifically, during T-tubule membrane formation, which is formed

by endomembrane derived vesicles fusing to each other and to the plasma membrane (*24*). Moreover, using VSVG trafficking experiments (unpublished data from studies conducted in the Michael A. Frohman laboratory by Danxia Ke, Stony Brook University), it was suggested that PLD3 might also have a role in regulating the secretory system.

Figure 1. 1 Mammalian Phospholipase D superfamily members.

A. Cartoon schematic of mammalian PLD superfamily members with recognizable domains. **B.** Classical PLD enzymatic activity performed by PLD1 and PLD2. **C.** Non-classical PLD enzymatic PLD activity performed by Mito-PLD.

A.

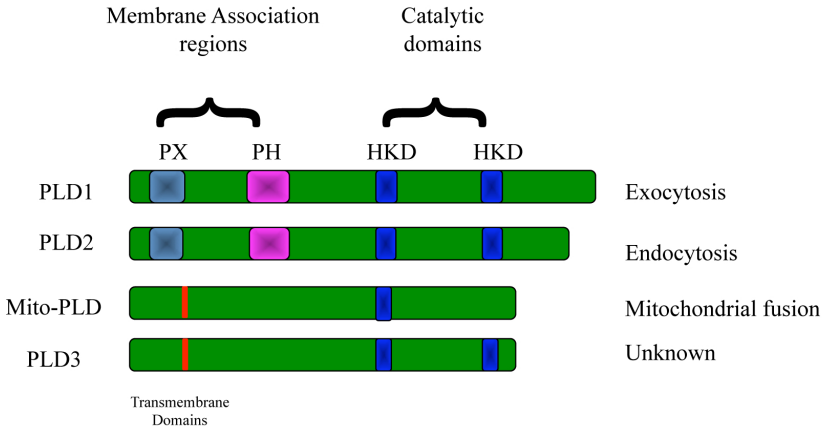
Membrane Association regions
Catalytic domains
PX
PH
HKD
HKD
PLD1
PLD2
Mito-PLD
PLD3
Exocytosis
Endocytosis
Mitochondrial fusion
Unknown
Transmembrane Domains

B.

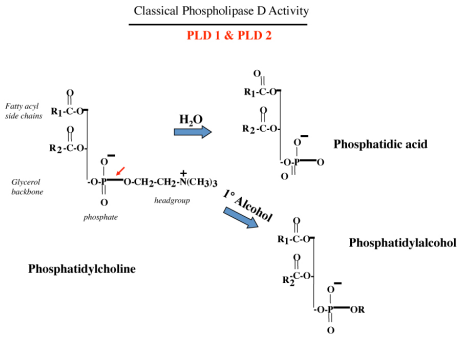
Classical Phospholipase D Activity
PLD 1 & PLD 2
Fatty acyl side chains
Glycerol backbone
phosphate
headgroup
H2O
1° Alcohol
Phosphatidic acid
Phosphatidylalcohol
Phosphatidylcholine

C.

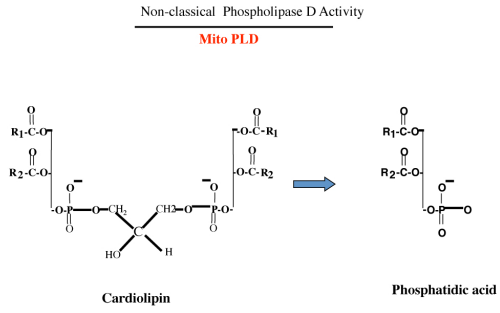
Non-classical Phospholipase D Activity
Mito PLD
Cardiolipin
Phosphatidic acid

Figure 1. 2 Cartoon Representation of Myogenesis.

Myogenesis is a multi-step process that occurs in two stages: initial myoblast-myoblast fusion to form nascent myotubes, followed by subsequent myotube-myoblast fusion to form mature muscle fibers.

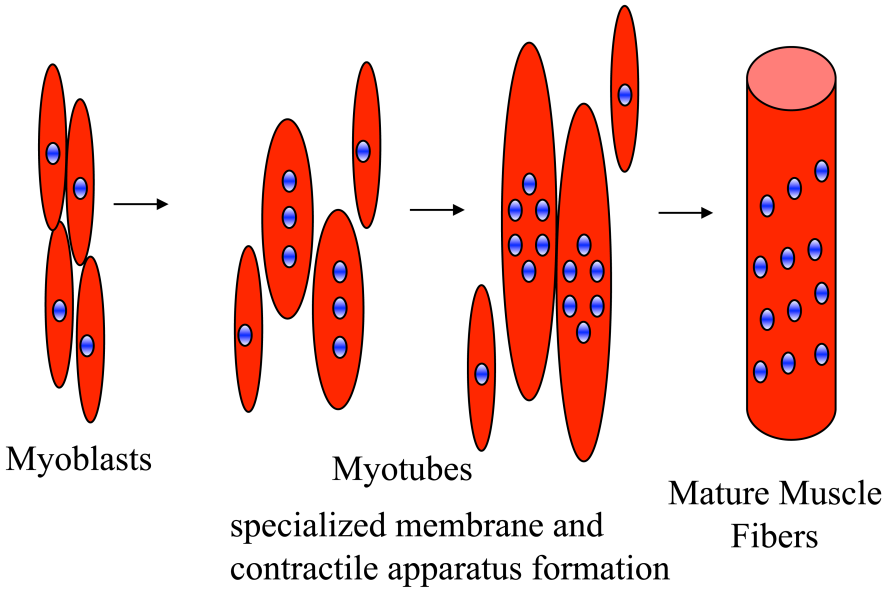
Myoblasts
Myotubes
specialized membrane and
contractile apparatus formation
Mature Muscle
Fibers

Chapter 2

Materials and Methods

2.1 General Reagents. All reagents used in this thesis were purchased from Sigma Aldrich unless otherwise stated.

2.2 Plasmid Construction

2.2.1 huPLD3-myc and huPLD3-K418R-myc constructs

huPLD3 and huPLD3 K418R were amplified using primer set 1, in chart 2.1. The amplified products were then digested with restriction enzymes NotI and BamHI and ligated to pQCXIP and pCDNA 3.1- zeo digested with the same enzymes.

2.2.2 PLD3 deletion mutants

Two PLD3 mutants were constructed in which the transmembrane domain was removed. The first mutant Δ37-60 had only the transmembrane domain (amino acids 37-60) removed. The second mutant Δ1-60, had amino acids 1-60 removed, which included the N-terminus and the transmembrane domain. To make Δ1-60, huPLD3 was amplified using primer set 2, which also added a myc

tag to the C-terminus. The Δ37-60 construct was made by fusion PCR. First the N-terminus (without the transmembrane domain) was amplified using primers set 3.1. The C-terminus was amplified using primer set 3.2. The final product was made using the forward primer from the N-terminus amplification and the reverse primer from the C-terminus amplification (primer set 3.3) and both the N and C terminal products as the templates for amplification. The Δ1-60 PCR product and the final Δ37-60 PCR products were digested with BamHI and Not I and ligated to the vector pCDNA 3.1- zeo digested with the same enzymes.

2.2.3 mito-tagged PLD3-Δ1-37

PLD3 Δ1-37 was amplified using primer set 4. Δ1-37 was digested with restriction enzymes BamHI and NotI and ligated into PCDNA 3.1 mito-mcherry that was digested with the same enzymes.

2.2.4 PLD3 N-terminal GFP/YFP fusion proteins

PLD3 1-37-GFP, PLD3 1-60-YFP and PLD3 37-60-YFP constructs were made by amplifying the indentified amino acid by PCR amplification using primer sets 6,7 and 8, respectively. The PCR products were then digested with BamHI and EcoRI and ligated to pCDNA 3.1- zeo digested with the same enzymes.

2.2.5 ER-mcherry

mcherry was amplified by PCR using primer set 5, to add an N-terminal calreticulin localization sequence and a C-terminal KDEL ER retention sequence. The PCR product was then digested with restriction enzymes NotI and BamHI. The digested product was then ligated to pQCXIP digested with the same enzymes.

2.2.6 PLD3-GFP

Mouse PLD3 was amplified using primer set 4. The PCR product was then digested with BamHI and EcoRI and ligated to pEYFPC-1 digested with the same enzymes.

2.2.7miR constructs

The mouse sequence of PLD3 was retrieved from NCBI gene bank (Accession # NM_011116.1). This sequence was then entered in Invitrogen's **BLOCK-iT** RNAi designer software/ program (https://rnaidesigner.invitrogen.com/rnaiexpress/) to retrieve sequences suitable for micro (miR) RNA sequences. Two sequences, denoted miR-1and miR-2 (chart 2.2) were chosen for use in RNAi experiments. The oligos for miR-1 and miR-2 contained the 5' and 3' sticky ends for BsmBI and were annealed by heating the

oligos to 100C in 1X NEB buffer 3. The annealed oligos were then ligated to the pSM155-GFP backbone that was cut with BsmBI. For pMscv-miR constructs, the miR sequences were removed by restriction digestion with enzymes SalI and EcoRI. The fragments were then ligated to pMscv cut with restriction enzymes EcoRI and XhoI.

2.2.8 shRNA constructs

As above with the miR constructs, the mouse PLD3 sequence was retrieved from NCBI gene bank and entered into the BLOCK-iT software to retrieve suitable sequence for shRNA-based knockdown. The sequences denoted shRNA-1 and shRNA-2 (chart 2.2), containing the sticky ends for restriction sites ACC65I and BglII, were annealed as above and place into a pSuper vector cut with the same restriction sites. For pSuperRetro, the sequences were removed from pSuper with restriction enzymes EcoRI and PmeI . The fragments were then ligated into pSuperRetro cut with Hinc II and EcoRI.

2.3 Cell culture and differentiation

All cells used in this thesis were maintained in a humidified incubator containing 5% CO2 at 37C and grown in DMEM supplemented with 10% fetal bovine serum (FBS), henceforth known as proliferation media (PM). C2C12 cells were differentiated by growing cells until confluent then switching from PM to differentiation media (DM), DMEM supplemented with 2% horse serum (HS).

PC12 cells were induced to differentiate by plating cell onto collagen and poly-l-lysine coated plated or coverslips and switching from PM to DM supplemented with 100 ng/ml 2.5S NGF (Invitrogen).

2.4 Cell transfection and infection

All transfections, except viral packaging cell transfections for retroviral infections, were conducted using Lipofectamine and Plus reagents (Invitrogen). Cells were seeded onto 35mm plates in OPTI-MEM I media for 15-30 min. While the cells were incubating in the OPTI-MEM I media, 1ug of DNA was complexed with the Plus reagent (Invitrogen) and Lipofectamine (Invitrogen) in OPTI-MEM, following the manufacturer's instructions.

siRNA transfections were conducted using siRNA oligos designed and produced by Invitrogen. C2C12 cells were seeded so that they were approximately 50% confluent at the time of transfection. The siRNA oligos were complex with the lipid transfection reagent Dharmafect 3 (Dharmacon) for 15 min followed a 24-hour incubation with seeded cells in PM.

For retroviral infections, Plat-E (*38*) retroviral packaging cells were seeded onto 10 cm plates so that they were 60% confluent at the time of transfection, by the calcium phosphate method. Twenty four hours after transfection, the media was replaced with fresh growth media for viral supernatant collection 24 hours later. To infect the cells, cells are seeded so that they were less

than 50% confluent at the time of infection. Viral supernatants was then added to the cells including 8 μg/mL polybrene and allowed to incubate on the cells for 24 -48 hours. The media on the cells was then replaced with fresh PM and selective antibiotics added 48 hours after viral supernatant removal.

2.5 Cell lysis and Western Blot analysis

Cells were washed in PBS and lysed in modified RIPA buffer (50mM Tris-HCl, pH 7.4, 1% Triton X-100, 150 mM NaCl, 1%Na-deoxycholate, 0.1% SDS, 1mM EDTA, 1mM EGTA 0.5% CHAPS) supplemented with a protease inhibitor cocktail (Roche). The lysates were then centrifuged at 3000 rpm for 10 min to remove nuclei. The samples were then added to 2X sample buffer containing 8M urea and ran on 8-15% SDS PAGE gels. The proteins were then transferred onto a nitrocellulose membrane. The membranes were then blocked with 1% casein in TBS, followed by incubation with the appropriate primary antibodies in 1% casein in TBST. Following the primary antibody incubation, membranes were then washed, three times for 5 min each in TBST followed by a one hour incubation with the appropriate secondary antibodies conjugated with either the Alexa 680 (Invitrogen) or IR Dye 800 (Rockland) fluorophores (1:5000 dilution) in 1% casein in TBST for one hour. The membranes were then washed 3 times for 5 min each in TBST followed by a 5 min wash in PBS. The membranes were then scanned by the Odyssey Infrared Scanner (LI-COR) to visualize protein bands.

2.6 Quantitative PCR

C2C12 myoblasts were allowed to differentiate for 5-6 days as stated above with cell pellets collected on a daily basis. RNA was extracted from the cells using the RNeasy mini kit (Qiagen), following the manufacturers directions. Once collected, RNA concentration was measured using the nanodrop and 1ng of total RNA was used for reverse transcription and amplification. Reverse transcription and amplification was conducted using the HotStart Sybr green one step qRT-PCR mastermix kit (USB) with PLD3 and GAPDH specific primers: (fwd 5' CTGAGGAACCGGAAGCTGT; rev 5' GGAAAGGGGTGGTCCTGA) and (fwd:5'TGGAGAAACCTGCCAAGTATG; rev 5'GTTGAAGTCGCAGG AGA CAAC), respectively.

2.7 Indirect Immunofluorescence Microscopy

Cells were seeded onto gelatin coated coverslips. When the cells were ready for staining they were washed 3 times in PBS then fixed in 4% formaldehyde for 10 min followed by permeabilization in 0.2% Triton-X 100. The cells were then blocked in 5%BSA with 5% goat serum diluted in PBS for 1 hour followed by a one-hour incubation in the appropriate primary antibodies. Afterwards, the cells were then washed with PBS 3X for 5 minutes each, and then incubated for one hour in the appropriate secondary antibodies and DAPI. The coverslips were mounted on to slides with Vector Mount and visualized by

confocal microscopy using either a Zeiss LSM 510 Meta or Leica SP-2 microscope. When preservation of delicate membrane structures was required, the Triton-X 100 permeabilization step was skipped and 0.1% Saponin was added to the blocking, primary and secondary steps for permeabilization.

2.8 Transient ER stress

Cells were allowed to grow until confluency in PM. Once confluent the cells were treated with DMSO, Brefeldin A (200μg/ml), tunicamycin (1μg/ml), tharpsigargin (200 nM), calcium ionophore A23187 (5-10 μM) or dithiothreitol (1μM-5μM) for 30 minutes to one hour. The cells were washed twice in warm PBS and immediately induced to differentiate by incubating the cells in DM supplemented with insulin (50nM) changing the media everyday for the duration of the experiment.

2.9 PLD3 Deglycosylation

PLD3 from differentiating myoblasts was deglycosylated using New England Biolab's EndoH and PNGaseF enzymes, following the companies suggested protocol. Briefly, whole cell lysates were denatured by adding urea to a final concentration of 2.4M for 10 minutes at room temperature. For PNGase F treatment, after denaturing 10X G7 reaction buffer and 10X NP-40 were added to a concentration of 1X, followed by 2ul of PNGase F per 10ul of lysate used. For EndoH, after denaturing, 10X G5 reaction buffer was added so that the final

concentration was 1X, followed by the addition of 2ul of EndoH per 10 ul of lysate used. The lysate endonuclease mix was then allowed to incubate for 2 hours at 37C. The reaction was stopped by the addition of 2X sample buffer, which also prepared the samples for SDS-PAGE.

2.10 Co-immunoprecipitation

C2C12 control and overexpression myoblasts were differentiated as mentioned above for 6 days in 10cm culture plates. The cells were then washed twice in ice cold PBS and scraped on ice into IP lysis buffer (1 % CHAPS and 1% octyl-glucopyranoside in PBS). The cells were then incubated in the lysis buffer for 20 minutes on ice. The lysate is then spun down at a low RPM for 20 minutes to remove nuclei and cell debris. The supernatant was then pre-cleared using non-conjugated agarose beads for 30 minutes. The lysate/bead mix is then spun down to pellet the agarose beads; the supernatant was then removed and incubated with anti-myc antibody bound agarose beads overnight. The beads were then washed 7 times with the lysis buffer and once with PBS to remove all detergents. Captured proteins are then removed from the myc-agarose beads incubating the beads with an acidic elution buffer (Pierce), followed by a 1 minute centrifugation at max speed on a table top centrifuge and the addition of pH9.5 Tris buffer for neutralization. The samples were then sent to Dr. Emily Chen for mass spectrometry analysis.

2.11 Conditioned media analysis

C2C12 parental and overexpression cells were allowed to grow until confluent and induced to differentiate. The cells were allowed to differentiate for 4 days in DM. The cells were then washed with PBS and switched from DM to DMEM supplemented with ITS (insulin transferrin and selenium) media supplement for two days. The conditioned media was collected; the cells were carefully washed once with PBS and added to the conditioned media. The media and PBS wash were briefly centrifuged to remove any cell debris and detached cells and concentrated by centrifugation 5mL at a time using an Amicon Ultra-15, molecular weight cut off 3kDa centrifugal filter in refrigerated centrifuge at 5000 RPM for 45 minutes each spin. The protein concentration was measured using the BioRad protein assay and sent to Dr. Emily Chen for mass spectrometry analysis.

2.12 Unfolded Protein Response detection

Cells were seeded so that they were approximately 50% confluent. The cells were then transfected with reporter plasmid 5X ATF6-Luc (firefly luciferase under the control of 5x ATF6 binding sites described in (*39, 40*)) and a β-galactosidase plasmid. Twenty-four hours after transfection myoblasts were induced to differentiate for 3 days. The cells were then lysed and both luciferase and β-galactosidase activity was measured using the Dual light detection kit

(Applied Biosystem) and 20/20 luminometer (Turner Biosystems). Luciferase activity values were normalized by β-galactosidase activity values that reflect transfection efficiency.

2.13 Heterotypic fusion assay

C2C12 myoblasts stably expressing β-galactosidase (β-gal) fragment proteins, 410α and 50ω (described in (*41*)), were infected with retroviruses containing ER-mcherry, PLD3-myc or PLD3-K418R-myc as stated above and selected for cells that stably express the above genes. For fusion analysis, equal proportions of cells expressing the split β-gal fragments, were seeded into 6-well plates and induced to differentiate for five days. The cells were paired as follows: ER-mcherry-410α/ ER-mcherry-50ω, PLD3-myc-50ω/PLD3-myc 410α, PLD3-myc-K418R-50ω/PLD3-myc-K418R-410α ER-mcherry-50ω/ PLD3-myc-410α, ER-mchery-50ω/ PLD3-K418R-myc-410α, ER-mcherry-410α/ PLD3-myc-50ω, ER-mcherry-410α/ PLD3-K418Rmyc-50ω, PLD3-myc-50ω/PLD3-K418R-myc-410α, and PLD3-myc-410α/ PLD3-K418R-myc-50ω. β-gal activity was measured daily including D0 using the Galato-star substrate reagents (Applied Biosystems).

Chart 1 Cloning Primers

	construct	Sequence
1	PLD3-myc and K418R	FWD 5′CGGCGGCCGCACC ATGAAGCCTAAACTG3′ REV 5′ GGATCCTCAGAGCAGGCGGCA
2	PLD3-Δ1-60-myc	FWD:5′CGCCCGCGGCCGCACCATGGAATACGGCGACTTG3′ REV:5′GGATCCTCACAGATCTTCTTCAGAAATTTGTTTTTGTTCG AGCAGGCGGCAGG3′
3	PLD3-Δ37-60-myc	1. FWD: 5′CGCCCGCGGCCGCACCATGAAGCCTAAACTG3′ REV: 5′GCAAGTCGCCGTATTGCGGGCTTTCTTTTC3′ 2. FWD: 5′GAAAAGAAAGCCCGCAATTACGGCGACTTGC3′ REV:5′GGATCCTCACAGATCTTCTTCAGAAATTTGTTTTTGTTCGAGCA GGCGGCAGG3′ 3. FWD: 5′CGCCCGCGGCCGCACCATGAAGCCTAAACTG3′ REV:5′GGATCCTCACAGATCTTCTTCAGAAATTTGTTTTTGTTCGAGCA GGCGGCAGG3′
3	Δ1-37	FWD: 5’CGCCCGCGGCCGC ACCATGAAGCCTAAACTGA REV:5’GGATCCTCACAGATCTTCTTCAGAAATTTGTTTTTGTTCG AGCAGGCGGCAGG3’
4	mPLD3-GFP	FWD: 5′ CCGGAATTCCATGAAGCCCAAACTG3′ REV: 5′ CGCGGATCCGGAAGCAGGCGGCAGGC3′
5	ER-mcherry	FWD5′GCGGCCGCATGCTGCTATCCGTGCCGTTGCTGCTCGGCCTCC TCGGCCTGGCCGTCGCCATGGTGAGCAAGGGCGAG REV: 5′ GGATCCTTACAGCTCGTCCTTCTTGTACAGCTCGTCCAT
6	1-37-GFP	FWD: GAATTCATGAAGCCTAAACTG REV: GGATCCGCGGGCTTTCTTTTC
7	1-60-YFP	5′ GAATTCACCATGAAGCCTAAACTG 3′ 5′ GGATCCtTCCATAGAAACAGCTGA 3′
9	37-60 YFP	5′ GAATTCACCATGCGCTGGGTC 3′ 5′ GGATCCTTCCATAGAAACAGCTG 3′

Chart 2. miRNA and shRNA primers/ sequences.

	Primer sequence. *Target sequence in red
miRNA-1	5'TGCTGTTCAGCTCCTGGTACATCAGTGTTTTGGCCACTGACTGACACTGATGCCAGGAGCTGAAAAG3' 5'CCTGTTCAGCTCCTGGCATCAGTGTCAGTCAGTGGCCAAAACACTGATGTACCAGGAGCTGAAC3'
miRNA-2	5'TGCTGACCAGTTGGAGGTTCCAATGTGTTTTGGCCACTGACTGACACATTGGCCTCCAACTGGTAAG3' 5'CCTGGACCAGTTGGAGGCCAATGTGTCAGTCAGTGGCCAAAACACATTGGAACCTCCAACTGGTC3'
shRNA-1 (167)	5'GATCCCCGGAAGGCAGCAGAGAAGAATTCAAGAGATTCTTCTCTGCTGCCTTCCTTTTTGGAAG3' 5'GTACCTTCCAAAAAGGAAGGCAGCAGAGAAGAATCTCTTGAATTCTTCTCTGCTGCCTTCCGGG3'
shRNA-2 (1028)	5'GATCCCCCCCGAAGCTTCATCTACATTTCAAGAGAATGTAGATGAAGCTTCTTTTTTTTGGAAG3' 5'GTACCTTCCAAAAACCCGAAGCTTCATCTACATTCTCTTGAATGTAGATGAAGCTTCTTTGGG3'

Chart 3. siRNA oligo sequences

Oligo	Sequence
1	5'UAA UAU AGC CCA CAG UUU CCU GGC G 3' 3'AUU AUA UCG GGU GUC AAA GGA CCG C 5'
2	5'GAC AGU GCC CGA AGC UUC AUC UAC A3' 3'CUG UCA CGG GCU UCG AAG UAG AUG U5'
3	5'CCU UCU ACU GGA CCC UCA CAA AUA A5' 3'GGA AGA UGA CCU GGG AGU GUU UAU U3'

Chapter 3
Characterization of PLD3 during Myogenesis

3.1 PLD3 expression increases during C2C12 in vitro myogenesis.

3.1.1 Introduction

Tomzack et. al. showed that there was an increase in PLD3 mRNA expression during C2C12 *in vitro* differentiation (*29*), suggesting that PLD3 has a role in myogenic differentiation and thus inspired the start of this thesis. It was important to examine both mRNA and PLD3 protein levels during differentiation to both confirm the previous publication and to determine if the presumed increase in mRNA coincided with an increase with protein expression.

3.1.2 Results

To confirm if there was truly an increase in PLD3 mRNA expression, C2C12 myoblasts were grown until confluent and induced to differentiate by

incubating myoblast in differentiation media (DM) for six days. Total RNA was extracted from the differentiating cells, using the Qiagen RNeasy RNA purification kit, every day for the duration of the experiment including day 0 (D0), the day differentiation was induced. 1 ng of RNA, as determined by a nano-drop spectrophotometer RNA measurements, was then used for quantitative PCR (qPCR) using PLD3 and GAPDH specific primers (section 2.6) and a sybr green one-step qPCR kit (USB). Both amplification and analysis was conducted using the Roche lightcycler 480 machine and software. PLD3 levels were normalized to GAPDH and compared to D0 levels. As seen in figure 3.1A, PLD3 mRNA levels had a general increase in expression, reaching a maximum level of expression at day 4 post differentiation induction.

To determine the expression profile for PLD3 protein, C2C12 myoblasts were differentiated as above for 12 days. Total cell lysates were collected from cells every day for the first 6 days and every other day there after. The cells were collected and lysed in a modified RIPA buffer, followed by low RPM centrifugation to remove nuclei and cell debris. Equal amounts of protein, as determined by Bradford reagent (Biorad), were then separated on a 10% SDS-PAGE gel and transferred onto a nitrocellulose membrane. The membrane was then probed with anti-PLD3 and anti-GAPDH antibodies, with GAPDH used as a loading control. As seen in figure 3.1B, there was a steady an increase in PLD3 protein expression as C212 cells differentiated, which further validates the mRNA data and the previous results.

3.1.3 Discussion

In undifferentiated myoblasts, there are no detectable levels of PLD3 protein expression. However, within 24 hours of differentiation induction, PLD3 protein and mRNA levels rose significantly, confirming the previously published data and demonstrating that PLD3 protein is also expressed during differentiation. Wile there is not a direct correlation between expression and function, it is unlikely for PLD3 have such levels of induction and not have a function during differentiation. There is a noticeable difference in the expression levels and mRNA levels. However, this can be explained by the fact that there is not always a complete correlation between mRNA and protein expression and also perhaps, that PLD3 protein is very stable.

3.2 In proliferating myoblasts, the transmembrane domain of PLD3 directs localization of PLD3 to the endoplasmic reticulum.

3.2.1 Introduction

A previous study on PLD3 showed that PLD3 was a glycosylated, type II transmembrane protein, associated with the endoplasmic reticulum (*27*). The previous study was conducted in Cos7 cells which, to date, have not been shown to express endogenous PLD3 protein. However, since C2C12 cells do endogenously express PLD3 protein, during differentiation and may have a different localization in both undifferentiated and the differentiated cells, it was important to this thesis to confirm endoplasmic reticulum localization in both differentiated and undifferentiated C2C12 cells. Below is the data for proliferating cells; differentiating cells will be discussed later in the chapter.

3.2.2 Results

In order to confirm endoplasmic reticulum (ER) localization of PLD3 in proliferating myoblasts, proliferating C2C12 myoblasts transiently transfected with myc-tagged PLD3 underwent indirect immunofluorescence using anti-myc and anti-KDEL antibodies to detect PLD3 and the ER, respectively. The stained cells were then mounted onto slides and visualized by confocal microscopy using

a Zeiss LSM510 Meta confocal microscope. The staining showed that there was uniform co-localization between PLD3-myc and KDEL (figure 3.2), confirming the previously reported data.

To further study the localization pattern of PLD3, determining if there is a ER localization site in PLD3, two PLD3 deletion mutants (Δ1-60 and Δ37-60) were constructed by PCR based mutagenesis, in which the transmembrane domain was removed. The Δ1-60 mutant removed the first 60 amino acids including the transmembrane domain, while the Δ37-60 mutant removed just the transmembrane domain (figure 3.3A). C2C12 cells were transfected with the above constructs, and subjected to indirect immunofluorescence staining and analysis using anti-myc and anti-KDEL antibodies to detect the deletion mutants and the endoplasmic reticulum, respectively. The staining showed that the localization of the protein changed significantly, no longer localizing to the ER when the transmembrane region was removed. Both mutants localized to unknown vesicles and the nucleus with very little to no ER localization (figure 3.3 B-C), suggesting that the transmembrane domain is the minimal region required for PLD3 localization to the ER in proliferating cells.

This was further supported by the use of a mito-tagged Δ1-37 PLD3 mutant in which the N-terminal amino acids, not including the transmembrane domain (figure 3.3A), were deleted. C2C12 cells were transfected with the mito-tagged Δ1-37 mutant and stained by indirect immunofluorescence. The mito-

tagged Δ1-37 mutant retained its ability to localize to the ER (figure 3.3D). This showed that the transmembrane region is largely responsible for PLD3 localization and that the transmembrane domain may be the minimal element required for endoplasmic reticulum localization of PLD3 in proliferating cells. In the Δ37-60mutant, it was also observed that, occasionally, the endoplasmic reticulum is underdeveloped as there was less ER less staining in these cells compared to cells expressing the Δ1-60 or full length PLD3 constructs. This observation will be discussed in detail later in this section.

In order to determine if that the transmembrane domain of PLD3 was the minimal element required for PLD3 localization, YFP/GFP fusion proteins were constructed. Three fusion plasmids were made: PLD3 1-37GFP (the first 37 amino acids of PLD3 with out the transmembrane domain), PLD3 1-60-YFP (N-terminus of PLD3 plus the transmembrane domain), and PLD3 37-60-YFP (only the transmembrane domain of PLD3). All three constructs were transfected into NIH3T3 cells. After transfection, the cells were then stained by indirect immunofluorescence with an anti-KDEL antibody to stain the ER, followed by confocal microscopy analysis to determine if there was co-localization. The two constructs containing the transmembrane domain, 1-60-YFP and 37-60-YFP, localized to the ER (figure 3.4 B-C); further suggesting the transmembrane domain of PLD3 as the minimal element required for PLD3 localization. The PLD3 1-37-GFP construct did not localize to the ER, instead it had a fairly ubiquitous localization, localizing mainly to the cytoplasm (figure 3.4 A). This

data further confirmed the above data showing that the transmembrane domain is largely responsible for PLD3 localization to the ER in proliferating cells, and is the minimal element required for PLD3 localization. It was, however, noticed that the endoplasmic reticulum had distorted shape with the expression of the transmembrane-YFP constructs.

As mentioned earlier, the PLD3 deletion mutant Δ37-60, showed a decrease in ER staining. To further study this phenomenon, Cos7 cells were transfected with a, presumably, inactivated Δ37-60 construct, Δ37-60 K418R, which has a mutation in the second HKD domain. The cells were also transfected with WT Δ37-60 or Δ1-60WT. After transfection, the cells were stained, by indirect immunofluorescence with anti-myc and anti-KDEL antibodies. As seen in figure 3.5, cells expressing the active Δ37-60 WT mutant exhibited a decrease in ER staining compared to the cells expressing the inactive Δ37-60 K418R and Δ1-60 WT mutants. Together the data, suggested that the decrease in ER staining observed is dependent on the protein having intact HKD domains and therefore PLD3 activity. To examine the ER specificity of this trend, cells transfected with Δ37-60 active were stained with an anti-Gm130 to visualize the Golgi. As seen in figure 3.5D, the Golgi was still intact, with very little observable changes to its architecture, suggesting that this phenomenon only affects the ER.

3.2.3 Discussion

Overexpression in proliferating cells, PLD3 localizes to the ER; also confirmed above. PLD3 was predicted to have a secretory sequence, which directed its localization to the ER. However, contrary to beliefs that the N-terminal secretory sequence is responsible for the localization of PLD3, I demonstrated that PLD3 localization is controlled mainly by the transmembrane region, as shown by the transmembrane only fusion protein, which was able to direct ER localization. In fact, the transmembrane domain is the minimal region required for ER localization in proliferating cells. Without the transmembrane domain, PLD3 localizes to unknown vesicles as well as to the nucleus. The localization of the truncated protein to the nucleus is a very interesting phenomenon, since the protein does not contain a recognizable nuclear localization signal and is too large to enter the nucleus by simple diffusion. Perhaps truncated PLD3 binds to proteins capable of transporting PLD3 to the nucleus. This phenomenon also leads to an interesting question: Can nuclear PLD3 bind and modify DNA like vK4L? Since vK4L binds and modifies DNA (*30*), it could be that the function of nuclear localized PLD3 is the same. Since full length PLD3 has not been observed to enter the nucleus, differential splicing events may control when and where truncated PLD3 could be expressed. Endonuclease activity for nuclear PLD3 could explain how PLD3 could promote

differentiation in some cells/tissues (i.e. neurogenesis and myogenesis) and increased self-renewal properties in hematopoietic stem cells.

Since we have shown that the transmembrane domain is very important for PLD3 localization, is it possible for the transmembrane region to also control PLD3 activity? As seen above, removal of PLD3's transmembrane domain, unexpectedly, leads to a decrease in ER staining/structure. How and why the transmembrane would control PLD3 activity is unknown; however it is possible that the primary method of transmembrane control over PLD3 activity is through localization. Keeping PLD3 sequestered in the ER away from substrate molecules, possibly located on the ER surface or other membrane surfaces, would inhibit PLD3 activity. The second possible reason for transmembrane domain control over PLD3 activity is through protein folding. As mentioned above, the deletion mutant Δ1-60 also loses it localization to the ER; however, it does not alter ER structure as the Δ37-60 mutant. It is possible that active domain(s) of PLD3 is more exposed in the Δ37-60 mutant than the Δ1-60 mutant, leading to the differences in ER staining structure observed above.

3.3 Localization of PLD3 in differentiating C2C12 cells

3.3.1 Introduction

Localization of PLD3 can suggest function and possibly give insight into biochemical activity. As mentioned above, PLD3 localizes to the ER when overexpressed in proliferating cells; however, protein localization during forced expression does not always correlate to localization pattern when endogenously expressed. Since above it was demonstrated that the transmembrane domain directs PLD3 localization to the ER, it was hypothesized that PLD3 would localize to the ER or an ER-derived membrane system during differentiation. In addition to the above, based on the role of Spo14 during yeast prospore membrane formation (11), it was believed that PLD3 may localize to and aid in the formation of the T-tubule membrane formation.

3.3.2 Results

To determine the localization of PLD3 during *in vitro* myogenesis, C2C12 cells were allowed to differentiate for 5- 6 days on gelatin-coated coverslips. The cells were then fixed and immunoflourescent staining performed on the cells as stated above using anti-KDEL and anti-PLD3 antibodies. As seen in figure 3.6A,

there was minimal co-localization between the PLD3 antibody and the ER/SR marker antibody KDEL; suggesting that PLD3 does not localize to traditional ER membranes during myoblast differentiation. However, there was a noticeable association between KDEL positive vesicles and PLD3 positive vesicles. Since there was a noticeable association between PLD3 and KDEL positive vesicles, differentiating myotubes were treated with DMSO or Brefeldin A (BFA) (10μg/ml) for one hour to increase ER volume, as BFA prevents ER-Golgi trafficking. The inhibition of ER-Golgi trafficking leads to an accumulation of protein in the ER, ultimately leading to an increase in ER volume. As seen in figure 3.6 B, PLD3 still did not localize to KDEL positive vesicles/membranes. This was further examined by using PC12 cells, which like myoblast differentiation express PLD3 upon neurogenic differentiation induction (figure3.7 A). PC12 cells were induced to differentiate for 4 to 8 days and subjected to immunoflourescent staining with anti-PLD3 and anti-KDEL antibodies. As above, there were no points of co-localization between PLD3 and KDEL (figure 3.7B), confirming that PLD3 does not localize to ER membranes during PC12 differentiation, and differentiation events in general.

As stated above, based on the role of Spo14 in yeast prospore membrane development, it was believed that PLD3 localized to and aided in the formation of the T-tubule system. The myotubes were tested for localization of PLD3 to the developing T-tubules by immunoflourescent staining using a caveolin 3 antibody, which localizes to early T-tubule membranes (*42*), and the PLD3 antibody. There

were no significant points of localization between PLD3 positive vesicles and caveolin 3 positive membranes (3.8 A), suggesting that not only does PLD3 not localize to developing T-tubules, it does not directly aid in T-tubule development.

Myotubes were also stained with markers for secretory vesicles, early endosomes, mitochondria, cis-Golgi, autophagosomes, and peroxisomes, with no significant amount of co-localization between PLD3 and the above markers (figure3.8 B-G) in differentiating myotubes. While there was not a significant localization between PLD3 and the mitochondria marker cytochrome C (cyto-c) (3.8 D) in myotubes, there was a remarkable amount of co-localization between cytochrome c and PLD3 in a myoblast fusing to a larger myotube that resembled contact points between the ER and the mitochondria. This above data suggests that PLD3 resides in the ER of non-fused, differentiating/fusing myoblasts before they have fused and rearranged their ER membranes; it also suggests that PLD3 may localize to ER-derived or highly specialized ER membranes during differentiation.

To determine if PLD3 passed through the Golgi, no longer localizing to ER membranes during differentiation, PLD3 protein from the whole cell lysates of differentiating C2C12 myoblasts expressing ER-mcherry or PLD3-myc was subjected to deglycosylation with EndoH and PNGaseF, followed by western blot analysis for shifts in PLD3 size and thus glycosylation status. Both of the above enzymes act to deglycosylate N-glycosylated proteins, with PNGaseF acting on

almost all N-glycosylated proteins and EndoH acting only on glycosylated proteins that have not been passed through the Golgi. PLD3 showed a decrease in size with PNGaseF treatment, but not with EndoH treatment (3.9), suggesting that not only does PLD3 not retain ER localization during differentiation, but also that it passes through the Golgi and is most likely a part of the secretory system.

To see if we could determine the localization of PLD3 by placing it within a signaling pathway (ie. determining if inhibiting or activating signaling pathways would change localization of PLD3), I treated PLD3-myc overexpressing, differentiating myotubes with Brefeldin A (20μM) (prevents ER-Golgi protein trafficking), tunicamycin (2mg/ml) (inhibits protein glycoslylation), tharpsigargin (1mM) (inhibits ER calcium pumps), amphotericin B (25μg/ml) (disturbes membranes systems by sequestering cholesterol) or wortmanin (10μM) (inhibits PI3 Kinases signaling) for 4 hours followed by indirect immunoflourescent staining with anti-myc and anti-KDEL antibodies. As seen in figure 3.10, most of the treatments did not cause a change in the localization pattern of PLD3, except tharpsigargin. Treatment of these myotubes with tharpsigargin showed an increase in PLD3 localization to the ER (figure 3.10D); however, it is unknown why this would occur, but as seen in section 3.5, tharpsigargin can and is most likely increasing PLD3 expression.

3.3.3 Discussion

As mentioned above, prior to differentiation, overexpressed PLD3 localized to the endoplasmic reticulum. We have even shown that PLD3 localizes to what looks like ER/ ER-mitochondrial localization sites in differentiating, no-fused myoblasts. However, we have shown that once differentiated, PLD3 no longer localizes to "traditional" ER-membranes, as it is not detected in KDEL positive membranes/vesicles. The EndoH resistance of PLD3 in differentiating cells, seen above, further suggesting that PLD3 no longer localizes to the ER in differentiating myotubes. In fact, the EndoH resistance of PLD3 suggests that it passes through the Golgi and is most likely a part of the secretory system. However, the status of PLD3's EndoH resistance can be questioned due to the hydrophobic nature of PLD3. Denaturing PLD3 by boiling leads to PLD3 precipitation out of solution and a failure to detect PLD3 by western blot analysis, which is why urea was chosen for PLD3 denaturating. With that, it is possible for PLD3 to be EndoH resistant, since it is possible that PLD3 was not sufficiently denatured for EndoH enzymatic processing.

We next tested to see if PLD3 localized to developing T-tubules; however, there was no co-localization between PLD3 and the T-tubule marker caveolin 3, suggesting that PLD3 did not have a role in developing T-tubules. This was further confirmed by treating myotubes with amph B, which leads to the collapse

of the T-tubule system (*42*), with no change in the localization PLD3; showing that PLD3 is not a part of the T-tubule system.

PLD3 localization was further tested using an array of antibody markers, as seen above, oddly with none of the makers showing any significant co-localization with PLD3. This lead us to believe that PLD3 may localize to uncharacterized vesicles in differentiating myotubes. These are most likely associated with the ER since, as above, we have shown that tharpsigargin leads to an increase in the association between PLD3 and the ER, but more importantly since, as I show later, tharpsigargin is able to increase PLD3 protein expression in differentiating myotubes.

3.4 PLD3 overexpression enhances myotube formation in C2C12 myoblasts

3.4.1 Introduction

In an effort to determine PLD3 localization during differentiation, a PLD3-mcherry construct was made and stably expressed in C2C12 myoblasts. While differentiating PLD3-mcherry overexpressing myoblasts, it was noticed that the cells looked and behave differently than the non-overexpressing cells, specifically showing a fragmented ER membrane before differentiation was induced as well a decrease in fusion once cells were induced to differentiate (data not shown). Previous studies overexpressing PLD3 did not yield a phenotype, so this was very unexpected phenotype that required further exploration using a myc-tagged PLD3 in both the active and inactive (contains a mutation in the second HKD domain, K418R, to inactivate PLD3 activity) forms, since it was also noticed that the PLD3-mcherry protein aggregated during differentiation.

3.4.2 Results

To further explore the above observation, C2C12 myoblast populations stably expressing ER-mcherry, PLD3-myc, and inactive PLD3, PLD3-K418R-myc were created by retroviral infection. After selection all three cells were

induced to differentiate for 6 days. The PLD3 overexpression cells (active and inactive) showed an initial delay in fusion (3.11A); however, the wild-type (wt) PLD3-overexpressing cells eventually showed a significant increase myoblast fusion (figure 3.11A). By day 5 post differentiation induction, wt PLD3-overexpressing myoblasts had a higher fusion index (percentage of nuclei in myotubes with three or more nuclei over total nuclei) than both the control and PLD3-K418R-overexpressing myoblasts (figure 3.11 B). By day 6 post induction the wt PLD3 cells maintained the increased fusion index, having enhanced myotube formation compared to the control and PLD3-K418R myoblasts (3.11B). To determine if increase in myotube formation was due to an increase in nuclei per myotube, a fusion index representing the percentage of myonuclei (nuclei in myotubes with three or more nuclei) in myotubes with 3-10, 11-20, or >20 nuclei was determined for each of the cell populations. It was observed that there was no significant difference in the amount of nuclear incorporation between the ER-mcherry overexpressing and the wt PLD3-myc overexpressing myotubes; however, it also was observed that the PLD3-K418R-myc cells, based on nuclear incorporation, formed smaller myotubes than the control and PLD3-myc cells (figure 3.12). This fusion phenotype was further confirmed by using a different myoblast cell line, Sol8, which showed a phenotype similar to the C2C12 myoblasts in which, visually, the wt PLD3-myc overexpressing myoblasts fused more efficiently than the ER-mcherry and PLD3-K418R overexpressing myoblasts (figure 3.13).

To further examine the altered fusion indices between the three cell populations, C2C12 PLD3 and ER-mcherry overexpression myoblasts were examined for altered expression of the myogenic differentiation markers myosin heavy chain (MHC) and calsequestrin (CSQ), which measures the formation of the contractile apparatus and specialized membranes, respectively. By Western blot analysis, there were no significant differences in expression of MHC and CSQ between the control cells and the PLD3 overexpression cells (figure 3.14 A). There was however, a slight delay in the expression of MHC in the PLD3-K418R-myc cells. To determine if the change in fusion was due to a change in the expression of fusion-related proteins I examine the expression of cell surface, myofusion markers m-cadherin and calpain-1 by western blot analysis. As with the above myogenic markers, m-cadherin and calpain-1 did not show significant changes in protein expression between the three cell populations (figure 3.14 B).

To further attempt to dissect why and how PLD3 expression alters myotube formation, I examined if there were changes in secreted proteins by examining conditioned media from differentiating myoblasts, as well as deciphering if PLD3 binds to any proteins as part of its function or regulation by co-immunoprecipitation. For this approach, C2C12 myoblasts expressing ER-mcherry, huPLD3-myc, or huPLD3-K418R-myc were seeded into 15cm tissue culture plates and induced to differentiate in normal differentiation media. After four days of differentiation, the media was changed to serum-free medium (DMEM plus ITS media supplement). This was done to remove serum proteins

that would create high background during the subsequent mass spectrometry analysis. The cells were then allowed to differentiate for 2 more days to "condition" the media. On day 6 post differentiation induction, the conditioned media was carefully collected and pooled with a washing of the cells in PBS. The pooled media and PBS wash was then concentrated and separated on an 8-20% gel. The gel was then stained by either Coomassie blue or silver staining to visualize proteins and determine if there were any differences. The cells were processed for co-immunoprecipitation (co-IP) using the Pierce Myc tag co-immunoprecipitation kit.

The preliminary results for the conditioned media were very promising, based on gel electrophoresis and mass spec analysis. Visually, by gel-electrophoresis, there appeared to be differences in the secretome between the cell populations (figure 3.15); more importantly, mass spectrometry analysis showed that there was an increase in "pre-pro" proteins in the conditioned media from cells expressing huPLD3-K418R-myc compared to the ER-mcherry and PLD3-myc-expressing cells (Appendix 1). However, when the experiment was repeated, there were problems with reproducibility (Appendix 2) as there were fewer proteins indentified, and the high levels of "pre-pro" proteins were no longer observed.

The preliminary results for the co-IP were not promising. There were few differences in eluted proteins between the cell populations based on gel

electrophoresis and silver staining. The mass spectrometry analysis results were similar to the above gel showing there no differences in the protein contents of the samples. The co-IP was then repeated, but based on western blot analysis of the beads used for IP, the PLD3-myc protein was not efficiently eluted from the beads. It was also observed that the PLD3-K418R was not being pulled out of solution efficiently either (figure 3.16).

Since the above proteomics approaches to determine why PLD3 overexpression changes myoblast fusion were unsuccessful, I decided to use a heterofusion assay to determine if myoblasts with altered PLD3 expression could cause a change in the fusion of cells without altered PLD3 expression. The heterofusion assay consisted of mixing ER-mcherry myoblasts with PLD3-myc or PLD3-K418R-myc myoblasts as well as mixing PLD3-myc and PLD3-K418R myc. For this, I employed the use of the split β-gal complementation system as previously described (*41, 43, 44*), to measure the amount of fusion that is occurring between the cell populations via β-gal activity. As seen in figure 3.17A, the β-gal complementation fusion assay confirmed that PLD3-myc overexpressing myoblasts had a higher fusion index than the ER-mcherry and PLD3-K418R-myc myoblasts. More importantly, we see that population mixes containing the PLD3-myc overexpressing myoblast tended to have higher fusion indices than the cell populations without PLD3-myc (figure 3.17B-C); suggesting that either the PLD3-myc myoblasts are secreting more "pro-fusion" factors than

the other myoblast populations or, there may be changes to fusion machinery in either concentration, localization, or activity.

3.4.3 Discussion

Above, I showed that PLD3 overexpression promotes myotube formation. Cells overexpressing PLD3 had larger myotubes than both the control and the PLD3-inactive overexpressing cells. However, how PLD3 is able to achieve this is unknown. It is unlikely that the increase in myotubes was due to accelerated differentiation, as there was not an increase or acceleration in the expression of differentiation markers MHC and CSQ, as seen above. However, it is possible for there to be other differentiation markers that might show altered expression between the cell populations during differentiation including caveolin 3, which if altered, would have signaling implications specific to the Phosphoinositide-3-kinase cascade (*45*); however, this is unlikely. As seen in the previous section PLD3 localization in differentiating myotubes was not altered by treating myotubes with the Phosphoinositide-3-kinase inhibitor wortmanin. It is also, possible that there are changes to the cell surface, even though, as mentioned above, there were no changes to the myofusion markers m-cadherin and calpin-1, which localize to the cell surface. More importantly, as in reference (*41*), it is possible for there to be no change in the expression of fusion and cell surface proteins, while the activities of these proteins are altered, leading to a change in

fusion rates. In this scenario PLD3 activity would control signaling cascades that control the activities of fusion machinery proteins. Another possible explanation for changes in the fusion index of the cells is that PLD3 is not altering myotube formation, but is instead changing/controlling myotube trophic status by inhibiting atrophy. In this scenario, PLD3 overexpressing cells are more resistant to atrophy and therefore more resistant to cells wasting away, leaving the ratio of polynuclear cells to mononuclear cells higher and thus a higher fusion index. However, another, less likely, possibility is that PLD3 may regulate myotube twitching. In culture, it is common for C2C12 cells to spontaneously contract or twitch. This twitching, usually leads to a loss of myotubes if the substratum is not strong enough to withstand the shear force and as a result, myotubes lift off the plate (*46*), and once again, the ratio between polynuclear and mononuclear cells would shift.

We attempted to determine if the increase in myotube formation was because of alterations in the secretome; however a more sensitive method for secretome studies is needed. There is a strong possibility for an altered secretome based on earlier unpublished lab data, which showed alter VSVG trafficking and localization in cells overexpressing PLD3. If there are changes to the secretome, it is most likely coming from changes in cytokine secretion, specifically, IL-4, since it has been shown to promote fusion when exogenously expressed and inhibit fusion when it is inhibited (*47*). However, the likelihood of this possibility is questionable due to the results of the heterotypic fusion assay. If there is an

altered secretion of “profusion” factors, then one would expect that the fusion index of myoblast populations containing PLD3-myc myoblasts and non-PLD3-myc myoblasts to rise to or above the level of the PLD3-myc only myoblasts.

3.5 Transient ER-stress increases PLD3 expression during myogenesis

3.5.1 Introduction

According to Nakanashi et. al., transient ER-stress leads to an increase in myofiber formation (*48*). In and effort to improve myotube formation, I placed C2C12 myoblasts under transient ER-stress induced by using the sarcoplasmic/endoplasmic reticulum Ca2+ -ATPase inhibitor, tharpsigargin (TG) (1uM) to inhibit ER function by depleting ER calcium stores or the solvent control DMSO, for 30 min to one hour before differentiation induction as used by Nakanashi et. al. (*48*). Interestingly, an increase in myofiber formation was not seen; instead, all of the TG treated cells died within 48 hours of treatment and differentiation induction. However, when the protein samples of the treated and non-treated cells were analyzed by western blot for PLD3 expression, TG treated cells showed a marked increase in PLD3 expression compared to the non-treated cells (not shown).

3.5.2 Results

To expand the above observation, C2C12 myoblasts were placed under transient ER-stress induced by tunicamycin (TN) (1μg/ml), tharpsigargin (TG)

(250nM) or Brefeldin-A (BFA) (200µg/ml) exposure in DMEM supplemented with 20%FBS for 30 minutes to 1 hour immediately before differentiation was induced in DM supplemented with insulin (167nM). TG induces ER-stress, as mentioned above, by depleting ER-calcium stores, while BFA and TN induce ER stress by stimulating an accumulation of proteins within the ER, by either inhibiting ER-Golgi trafficking (BFA) or inhibiting protein glycosylation and proper protein folding (TN). Cell lysates were collected on D0 (day of stress and differentiation induction) and everyday afterwards for 5 days. Western blot analysis was performed on the lysates probing for PLD3 and GAPDH (loading control). PLD3 expression was increased in the TN and TG treated cells compared to the DMSO treated cells, but not in the BFA treated cells (figure 3.18). This increase in PLD3 expression was sustained throughout the observed time. I also noticed that the TN and the TG treated cells showed a high amount of cell death compared to the DMSO and BFA treated cells (data not shown). Once again, the TG treated cells, as well as the TN treated cells, did not show an increase in myotube formation compared to the DMSO and the BFA treated cells. I next tested to see if the increase in PLD3 expression was due to ER-stress only or a combination of ER-stress and differentiation. To do this, ER stress was induced in proliferating C2C12 cells with BFA, TN or TG in proliferation media for 4, 8 or 24 hours. As seen in figure 3.19 A, PLD3 was not induced in proliferating cells treated with the ER-stressors; suggesting that PLD3 induction was due to a combination of both ER-stress and differentiation. To further

confirm that the increased PLD3 expression in TG and TN treated myoblasts was due to a combination of both ER-stress and differentiation, ER- stress induced in HeLa cells with TN as above with a serum reduction time of 3 days to simulate C2C12 differentiation conditions, and in proliferation media for 4, 8, and 24 hours. In both modes of stress induction, there was no induction of PLD3 expression in HeLa cells (figure 3.19 B); confirming that the increase in PLD3 expression following ER stress in differentiating myoblasts was due to the combined effects of ER-stress and differentiation.

After the above observations, the question asked was: why do the combined events of differentiation and ER-stress increase PLD3 expression? It has been reported that TG, by increasing intracellular calcium levels, acts to stimulate the calcineurin/NFAT pathway (*45*); which may place PLD3 in the calcineurin pathway; and going along this same line of reasoning, TN would be weakly acting the same way since, in addition to inhibiting glycosylation, it has also been shown to increase intracellular calcium levels (*49*). TN and TG could also be activating the unfolded protein response (UPR), thus stimulating ATF6 activation, a response/ pathway that both agents have been shown to activate (*50*) in order to stimulate ER expansion. There have been several reports stating a role for ATF6/ ER-stress/ UPR as apart of differentiation in several cell types and possibly myogenesis as well (*51-56*). In addition to the above possibilities, TN and TG have both been reported to activate ER-stress induced oxidative stress (*57*).

To determine why transient ER increased PLD3 expression, I began by testing if increased intracellular calcium levels can stimulate increase PLD3 levels. In order to test this, C2C12 cells were treated with calcium ionophore A23187 (10μM) for 30 min to one hour before the induction of differentiation and allowed to differentiate for three days. The cells treated with calcium ionophore did not show an increase in PLD3 compared to non-treated cells (figure 3.20 A). Myoblasts were then pre-treated with DTT, a potent UPR inducer, to induce an unfolded protein response, by blocking disulfide linked protein folding without a severe change in calcium levels in the cytoplasm or ER-lumen. The cells were also pretreated with a DTT calcium ionophore mix to determine if calcium and UPR induction were the necessary treatments to induce PLD3 expression. As seen in figure 3.20 A, DTT and DTT/ calcium ionophore pre-treatments did not show an increase PLD3 expression in differentiating cells; suggesting that PLD3 induction was not to the activation of the UPR. This was further examined by transfecting myoblasts stably expressing ER-mcherry, PLD3-myc or PLD3-K418R-myc with the 5X ATF6 reporter gene (described in (*39, 40*). This reporter genes was used to determine if there are differences in the activation of ATF6 and thus activation of the UPR, since upon ER-stress/ UPR activation ATF6 ultimately enters the nucleus as a transcription factor and stimulates the expression of UPR genes (*58*). As seen in figure 3.21, there were no differences in the activation of the UPR between the 3 cell populations, confirming that PLD3 does not alter the activation of the UPR.

To determine if the TG induced PLD3 expression was due to an oxidative stress response, myoblasts were treated with ascorbic acid, a reactive oxygen species scavenger to inhibit oxidative stress responses, during and after TG pretreatment and allowed to differentiate for three days as above. As seen in figure 3.20 A, the ascorbic acid and PLD3 ascorbic acid treated cells showed a level of PLD3 induction similar to the control cells, while the expression of PLD3 in the TG only treated cells remained high. The level of cell death in the TG/ ascorbic acid treated cells was also less than the amount of cell death in the TG only treated cells (data not shown). This suggested that PLD3 induction was due to, in part, activation of oxidative stress responses. This was further confirmed by the use of L-canavanine to inhibit TG induced oxidative stress by inhibiting iNOS activity (*57*). While there was not a reduction in the level of cell death between TG and TG/ L-canavanine (data not shown), there was less PLD3 induction in the cells treated with TG/ L-canavanine, compared to the control cells, (figure 3.20 B).

3.5.3 Discussion

As mentioned above, it is not uncommon for differentiating cells to induce the expression of UPR genes as a part of the differentiation program. Since we have determined that pre-treatment of myoblasts with ER-stress inducing agents TN and TG, leads to an increase in the expression of PLD3, it was assumed that PLD3 played a role in the activation or modulation of the UPR. However, as seen

above, with the use of the 5X ATF6 reporter gene and with DTT pre-treatment, there was no observable link between PLD3 and UPR activation during differentiation.

As seen above, there was a slight decrease in the induction of PLD3 with the pretreatment of myoblasts with L-canavanine and a large decrease in PLD3 induction with ascorbic acid treatment, suggesting that PLD3 may be involved in modulating oxidative stress response. However, inhibiting iNOS activity, with L-canavanine can inhibit differentiation, by reducing the amount of nitric oxide produced, which is very important for myoblast fusion, making the results for the L-canavanine treated cells questionable, since a decrease in myogenic induction could lead to a global decrease in the expression of myogenic factors, including PLD3 . The fact that there was a decrease in PLD3 expression without a decrease in the amount of cell death in L-canavanine treated cells, but more importantly, no observable decrease of PLD3 expression in ascorbic acid only treated cells makes the suggestion of a link between PLD3 and oxidative stress questionable. Furthermore, in osteoclasts, TG has been show to enhance osteoclast differentiation at lows levels through attenuation of reactive oxygen species production as well as to induce the expression of ATF4, which is another ER-stress activated protein, shown to be crucial in osteoclastogenesis (*59, 60*). Since we have shown that there is a link between TG and PLD3 induction as well as PLD3 and oxidative stress perhaps, as in osteoclast differentiation, PLD3 activity may be linked to ATF4 activation during myogenesis.

3.6 PLD3 knockdown during myogenesis

3.6.1 Introduction:

As mentioned in section 3.3.1, we hypothesized that PLD3 aided in membrane trafficking or reorganization events; specifically, we speculated that PLD3 would aid in formation of the T-tubule system. To investigate this, I sought to knockdown PLD3 expression by RNAi to determine a functional role for it during myogenic differentiation, and specifically to determine if PLD3 knockdown disrupted the known changes in membrane structures that occur during myogenesis. To date, there have not been any documented functional roles for PLD3 in myogenesis, nor have then been any major studies using RNAi to study PLD3 function or activity. Recently, in an RNAi screen, PLD3 was implicated in increasing sensitivity to oxidative stress; however, this paper failed to show a definite knockdown for PLD3 or a link between PLD3 expression and oxidative stress sensitivity (*36*).

3.6.2 Results

In order to knockdown PLD3 expression in C2C12 myoblasts, 4 shRNA and miRNA sequences (chart 2) were designed and constructed using the

invitrogen Block-It software. The 2 shRNA sequences were placed into the pSuper and pSuper retro backbones and the 2 miRNA sequences placed into the pSM155-GFP and pMscv-GFP backbones following the cloning details in (sec.2.24). Upon initial testing with transient co-transfections, the sequences did very well showing promising levels of PLD3 knockdown (data not shown). The myoblasts were infected with pSuper or pMscv-GFP retroviruses containing the selected sequences to make cells stably expressing the sh or miRNA sequences. There were initial troubles in obtaining stably expressing colonies with the pMscv-gfp-miR sequences, most likely due to dsRNA processing before the production of usable retroviral particles, so the use of the miR sequences was suspended. The colonies from the pSuper selection were then pooled together to form a population and used for knockdown studies.

The populations were then tested for PLD3 knockdown by transient transfection with mouse PLD-GFP followed by western blot analysis of PLD3 expression. The subsequent western blot analysis showed a high degree of PLD3 knockdown in the proliferating PLD3 shRNA expressing populations (figure 3.22 A). The cells were then tested for knockdown of endogenous PLD3 and potential consequences of PLD3 knockdown. The initial results from the knockdown experiments were very promising. The myoblast expressing the PLD3 shRNA showed an astonishing decrease in the formation of myotubes, with the population harboring sequence shRNA-1 showing the greatest amount of decreased fusion (figure 3.22 B). However, upon further testing I noticed that the PLD3 shRNA

expressing myoblasts exhibited full expression of PLD3 compared to the shRNA-Luc expressing cells at D4 post differentiation induction (figure 3.22 C). This suggested that the cells could have lost fusion competency for reasons unrelated to a decrease in PLD3 expression. The cell populations were remade in two different C2C12 parental backgrounds to ensure that there was not a general loss of fusion competency, but similar results were obtained. This suggested that the PLD3 shRNA expressing populations selected for cells that had the least amount of shRNA expression or the cells were reducing the amount of shRNA expression via heterochromatin formation.

To solve the above problems, I returned to the miR constructs in the pSM155-gfp backbones because the miR sequences are contained within an intron of a GFP expression cassette, allowing GFP expression to be a direct marker for the expression of the miRNA sequences. For this approach, C2C12 cells were transfected with the pSM155 miR constructs and subjected to antibiotic selection. Once colonies formed, a sterile flow-cytometry cell sort was used to select populations of cells with the highest amount of GFP expression for each of the miR sequences. Initially, as above, the cells showed a decrease in myoblast fusion with cells expression miRNA-2 showing the greatest decrease in fusion (3.23 A). Both cell populations exhibited a modest decrease in PLD3 expression by D4 post differentiation induction (data not shown). Upon further observation, the PLD3 miRNA populations showed an odd change in fusion dynamics, with the miR-1 expressing cells showing an increase in myotube formation compared to the

control miR-Luc expressing cells, and the cells expressing the miR-2 sequence maintaining decreased fusion compared to the miR-Luc cells (3.23 B). More importantly, there was an odd occurrence with the expression of PLD3 when examined earlier in differentiation; specifically, the PLD3 miRNA-expressing myoblasts showed a decrease in PLD3 expression at day 2 post differentiation induction, but by day 4, the myoblasts had normal levels of PLD3 expression (3.23 C).

With very little success with DNA-based RNAi knockdown, due to what was believed to be compensatory mechanisms within the cells that were constantly expressing the RNAi plasmids, it was decided to employ the use of 3 siRNA oligos designed and produced by Invitrogen (see chart 2.2). Preliminary results were very impressive and coincided with the preliminary results from the DNA-based methods. Compared to the cells treated with luciferase targeted oligos and the siGlo transfection control, cells treated with oligos 2 and 3 against PLD3, showed a decrease in fusion and an increase in cell death, especially cells treated with oligo 2 (figure 3.24). However, upon western blot analysis of PLD3 expression, PLD 3 did not seem to be knocked down in cells treated with oligos 2 and 3. Based on western blot analysis, the cells expressing oligos 2 and 3 had the highest amount of PLD3 protein compared to the luciferase and siGlo controls (figure 3.25). To determine if the results were based on abnormal activation of the unfolded protein response (UPR) in myoblasts with forced, lowered PLD3 expression, differentiating myoblasts transfected with the siRNA oligos were

analyzed by western blot analysis for Bip expression. The resulting western blot showed that were no significant differences in the expression of Bip (figure 3.26 A), which increases during ER-stress (*61*); suggesting, there was no difference in the activation of the UPR between the control cells and the presumptive PLD3 knockdown cells. To further explore this, and make sure there were no differences in the activation of the UPR, I decided to use the reporter gene 5X ATF6-Luc. To do this, C2C12 cells were transfected with 100nM siRNA oligos along with 0.5μg 5X ATF6-Luc, 0.5μg β-galactosidase (transfection control for luciferase normalization) and 1μg EYFPN-1 (visual transfection monitor). After transfection, the cells were allowed to differentiate for 3 days. The lysates were then collected and processed for β-galactosidase and luciferase activity using the dual lights detection kit (Applied Biosystems). As with Bip, there were no differences in the activation of the ATF6 compared to the control (figure 3.19); suggesting that treatment of differentiation myoblasts with PLD3 targeted oligos does not alter the activation of the UPR (figure 3.26 B). However, it is unknown why the myoblasts treated with oligo 2 and 3 showed an increase in both PLD3 and cell death during differentiation.

3.6.3 Discussion:

I was not able to successfully knockdown and sustain decreased expression of PLD3. Attempts to knockdown PLD3 expression by RNAi led to no change in PLD3 to elevated expression of PLD3. It is very possible for PLD3

expression to be vital for differentiation and therefore, when the sh, mi or siRNA sequences were expressed in differentiating cells, a response to increase PLD3 expression, overwhelming the RNAi sequences and machinery, occurred as seen in figure 3.23C where by D3 post differentiation induction miR-1 and miR-2 were able to knockdown PLD3 expression, but by D6 the cells recovered full PLD3 expression. This is further supported by a report claiming that differentiating myoblasts have decreased dicer expression and activity during myogenesis (*62*).

While the use of RNAi has evolved incredibly in the past few years, it is still not a perfect science. Picking sequences that will knockdown a particular gene of interest without off-target effects is still a challenge. With that, it is possible that the siRNA oligos 2 and 3, which showed the most dramatic phenotype with an increase in PLD3 protein expression, have off-target effects that may have lead to both the increase in PLD3 expression and the elevated levels of cell death with differentiation. However, it is cleat that the increased cell death is not due to an increase in the activation of the UPR.

Figure 3. 1 PLD3 expression increases during myogenic differentiation.

A. C2C12 cells were induced to differentiate and RNA extracts collected for the above indicated times. Equal amounts of RNA were used as a template in quantitative RT-PCR with PLD3 and GAPDH specific primers used for amplification. The amount of PLD3 mRNA was normalized to GAPDH levels. (N=3) **B.** C2C12 cells were induced to differentiate for the indicated days and whole cell lysates were collected. Equal amounts of protein from the whole cell lysates, as determined by Bradford reagent, were loaded onto a SDS-polyarylamide gel, with the subsequent blot probed with anti-PLD3 and anti-GAPDH antibodies. Representative blot from 3 independent experments.

A.

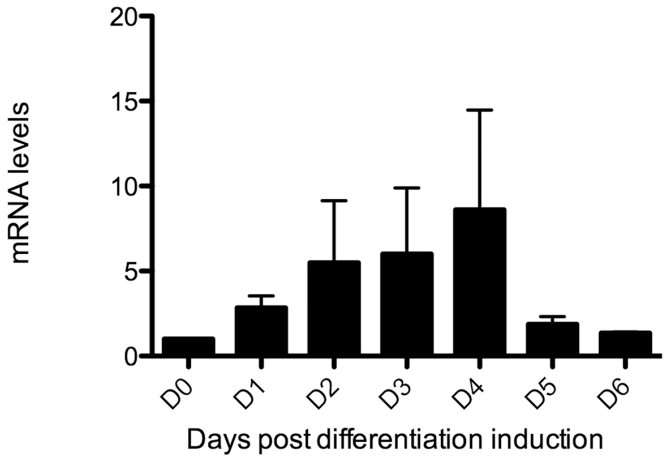
20
15
10
5
0
mRNA levels
D0
D1
D2
D3
D4
D5
D6
Days post differentiation induction

B.

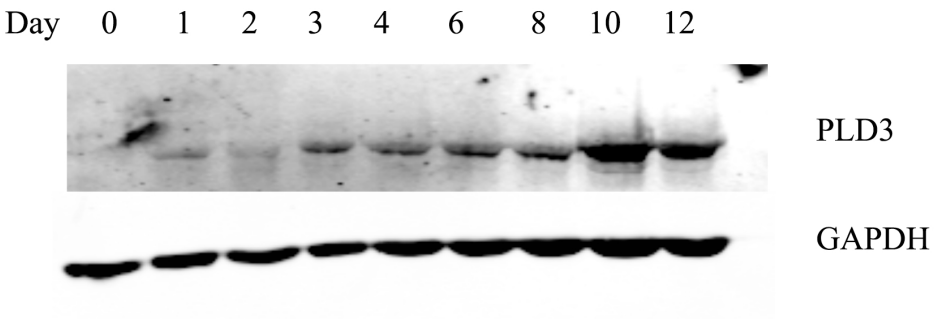
Day 0 1 2 3 4 6 8 10 12
PLD3
GAPDH

Figure 3. 2 PLD3 localizes to the endoplasmic reticulum in proliferating C2C12 myoblasts.

C2C12 cells were transfected with huPLD3-myc, followed by indirect immunofluorescence staining with calreticulin and myc antibodies to detect the endoplasmic reticulum and PLD3, respectively. Scale bar represents 10μm. Representative images from 3 independent experiments.

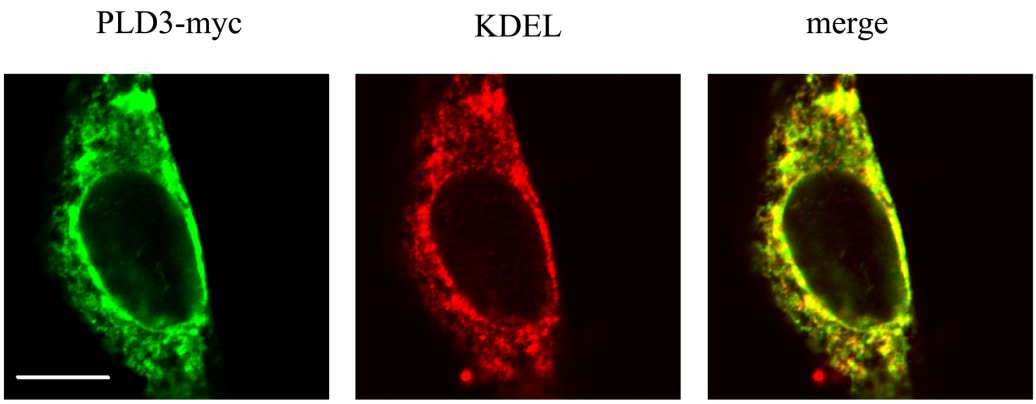
PLD3-myc
KDEL
merge

Figure 3. 3 The transmembrane domain controls PLD3 localization in proliferating cells.

A. Cartoon schematic of deletion mutants. C2C12 cells transfected with **B.** PLD3-Δ1-60-myc, **C.** PLD3-Δ37-60-myc or **D.** mito-tagged PLD3-Δ1-37 myc were fixed and stained by indirect immunofluorescence with anti-myc and ant-KDEL antibodies and visualized with a Zeiss LSM 510 confocal microscope. B-D are representative images from 3 independent experiments. Scale bar represent 10μm.

A.

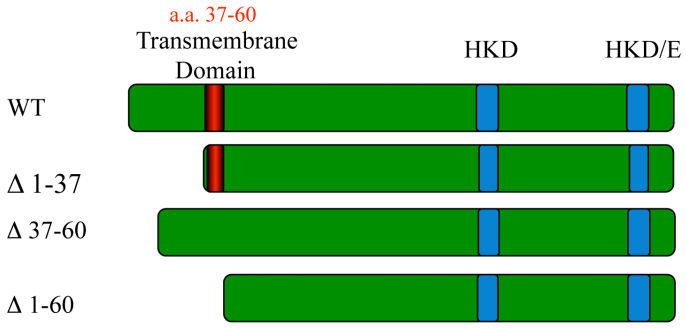
a.a. 37-60
Transmembrane Domain
HKD
HKD/E
WT
Δ 1-37
Δ 37-60
Δ 1-60

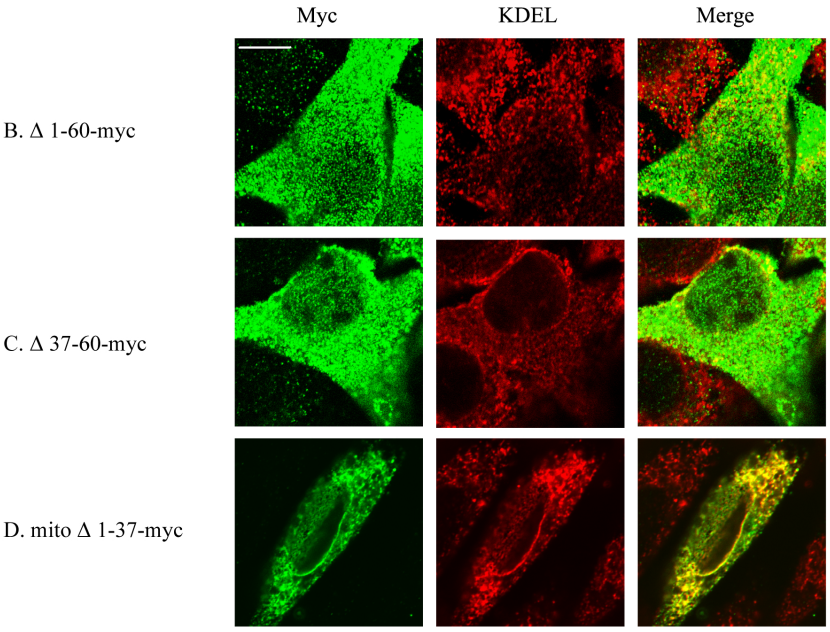
Myc
KDEL
Merge
B. Δ 1-60-myc
C. Δ 37-60-myc
D. mito Δ 1-37-myc

Figure 3. 4 The transmembrane of PLD3 is the minimal element required for PLD3 localization.

NIH 3T3 cells transfected with PLD3 **A.** 1-37-GFP, **B.** PLD3-1-60-YFP, or **C.** PLD3-37-60-YFP were fixed, stained by indirect immunofluorescence with anti-KDEL antibodies and visualized with a Zeiss LSM 510 Meta confocal microscope. All images are representative images from 3 independent experiments. Scale bar represent 10μm.

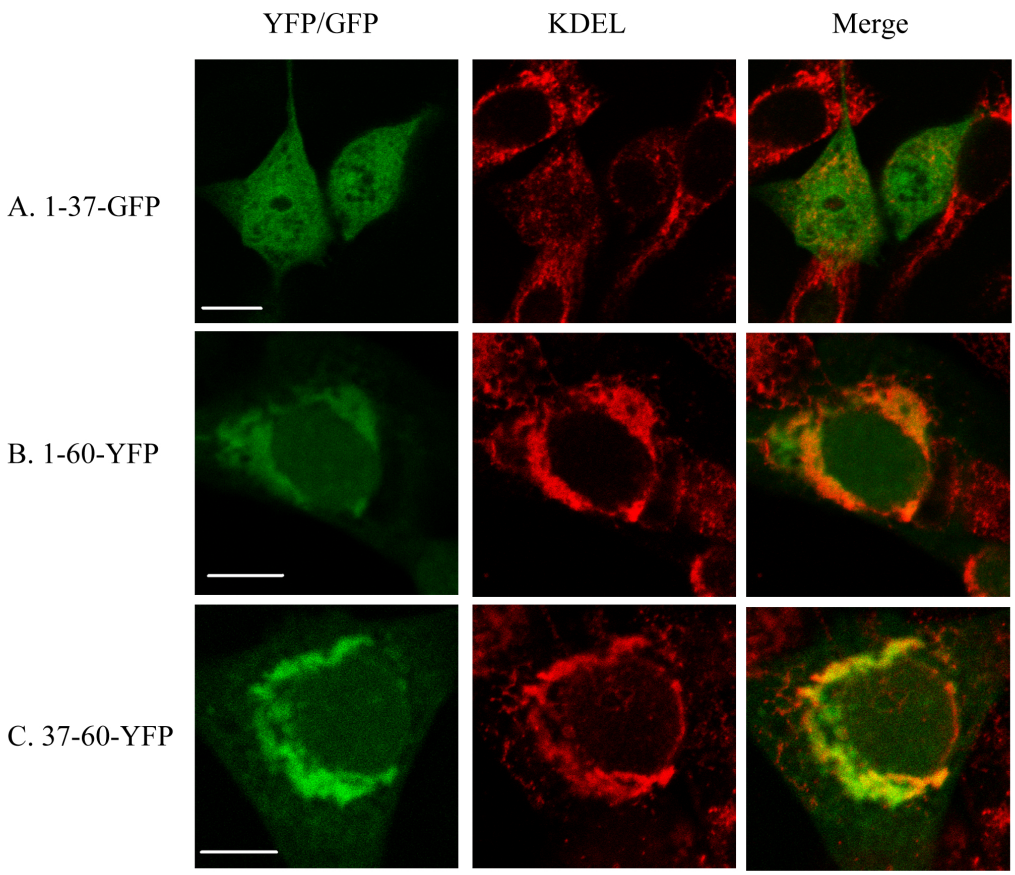
YFP/GFP
KDEL
Merge
A. 1-37-GFP
B. 1-60-YFP
C. 37-60-YFP

Figure 3. 5 Removal of the PLD3 transmembrane domain leads to a decrease in ER-staining.

Cos7 cells were transfected with **A.** Δ37-60 WT, **B.** Δ37-60 K418R, or **C.** Δ1-60 WT and stained by indirect immunofluorescence with anti-myc, anti-KDEL or **D.** anti-GM130 antibodies and visualized by confocal microscopy using a Zeiss 510 Meta confocal microscope. All images are representative images of 3 independent experiments. Scale bar represent 10μm.

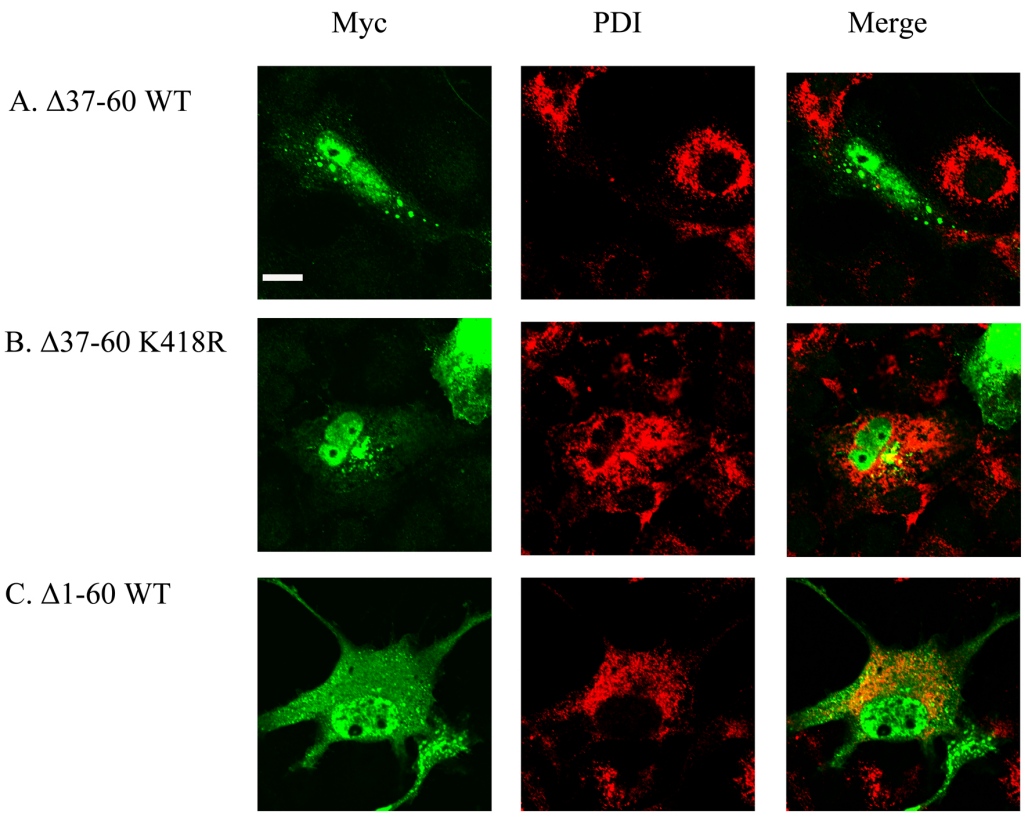
Myc
PDI
Merge
A. Δ37-60 WT
B. Δ37-60 K418R
C. Δ1-60 WT

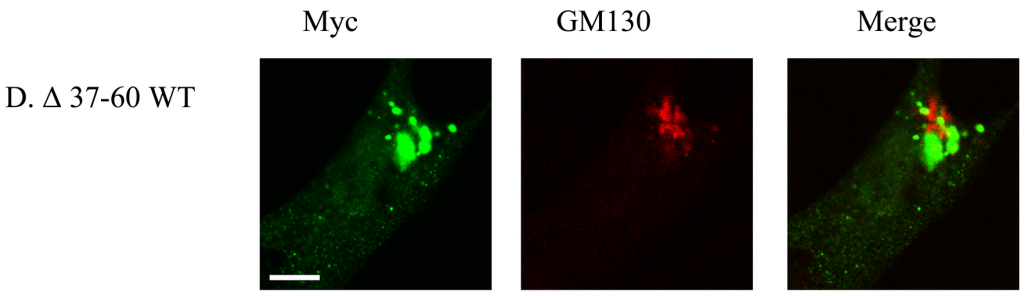
Myc
GM130
Merge
D. Δ 37-60 WT

Figure 3. 6 PLD3 does not localize to the endoplasmic reticulum in differentiating myotubes.

C2C12 myoblasts were induced to differentiate for 5 days and treated with **A.** DMSO or **B.** BFA for one hour. The cells were then fixed and stained by indirect immunoflourescent staining with anti-PLD3 and anti-KDEL antibodies. The cells were then visualized using a Zeiss LSM 510 Meta confocal microscope. Images are representative images of 3 independent experiments. Scale bar represent 10μm.

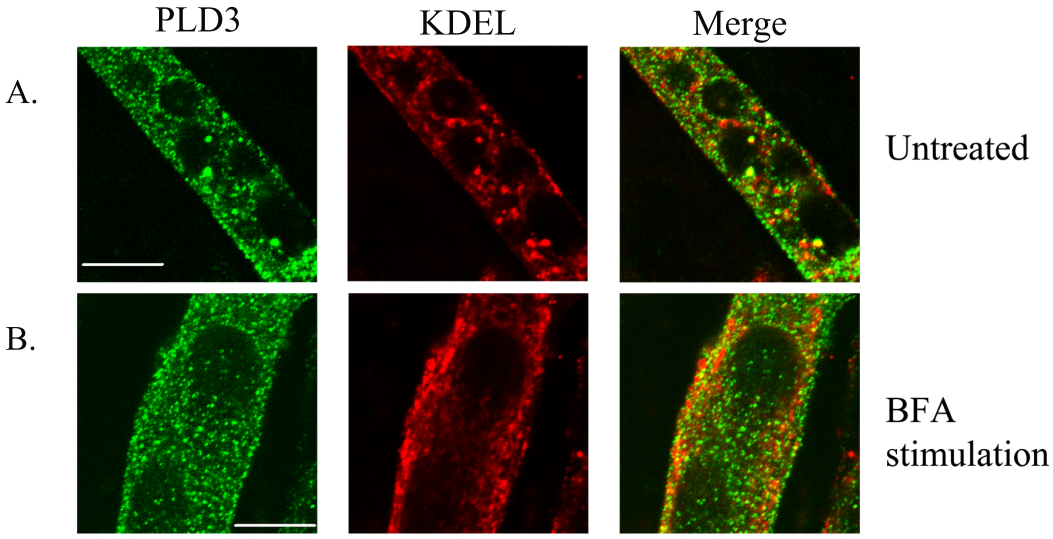
PLD3
KDEL
Merge
A.
Untreated
B.
BFA
stimulation

Figure 3. 7 PLD3 does not localize to the endoplasmic reticulum in differentiating in differentiating PC12 cells.

PC12 cells were induced to differentiate for 7 days. **A**. Whole cell lysates were collected on days 0,1,3,5, and 7 for western blot analysis for PLD3 expression, probing the subsequent blot with anti-PLD3 and anti-GAPDH antibodies. **B.** D4 cells were fixes and stained by indirect immunofluorescence using anti-PLD3 and anti-KDEL antibodies. Images are representative images of 3 independent experiments. Scale bar represent 20μm.

A.

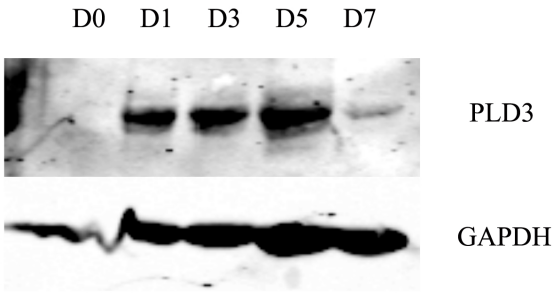

B.

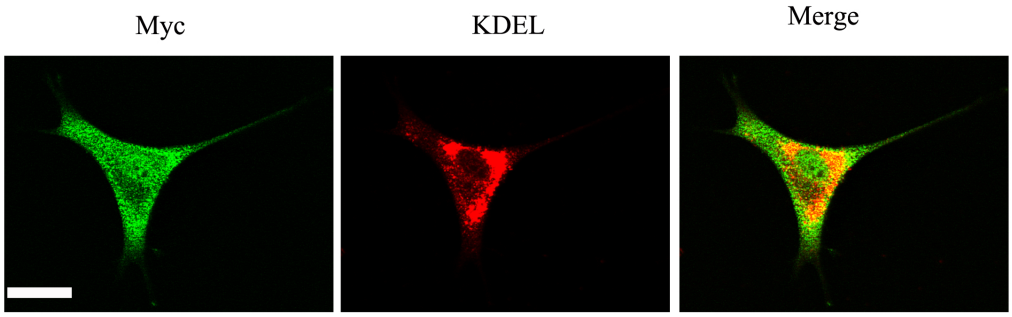

Figure 3. 8 PLD3 localizes to unknown vesicles in differentiating myotubes.

C2C12 myoblasts expressing either ER-mcherry or PLD3-myc were induced to differentiate for 6 days on gelatin-coated coverslips. Following differentiation, the cells were fixed and stained with anti-PLD3 and **A.** anti-cav3, **B.** anti-Rab27 **C.** 488 transferrin, **D.** anti-cytochrome c **E.** anti-Gm130 **F.** anti-LC3 A/B and **G.** anti-pmp70. The cells were visualized on a Zeiss LSM510 confocal microscope. All images are representative images of 3 independent experiments. Scale bar represent 10μm.

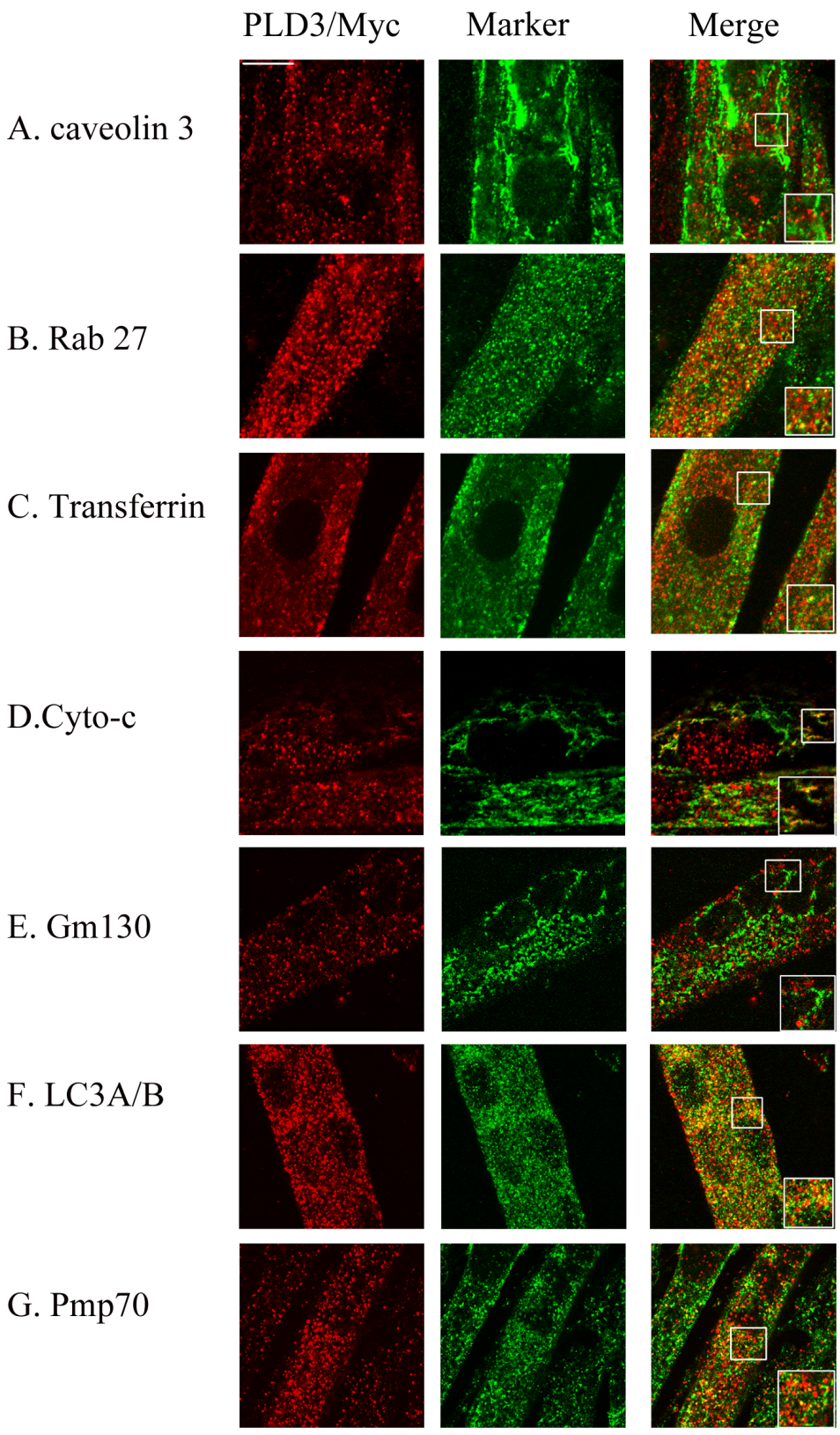
PLD3/Myc
Marker
Merge
A. caveolin 3
B. Rab 27
C. Transferrin
D.Cyto-c
E. Gm130
F. LC3A/B
G. Pmp70

Figure 3. 9 PLD3 is EndoH resistant in differentiating myotubes.

Whole cell lysates were extracted from differentiating myotubes and treated with EndoH or PNGaseF for 2 hours. The treated lysates were loaded onto a SDS-polyacrylamide gel, with the subsequent blot probed with anti-PLD3 and anti-GAPDH antibodies. Representative blot from 3 independent experiments.

ER-mcherry	+	+	+	-	-	-
PLD3 myc	-	-	-	+	+	+
untreated	+	-	-	+	-	-
Endo H	-	+	-	-	+	-
PNGaseF	-	-	+	-	-	+

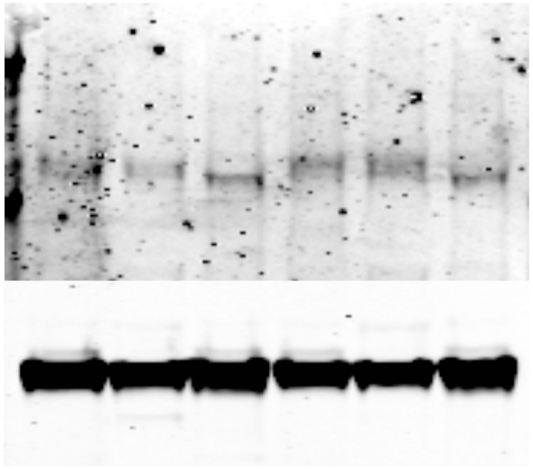

PLD3

GAPDH

Figure 3. 10 Tharpsigargin increases PLD3/ endoplasmic reticulum co-localization in differentiating myotubes.

PLD3-myc overexpressing myoblasts were differentiated for 6 days following incubation for 4 hours in **A.** DMSO, **B.** Brefeldin A, **C.** Tunicamycin, **D.** Tharpsigargin, **E.** Amphotericin B, or **F.** wortmanin. After the incubation, the cells were then stained by indirect immunofluorescence with anti-myc and anti-KDEL antibodies and visualized with a Zeiss LSM 510 Meta confocal microscope. Scale bar represent 10 μm. .

.

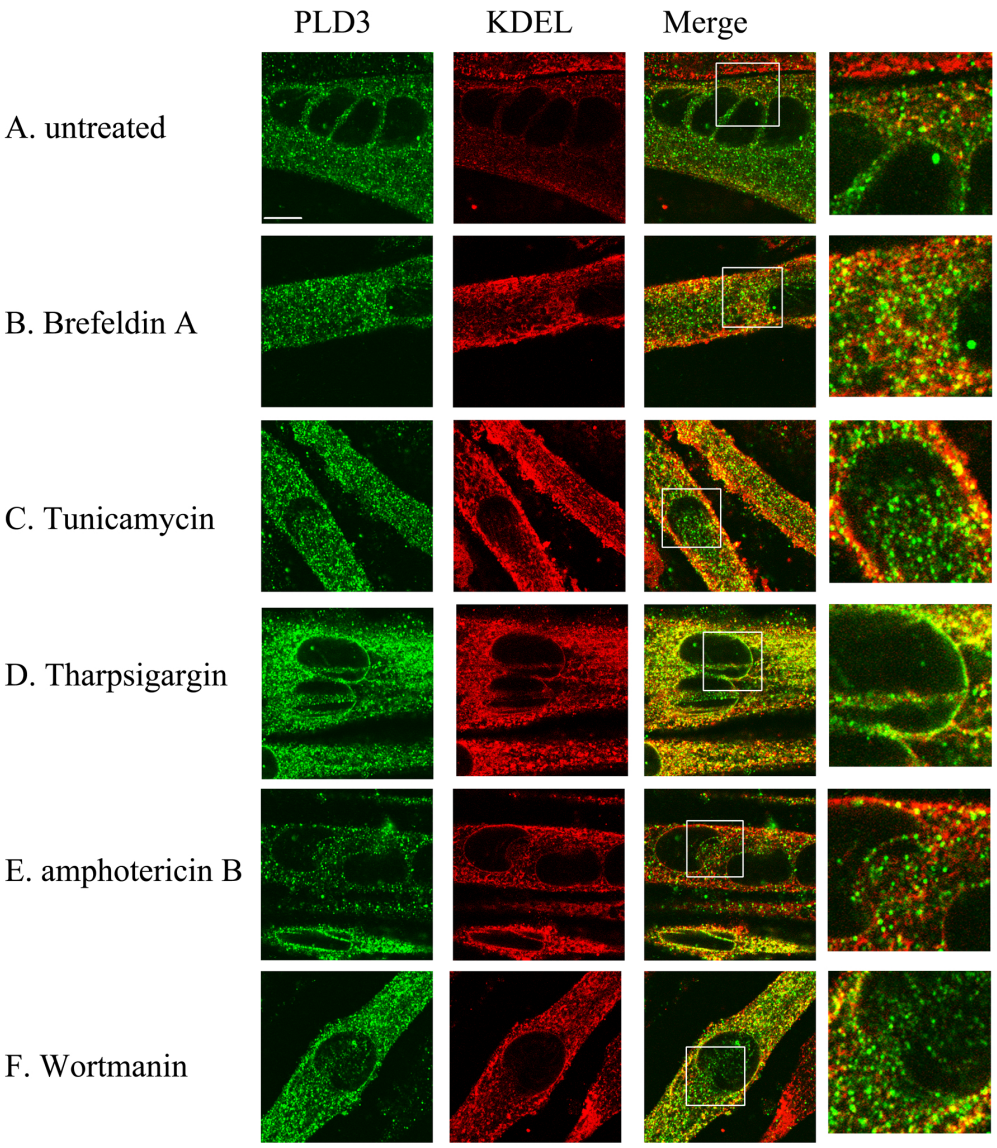
PLD3
KDEL
Merge
A. untreated
B. Brefeldin A
C. Tunicamycin
D. Tharpsigargin
E. amphotericin B
F. Wortmanin

Figure 3. 11 Overexpression of PLD3 promotes myotube formation.

A. C2C12 cells expressing PLD-myc, huPLD3-K418R-myc or ER-mcherry were induced to differentiate for 6 days on gelatin-coated coverslips. On the indicated days the cells were fixed in methanol at -20C, followed by giemsa dye staining. Images are representative images of 3 independent experiments. Scale bar represents 200 μm. **B.** Total fusion index analysis of differentiating C2C12 myoblasts expressing PLD-myc, huPLD3-K418R-myc or ER-mcherry, representing the number of nuclei in myotubes with 3 or more nuclei divided by the total number of nuclei in a field. Five fields were chosen at random for cell and nuclei counting. * represents $P< 0.05$ value as determined by one-way anova and Tukey post test from 3 independent experiments.

A.

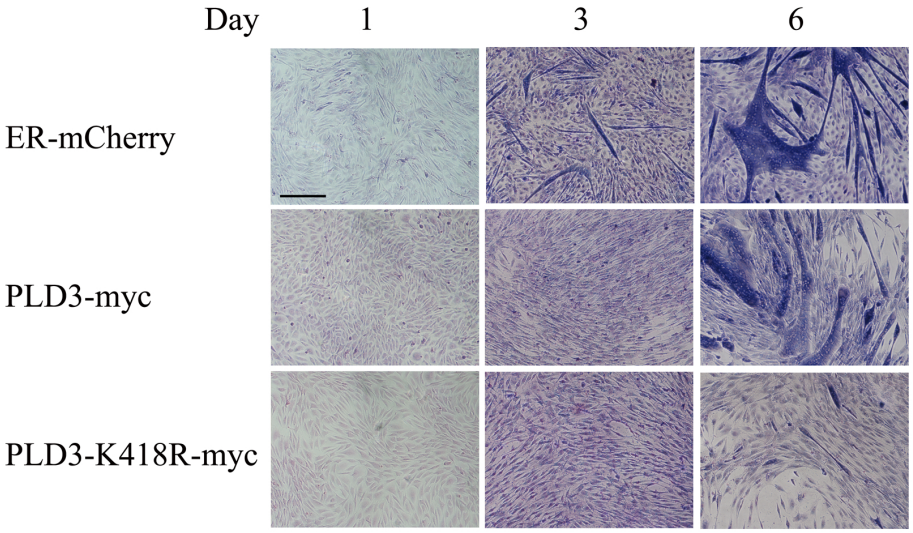
Day
1
3
6
ER-mCherry
PLD3-myc
PLD3-K418R-myc

B.

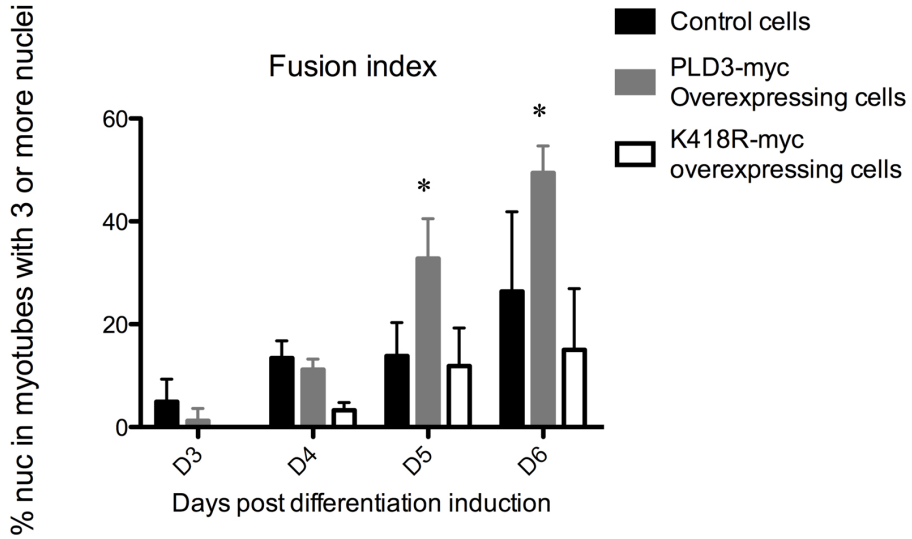
Fusion index
% nuc in myotubes with 3 or more nuclei
60
40
20
0
D3
D4
D5
D6
Days post differentiation induction
*
*
Control cells
PLD3-myc
Overexpressing cells
K418R-myc
overexpressing cells

Figure 3. 12 Overexpression of PLD3 does not increase nuclear incorporation into differentiating myotubes.

Fusion index representing the percentage of nuclei in myotubes with 3-10, 11-20, or >20 nuclei in A D5 myotubes and B. D6 myotubes. (N=3)

A.

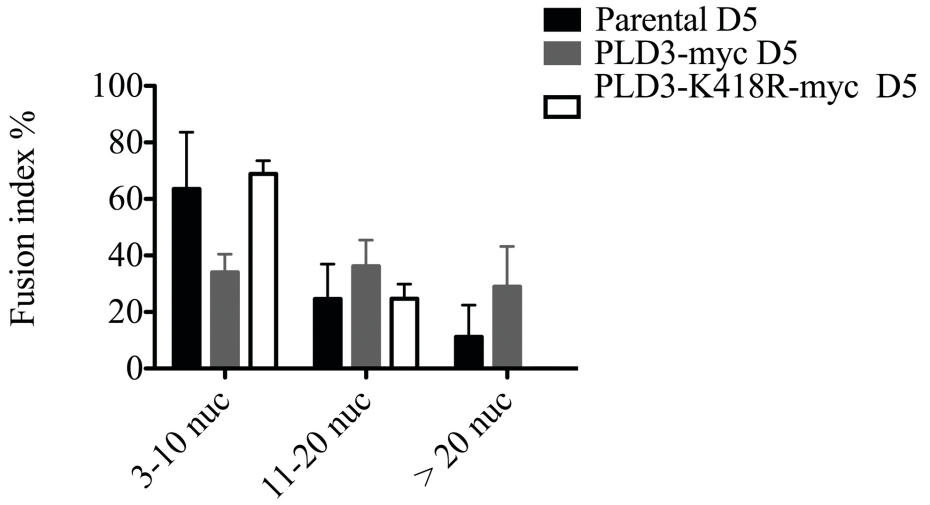
Parental D5
PLD3-myc D5
PLD3-K418R-myc D5
Fusion index %
100
80
60
40
20
0
3-10 nuc
11-20 nuc
> 20 nuc

B.

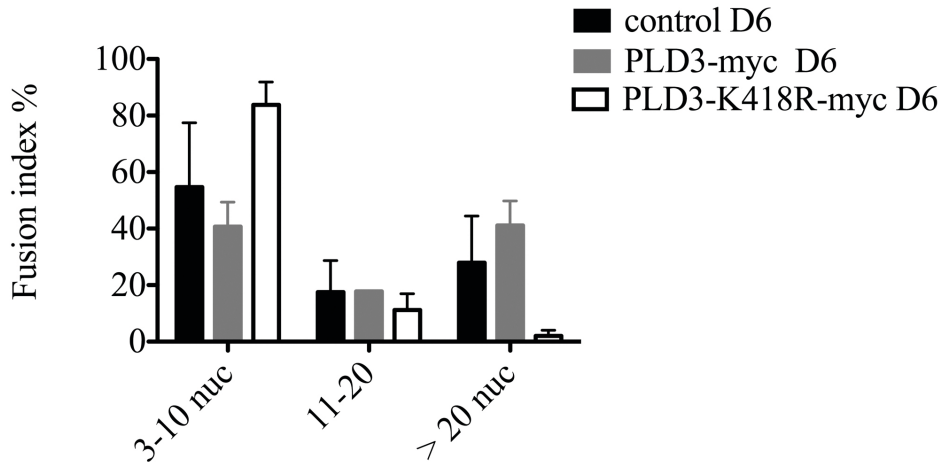
control D6
PLD3-myc D6
PLD3-K418R-myc D6
Fusion index %
100
80
60
40
20
0
3-10 nuc
11-20
> 20 nuc

Figure 3. 13 Overexpression of PLD3 increases fusion in Sol 8 myoblasts.

A. Brightfield image of Sol 8 myoblasts expressing PLD3-myc, PLD3-K418R-myc or ER-mcherry were induced to differentiate for 6 days. Images are representative images from 3 independent experiments. Scale bar represents 200μm. **B.** Fusion index of sol 8 myoblasts expressing huPLD3-myc, huPLD3-K418R-myc or ER-mchery, representing the number of nuclei in myotubes with 3 or more nuclei divided by the total number of nuclei in a field. Ten fields were chosen at random for cell and nuclei counting. (N= 3)

A.

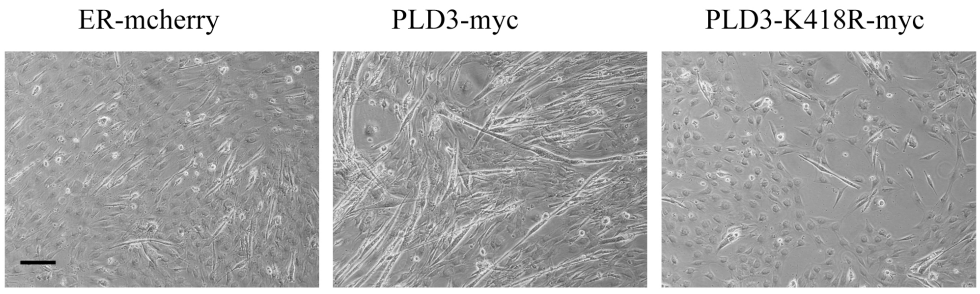
ER-mcherry
PLD3-myc
PLD3-K418R-myc

B.

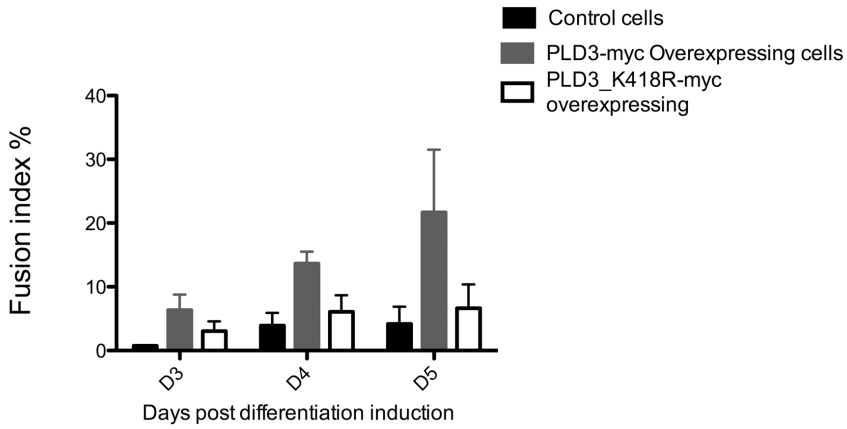
Control cells
PLD3-myc Overexpressing cells
PLD3_K418R-myc overexpressing
Fusion index %
40
30
20
10
0
D3
D4
D5
Days post differentiation induction

Figure 3. 14 Overexpression of PLD3 does not alter the expression of myogenic or fusion related markers during myotube differentiation.

C2C12 cells were induced to differentiate for the indicated days and whole cell lysates were collected. Equal amounts of protein from the whole cell lysates, as determined by Bradford reagent, were loaded onto a SDS-polyacrylamide gel, with the subsequent blot probed with **A.** anti-MHC, anti-CSQ and anti-GAPDH antibodies or **B.** anti-calpain-1 and anti m-cadherin antibodies. Representative blots from 3 independent experiments.

A.

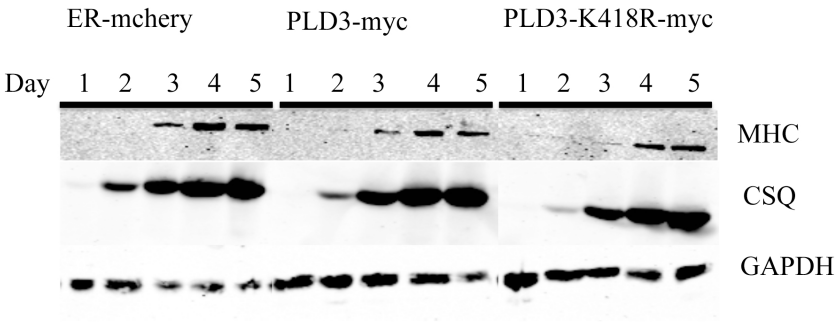
ER-mchery
PLD3-myc
PLD3-K418R-myc
Day 1 2 3 4 5 1 2 3 4 5 1 2 3 4 5
MHC
CSQ
GAPDH

B.

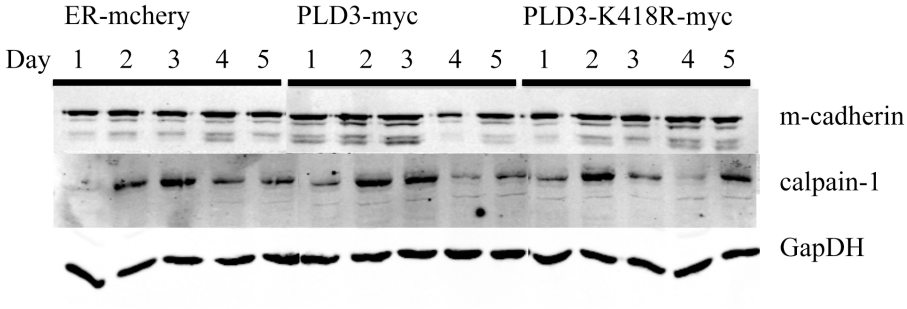
ER-mchery
PLD3-myc
PLD3-K418R-myc
Day 1 2 3 4 5 1 2 3 4 5 1 2 3 4 5
m-cadherin
calpain-1
GapDH

Figure 3. 15 Conditioned media analysis of myoblasts overexpressing ER-mcherry, PLD3-myc and PLD3-K418R-myc.

C2C12 myoblasts overexpressing ER-mcherry, PLD3-myc and PLD3-K418R-myc were induced to differentiate for 4 days in PM followed by 2 days in DMEM supplemented with ITS media supplement for 2 days. The 2 day conditioned media was then collected and concentrated. Proteins from the concentrated media were then resolved on a 4-20% SDS-PAGE gel that was stained with Coomassie dye after electrophoresis. Representative blot from 3 independent experiments. Arrows indicates proteins bands that are potentially different between the three cell populations.

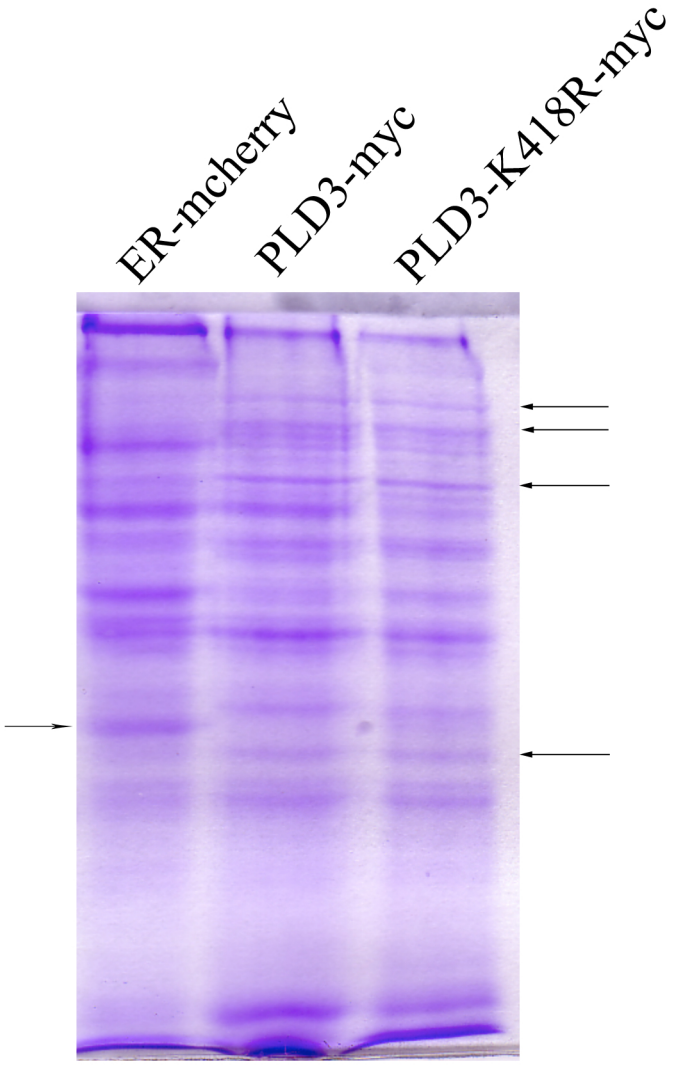
ER-mcherry
PLD3-myc
PLD3-K418R-myc

Figure 3. 16 Co-immunoprecipitation of PLD3-myc.

C2C12 myoblasts overexpressing ER-mcherry, PLD3-myc and PLD3-K418R-myc were induced to differentiate for 5 days, following which the cells were lysed and the lysates incubated with anti-myc antibodies conjugated to agarose beads overnight. After the overnight incubation, the beads were then spun out of solution, washed and bound proteins eluted using a low pH elution buffer. The eluted proteins were then loaded onto a SDS-PAGE gel, with the subsequent blot probed by anti-myc antibodies. Representative blot from 3 independent experiments.

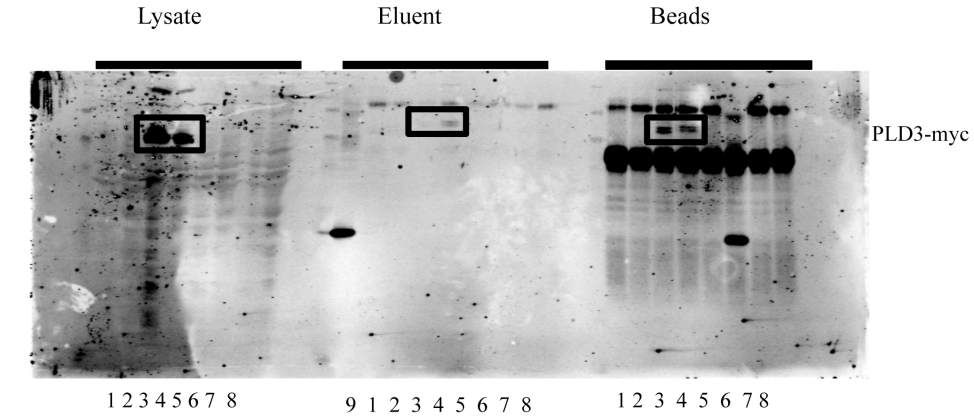

1. Parental D0	5. K418R D0	9. Myc positive control
2. Parental D6	6. K418R D6	
3. K4 D0	7. Non differentiate D0	
4. K4 D6	8. Non differentiate D6	

Figure 3. 17 PLD3-myc overexpressing myoblast improves the fusion efficiency of myoblasts not overexpressing PLD3-myc.

C2C12 myoblasts expressing ER-mcherry, PLD3-myc and PLD3-K418R-myc and either the 50ω or 410α fragments of β-gal were induced to differentiate for 5 days. Lysates for the differentiating pairs of myoblasts for **A.** homotypic fusion, **B.** ER-mcherry heterotypic fusion and **C.** PLD3-myc/ PLD3-K41R-myc heterotypic fusion were then collected and analyzed for β-gal activity. (N = 3)

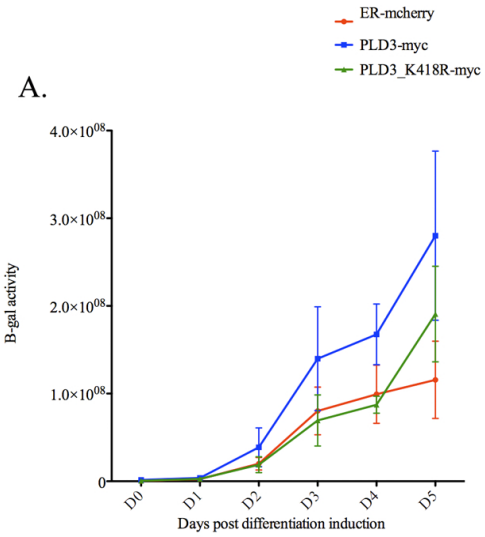
A.
ER-mcherry
PLD3-myc
PLD3_K418R-myc
B-gal activity
4.0×10^08
3.0×10^08
2.0×10^08
1.0×10^08
0
D0
D1
D2
D3
D4
D5
Days post differentiation induction

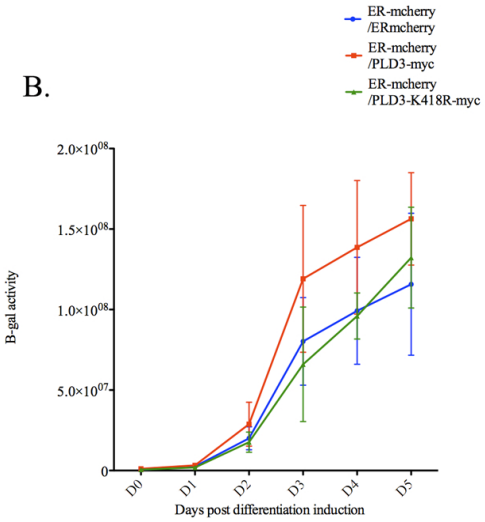
B.
ER-mcherry /ERmcherry
ER-mcherry /PLD3-myc
ER-mcherry /PLD3-K418R-myc
B-gal activity
2.0×10^08
1.5×10^08
1.0×10^08
5.0×10^07
0
D0
D1
D2
D3
D4
D5
Days post differentiation induction

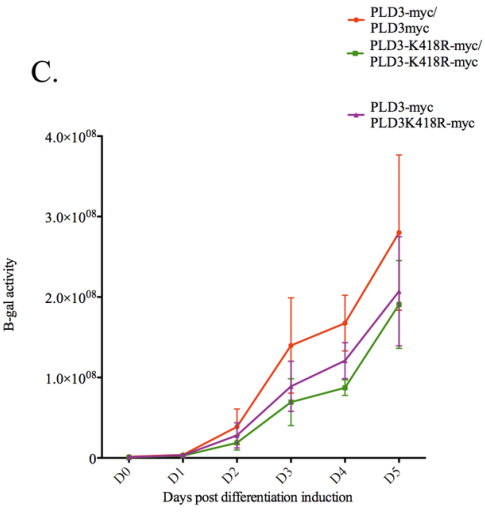
C.
PLD3-myc/ PLD3myc
PLD3-K418R-myc/ PLD3-K418R-myc
PLD3-myc PLD3K418R-myc
B-gal activity
4.0×10^08
3.0×10^08
2.0×10^08
1.0×10^08
0
D0
D1
D2
D3
D4
D5
Days post differentiation induction

Figure 3. 18 Transient ER-stress increases PLD3 expression during myogenesis.

C2C12 myoblasts were treated with TG, TN, BFA, or DMSO in complete media for 30 min. The cells were then washed with PBS and the placed in differentiation media to induce myogenic differentiation for the indicated days. Whole cell lysates were collected from the induced cells. Equal amounts of protein from the whole cell lysates, as determined by Bradford reagent, were loaded onto a SDS-polyacrylamide gel, with the subsequent blot probed with anti-PLD3 and anti-GAPDH antibodies. Representative blot from 3 independent experiments.

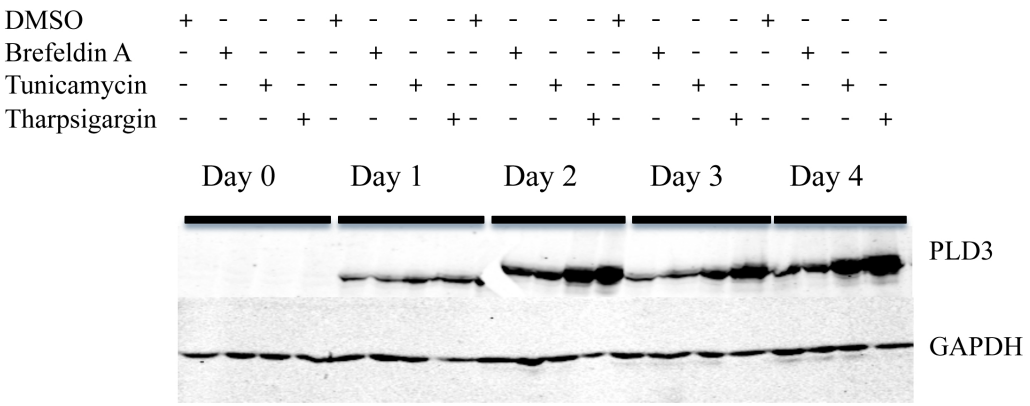
DMSO + - - - + - - - + - - - + - - - + - - -
Brefeldin A - + - - - + - - - + - - - + - - - + - -
Tunicamycin - - + - - - + - - - + - - - + - - - + -
Tharpsigargin - - - + - - - + - - - + - - - + - - - +
Day 0
Day 1
Day 2
Day 3
Day 4
PLD3
GAPDH

Figure 3. 19 The combined effects of transient ER-stress and differentiation induces PLD3 expression.

A. C2C12 cells were treated with BFA, TN or TG for 4,8 or 24 hours without differentiation induction in PM. **B.** HeLa cells were treated with TN for 30 min followed by incubation in DM for 0-3 days or treated with TN in PM for 24 or 48 hours. Whole cell lysates were collected from the treated cells and analyzed by western blot analysis with anti-PLD3 and anti-GAPDH antibodies. Representative blot from 3 independent experiments.

A.

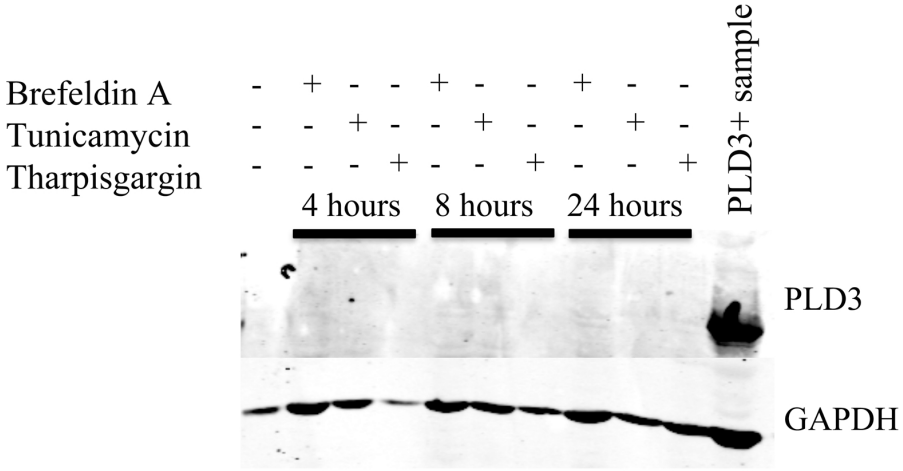
Brefeldin A
Tunicamycin
Tharpisgargin
- + - - + - - + - -
- - + - - + - - + -
- - - + - - + - - +
4 hours
8 hours
24 hours
PLD3+ sample
PLD3
GAPDH

B.

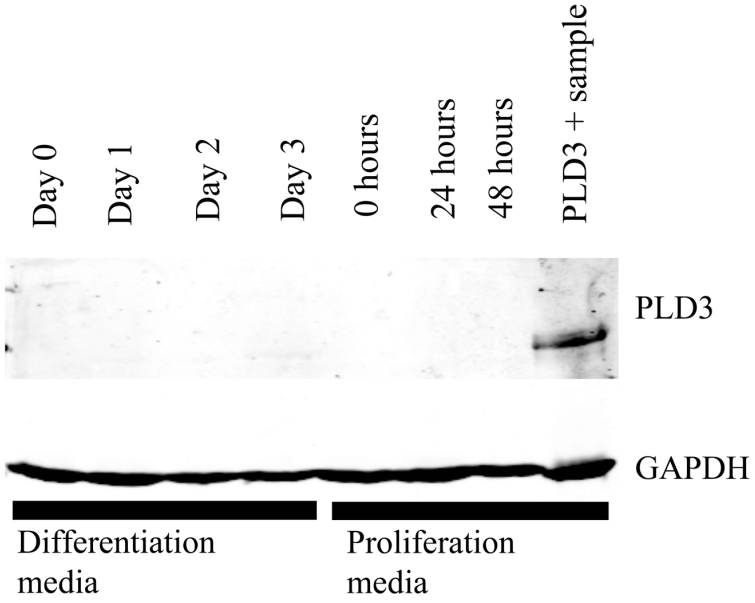
Day 0
Day 1
Day 2
Day 3
0 hours
24 hours
48 hours
PLD3 + sample
PLD3
GAPDH
Differentiation media
Proliferation media

Figure 3. 20 Oxidative stress may regulate PLD3 induction.

C2C12 myoblasts were treated with **A.** DMSO,TN, TN + ascorbic acid, TG, TG+ ascorbic acid, ascorbic acid only, DTT, calcium ionophore or calcium ionophore + DTT or **B.** DMSO,TG or TG and L-canavanine in complete media for 30 min. The cells were then washed with PBS and the placed in differentiation media to induce myogenic differentiation for the indicated days. Whole cell lysates were collected from the induced cells. Equal amounts of protein from the whole cell lysates, as determined by Bradford reagent, were loaded onto a SDS-polyacrylamide gel, with the subsequent blot probed with anti-PLD3 and anti-GAPDH antibodies PLD3 expression was determined by semi-quantitative analysis of PLD3 and GAPDH protein band density readings. Blots are representative of 3 independent experiments.

A.

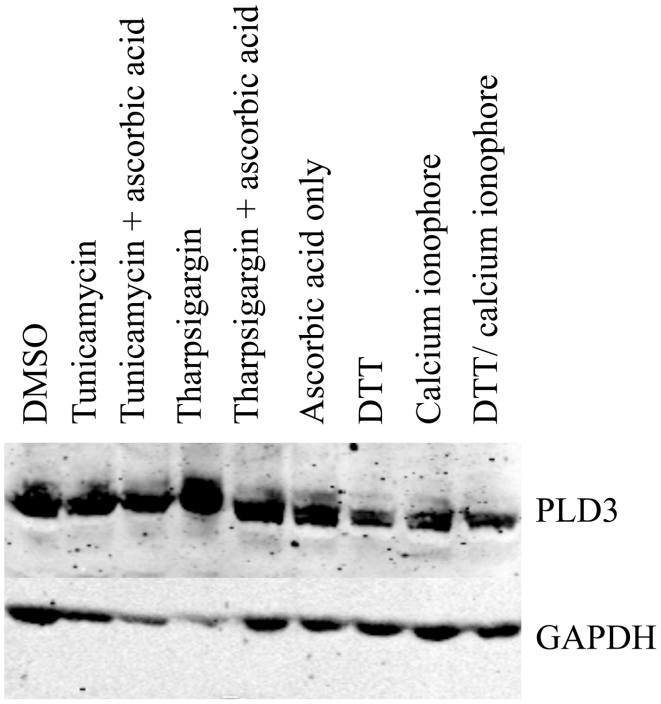

B.

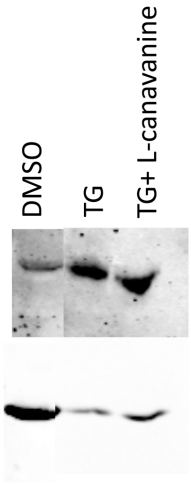

Treatment	Fold change
DMSO	O
TG only	93.5
TG+ Lcanavanine	43.9

Figure 3. 21 PLD3 overexpression does not alter UPR activation in differentiating myotubes.

C2C12 myoblasts overexpressing ER-mcherry, PLD3-myc or PLD3-K418R-myc were transfected with Lac-z and reporter gene 5X-ATF6-Luc at D-1. On D0 the cells were induced to differentiate for three days. Whole cell lysates were collected form the differentiating cells and analyzed for Luciferase and β-gal activity. (N = 3)

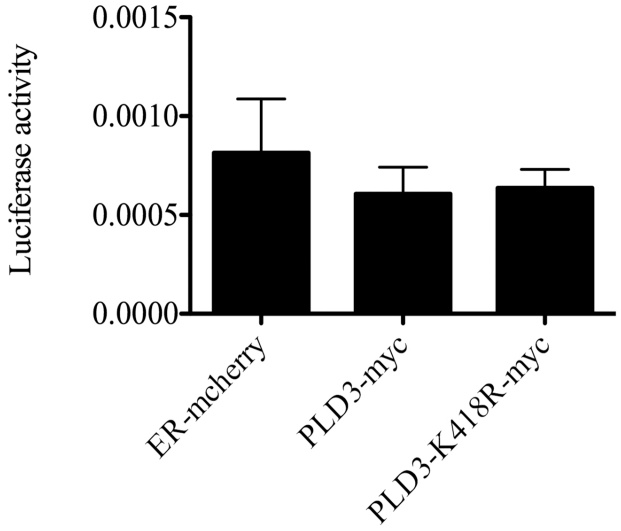

3 days post differentiation induction

Figure 3. 22 PLD3 knockdown with shRNA plasmids

A. C2C12 myoblasts stably expressing shRNA plasmids against PLD3 or luciferase were transiently transfected with PLD3-GFP. The cells were then lysed and analyzed for PLD3-GFP expression by western blot analysis using anti-GFP and anti-GAPDH antibodies. C2C12 stably expressing shRNA plasmids against PLD3 or luciferase were induced to differentiate for 4 days. **B.** C2C12 cells stably expressing shRNA plasmids against PLD3 were differentiated for 8 days and imaged by brightfield microscopy. Scale bar represents 200μm. **C.** Whole cell lysates from differentiating myoblasts stably expressing shRNA plasmids against PLD3 were analyzed by western blot using anti-PLD3 and anti-GAPDH antibodies. All images and blots are representative of 3 independent experiments.

A.

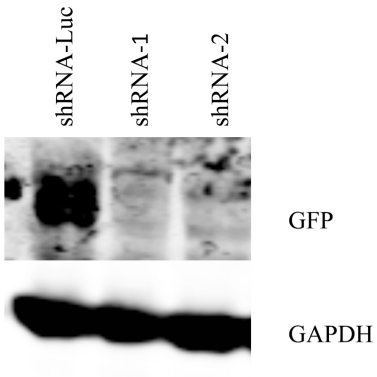
shRNA-Luc
shRNA-1
shRNA-2
GFP
GAPDH

B.

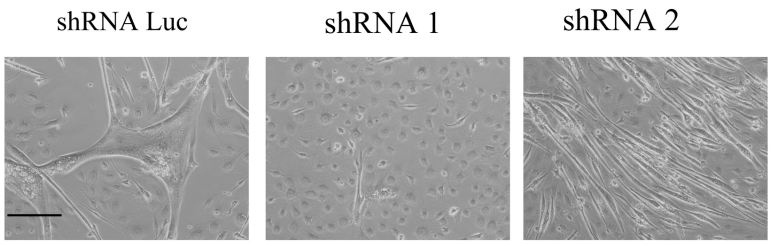
shRNA Luc
shRNA 1
shRNA 2

C.

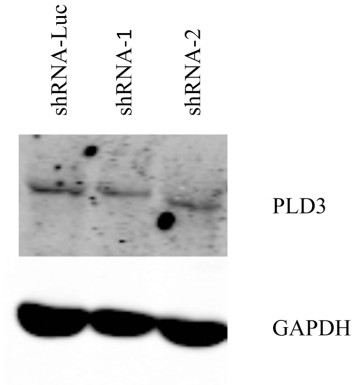
shRNA-Luc
shRNA-1
shRNA-2
PLD3
GAPDH

Figure 3. 23 PLD3 knockdown with miR plasmids

C2C12 myoblasts stably expressing miRNA plasmids against PLD3 or luciferase were induced to differentiate for 4 days. The cells **A–B.** were imaged by brightfield microscopy and **C.** whole cell lysates were analyzed by western blot using anti-PLD3 and anti-GAPDH antibodies. Images and blots are representative of 3 independent experiments.

A.

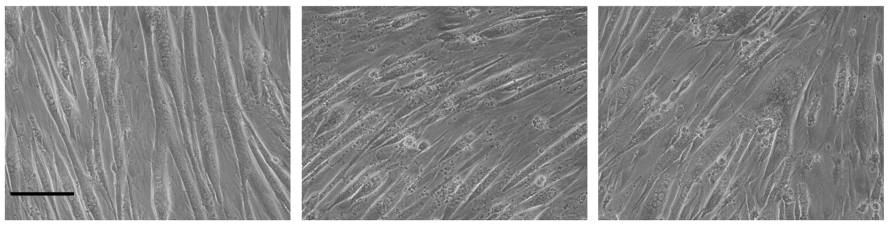

miRNA Luc miRNA 1 miRNA 2

B.

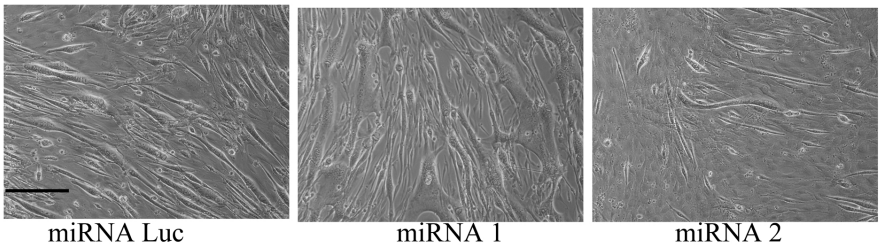

miRNA Luc miRNA 1 miRNA 2

C.

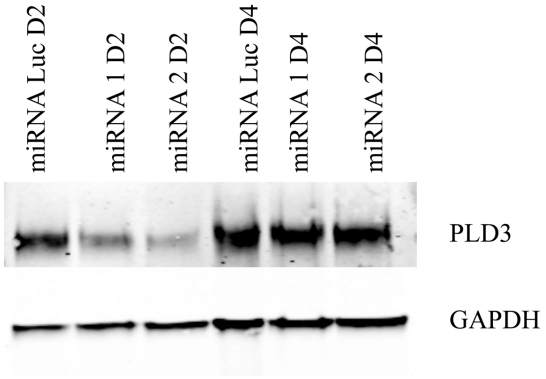

Figure 3. 24 PLD3 knockdown with siRNA oligos

C2C12 myoblasts transfected with siRNA oligos against PLD3, luciferase or siGlo transfection control were induced to differentiate for 5 days and imaged by brightfield microscopy on days 3 and 5. Representative images from 3 independent experiments. Scale bar represents 200μm.

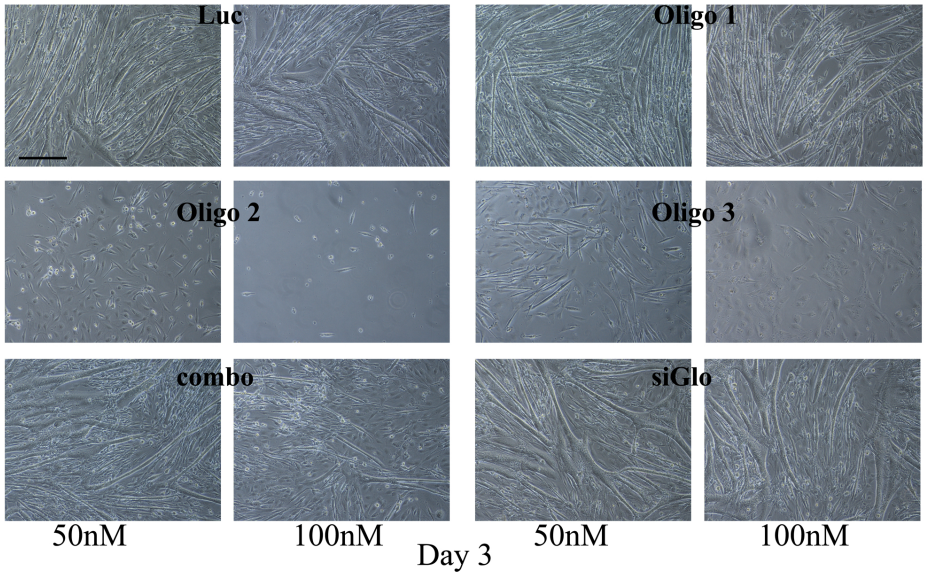
Luc
Oligo 1
Oligo 2
Oligo 3
combo
siGlo
50nM
100nM
50nM
100nM
Day 3

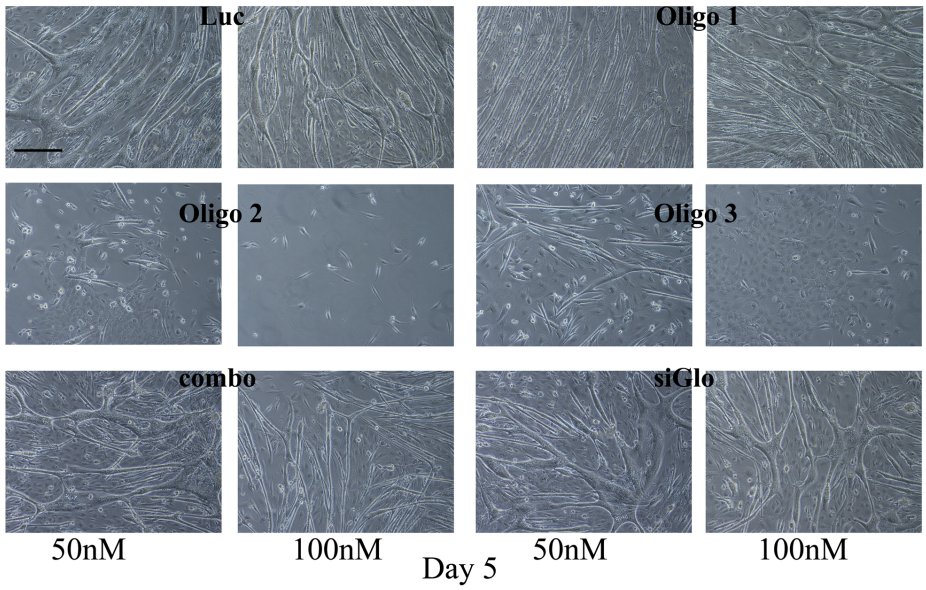
Luc
Oligo 1
Oligo 2
Oligo 3
combo
siGlo
50nM
100nM
50nM
100nM
Day 5

Figure 3. 25 siRNA against PLD3 promote PLD3 expression

C2C12 myoblasts transfected with siRNA oligos against PLD3, luciferase or siGlo transfection control were induced to differentiate for 5 days. Whole cell lysates were collected and analyzed by western blot using anti-PLD3 and anti-GAPDH antibodies. Representative blot from 3 independent experiments.

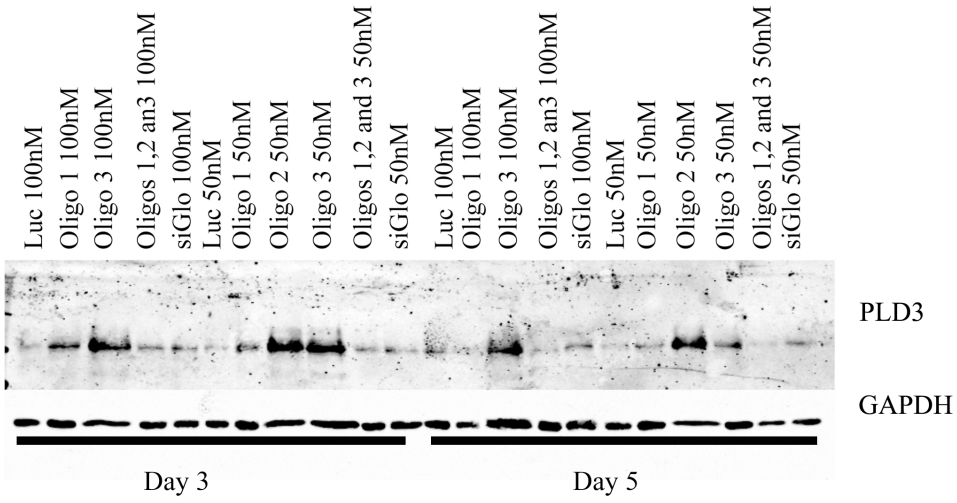
Luc 100nM
Oligo 1 100nM
Oligo 3 100nM
Oligos 1,2 an3 100nM
siGlo 100nM
Luc 50nM
Oligo 1 50nM
Oligo 2 50nM
Oligo 3 50nM
Oligos 1,2 and 3 50nM
siGlo 50nM
Luc 100nM
Oligo 1 100nM
Oligo 3 100nM
Oligos 1,2 an3 100nM
siGlo 100nM
Luc 50nM
Oligo 1 50nM
Oligo 2 50nM
Oligo 3 50nM
Oligos 1,2 and 3 50nM
siGlo 50nM
PLD3
GAPDH
Day 3
Day 5

Figure 3. 26 Cell treated with siRNA oligos against PLD3 do not have abnormal activation of the unfolded protein response.

A. C2C12 cells transfected with siRNA oligos against PLD3, luciferase or siGlo transfection control were induced to differentiate for 6 days. Whole cell lysates were collected and analyzed by western blot using anti-Bip and anti-GAPDH antibodies. Representative blot from 3 independent experiments. **B.** C2C12 cells were co-transfected with the 5XATF6 Luc reporter gene, Lac-Z and siRNA oligos against luciferase, PLD3 or the oligo transfection indicator siGlo. The cells were then allowed to differentiate for 3 days, followed by measuring luciferase and β-galactosidase activity. (N = 3)

A.

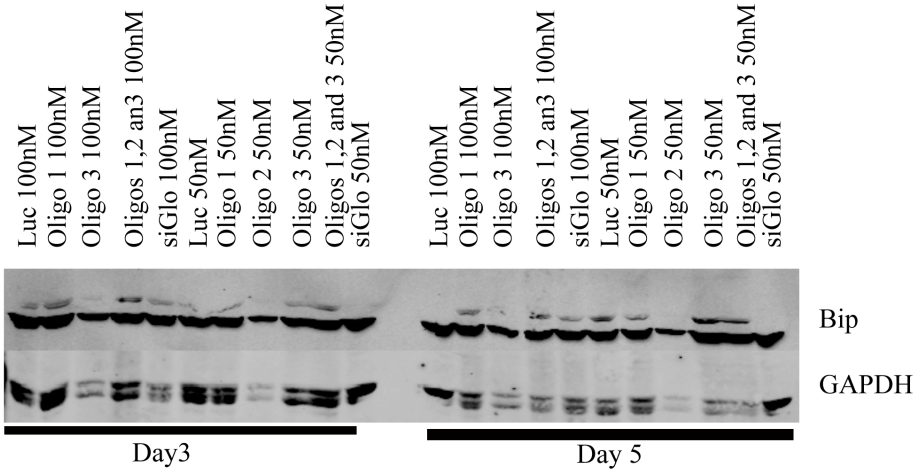
Luc 100nM
Oligo 1 100nM
Oligo 3 100nM
Oligos 1,2 an3 100nM
siGlo 100nM
Luc 50nM
Oligo 1 50nM
Oligo 2 50nM
Oligo 3 50nM
Oligos 1,2 and 3 50nM
siGlo 50nM
Luc 100nM
Oligo 1 100nM
Oligo 3 100nM
Oligos 1,2 an3 100nM
siGlo 100nM
Luc 50nM
Oligo 1 50nM
Oligo 2 50nM
Oligo 3 50nM
Oligos 1,2 and 3 50nM
siGlo 50nM
Bip
GAPDH
Day3
Day 5

B.

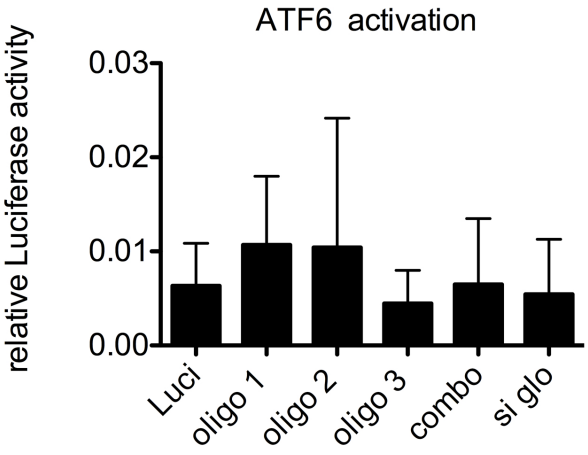
ATF6 activation
relative Luciferase activity
0.03
0.02
0.01
0.00
Luci
oligo 1
oligo 2
oligo 3
combo
si glo

Chapter 4

Conclusions and Future Considerations

4.1 Overall conclusions regarding PLD3 and Myogenesis

In the previous chapter, I showed that PLD3 is an unusual protein seemingly important for myogenesis. The transmembrane domain of PLD3 controls the localization of PLD3, and may also regulate PLD3 activity, as demonstrated by the use of the deletion and fusion mutants. While the localization of PLD3 is unknown, we showed that PLD3 localizes to unknown vesicles that seem to be derived from the ER as seem by points of co-localization between PLD3 positive vesicles and cyto-c positive membranes that resemble ER-mitochondrial contact points. I also showed that PLD3 activity enhances or stabilizes myotube formation, as demonstrated by the altered fusion indices of myoblasts overexpressing wild-type or inactive PLD3. However, the enzymatic activity or signaling pathways involved in PLD3-induced alteration of fusion are unknown, although it is clear that PLD3 activity is either modulated by or modulates the activation of ER stress or oxidative stress, as induced by TG.

4.2 Future considerations for studying PLD3

Does PLD3 act to produce phosphatidic acid?

The primary question that has plagued the PLD3 field for years is, whether or not PLD3 in a "true PLD", specifically, does PLD3 produce phosphatidic acid? As mentioned before, using a classical PLD assay, PLD3 has not shown any PLD activity (*28*). However, it is possible that the assay was not sensitive enough to detect PA produced by PLD3 since its catalytic HKD domains are luminal; more importantly, it is possible that PLD3 might produce PA using a substrate other than phosphatidylcholine. Moreover, unpublished data performed by Danxia Ke in the laboratory of Michael A. Frohman at Stony Brook University, in which cells transfected with either a PLD3 plasmid or an empty vector plasmid and labeld with tritiated palmitate, showed a difference in lipid species present once isolated. This data strongly suggested that PLD3 is a lipid modifying enzyme. To examine if PLD3 has phospholipase D activity, large-scale lipidomics should be conducted. While I have not found a specific location of PLD3 during myogenesis, it is clear that PLD3 is involved in ER / ER stress homeostasis and is most likely localizing to specialized ER or ER-derived microdomains.

Microsomes from developing myotubes, with and without PLD3 overexpression, should be isolated and examined for differences in lipid composition. And since I have demonstrated that tharpsigargin treatment increases PLD3 localization to the ER in myotubes, microsomes could also be prepared from differentiating myotubes treated with tharpsigargin for lipid analysis. Additionally, PLD3 protein purified using the baculovirus system could be incubated with typical ER lipids to determine if there are changes in the lipid composition, but more importantly, if it makes PA. The purified protein could also be incubated with purified whole cell lipids from differentiating myotubes. However, it is also very possible for PLD3 to not have PLD activity. It may, like its homologue F13L, show PLA or PLC activity instead, which would also be demonstrated in the above experiments.

Does PLD3 associate with other proteins?

It is not uncommon for PLD enzymes/proteins to interact with other proteins (binding partners) in order to regulate activity temporally or spatially. As mentioned earlier, I attempted to search for binding partners for PLD3 in order to help elucidate its function and potentially its localization during differentiation. However, there were a few mishaps in the process. In the future this could be re-examined by changing to a protein complementation assay (PCA), such as the life/ death PCA strategy described in (*63*), using cDNA from differentiating myoblasts. While the initial start-up would be time consuming and labor intensive, this would be a better method for determining binding partners because

it allows for a high throughput strategy and does not select against transient interaction as does co-immunoprecipitation.

Does PLD3 alter membrane structures in differentiating cells?

Earlier, I suggested PLD3 might promote changes in the structure of the endoplasmic reticulum by altering ER homeostasis through the UPR. I noticed that the ER membranes looked different in cells overexpressing PLD3-myc, PLD3-K418R or ER mcherry (Figure 4.1), but these observations were not conclusive at the level of magnification I used to image the cells. However, to determine this it would be necessary to have high magnification and resolution imaging of differentiating cells. Electron microscopy analysis of developing myotubes to examine: membrane fusion, fusion-related vesicle docking to the plasma membrane, ER structure and size should be conducted in the above cell lines for any changes. The above experiment would determine if PLD3 has a role in membrane trafficking events especially those mentioned above.

Does PLD3 alter cellular migration or cell-cell fusion rates in differentiating myoblasts/ myotubes?

Since I have shown that there are differences in the fusion indices of C2C12 myoblasts overexpressing PLD3 and that PLD3 overexpressing cells can improve the fusion indices of cells not overexpressing PLD3, the next question in why? There are several possible reasons how PLD3 is altering fusion. One possibility is that PLD3 is somehow altering the rate of cell migration, most likely

by changing the extracellular environment (i.e. secretion of cytokines) or by changing actin and microtubule dynamics reviewed in (*64*) or altering cellular fusion machinery in alternate ways. Setting up a multi-day live cell image of differentiating cells could test these theories by examining the migration and fusion dynamics of myoblasts in real time. This method would also allow one to see if there is a change in the actual fusion process rather than cell migration, which is another equally relevant suggestion.

Does Nuclear PLD3 have DNA binding and modulation ability?

I have shown with the PLD3 deletion mutants that loss of the transmembrane domain leads to a loss of ER localization in proliferating cells. More importantly, I demonstrated that these transmembrane mutants exhibited partial nuclear localization. As mentioned above, this was a very interesting occurrence since PLD3 does not have any noticeable NLS sequences, but more importantly, this was interesting because of the report suggesting that the viral homologue of PLD3, K4L is responsible for nicking and joining viral crucible DNA (*30*).

Can PLD3 alter secreted protein profiles in differentiating cells through the UPR or secretory pathway modulation?

Previous unpublished data from the lab using VSVG trafficking and PLD3 overexpression suggested that PLD3 might have a role in the secretory pathway. To further explore this, PLD3 expression and activity should be examined in the development of professional secretory cells, such as differentiating plasma cells, adipocytes, or osteoclasts. These cells are good systems for PLD3 study since I have shown there is a link between ER-stress and PLD3, and these cells are known to activate ER-stress/UPR genes to increase protein production secretory load during differentiation.

Figure 4. 1 ER-analysis in myoblasts overexpressing PLD3-mcherry, PLD3-myc and PLD3-K418R.

C2C12 myoblasts overexpressing PLD3-mcherry, PLD3-myc and PLD3-K418R wee induced to differentiate for 5 days and stained, by indirect immunofluorescence staining, with anti-KDEL antibodies. The cells were then visualized with a Zeiss LSM 510 Meta confocal.

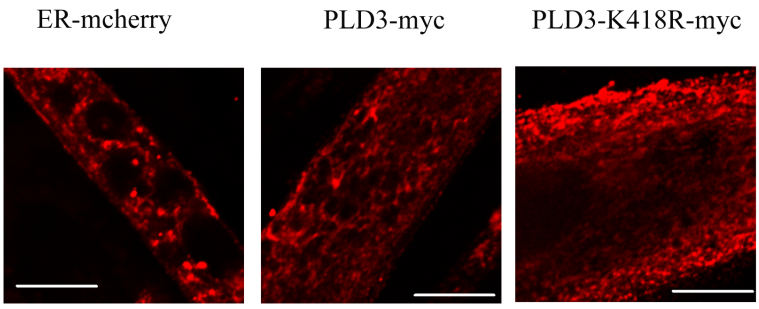
ER-mcherry
PLD3-myc
PLD3-K418R-myc

References

1. McDermott, M., Wakelam, M. J., and Morris, A. J. (2004) Phospholipase D, *Biochem Cell Biol 82*, 225-253.

2. Frohman, M. A., Sung, T. C., and Morris, A. J. (1999) Mammalian phospholipase D structure and regulation, *Biochim Biophys Acta 1439*, 175-186.

3. Jenkins, G. M., and Frohman, M. A. (2005) Phospholipase D: a lipid centric review, *Cell Mol Life Sci 62*, 2305-2316.

4. Sung, T. C., Roper, R. L., Zhang, Y., Rudge, S. A., Temel, R., Hammond, S. M., Morris, A. J., Moss, B., Engebrecht, J., and Frohman, M. A. (1997) Mutagenesis of phospholipase D defines a superfamily including a trans-Golgi viral protein required for poxvirus pathogenicity, *Embo J 16*, 4519-4530.

5. Bi, K., Roth, M. G., and Ktistakis, N. T. (1997) Phosphatidic acid formation by phospholipase D is required for transport from the endoplasmic reticulum to the Golgi complex, *Curr Biol 7*, 301-307.

6. Chen, Y. G., Siddhanta, A., Austin, C. D., Hammond, S. M., Sung, T. C., Frohman, M. A., Morris, A. J., and Shields, D. (1997) Phospholipase D stimulates release of nascent secretory vesicles from the trans-Golgi network, *J Cell Biol 138*, 495-504.

7. Hughes, W. E., Elgundi, Z., Huang, P., Frohman, M. A., and Biden, T. J. (2004) Phospholipase D1 regulates secretagogue-stimulated insulin release in pancreatic beta-cells, *J Biol Chem 279*, 27534-27541.

8. Huang, P., Altshuller, Y. M., Hou, J. C., Pessin, J. E., and Frohman, M. A. (2005) Insulin-stimulated plasma membrane fusion of Glut4 glucose transporter-containing vesicles is regulated by phospholipase D1, *Mol Biol Cell 16*, 2614-2623.

9. Du, G., Huang, P., Liang, B. T., and Frohman, M. A. (2004) Phospholipase D2 localizes to the plasma membrane and regulates angiotensin II receptor endocytosis, *Mol Biol Cell 15*, 1024-1030.

10. Knoepp, S. M., Chahal, M. S., Xie, Y., Zhang, Z., Brauner, D. J., Hallman, M. A., Robinson, S. A., Han, S., Imai, M., Tomlinson, S., and Meier, K. E. (2008) Effects of active and inactive phospholipase D2 on signal transduction, adhesion, migration, invasion, and metastasis in EL4 lymphoma cells, *Mol Pharmacol 74*, 574-584.

11. Nakanishi, H., Morishita, M., Schwartz, C. L., Coluccio, A., Engebrecht, J., and Neiman, A. M. (2006) Phospholipase D and the SNARE Sso1p are necessary for vesicle fusion during sporulation in yeast, *J Cell Sci 119*, 1406-1415.

12. Moreno-Borchart, A. C., and Knop, M. (2003) Prospore membrane formation: how budding yeast gets shaped in meiosis, *Microbiol Res 158*, 83-90.

13. Choi, S. Y., Huang, P., Jenkins, G. M., Chan, D. C., Schiller, J., and Frohman, M. A. (2006) A common lipid links Mfn-mediated mitochondrial fusion and SNARE-regulated exocytosis, *Nat Cell Biol 8*, 1255-1262.

14. Komati, H., Naro, F., Mebarek, S., De Arcangelis, V., Adamo, S., Lagarde, M., Prigent, A. F., and Nemoz, G. (2005) Phospholipase D is involved in myogenic differentiation through remodeling of actin cytoskeleton, *Mol Biol Cell 16*, 1232-1244.

15. Abmayr, S. M., Balagopalan, L., Galletta, B. J., and Hong, S. J. (2003) Cell and molecular biology of myoblast fusion, *Int Rev Cytol 225*, 33-89.

16. Potthoff, M. J., and Olson, E. N. (2007) MEF2: a central regulator of diverse developmental programs, *Development 134*, 4131-4140.

17. Bryson-Richardson, R. J., and Currie, P. D. (2008) The genetics of vertebrate myogenesis, *Nat Rev Genet 9*, 632-646.

18. Molkentin, J. D., and Olson, E. N. (1996) Defining the regulatory networks for muscle development, *Curr Opin Genet Dev 6*, 445-453.

19. Horsley, V., and Pavlath, G. K. (2004) Forming a multinucleated cell: molecules that regulate myoblast fusion, *Cells Tissues Organs 176*, 67-78.

20. Sorrentino, V. (2004) Molecular determinants of the structural and functional organization of the sarcoplasmic reticulum, *Biochim Biophys Acta 1742*, 113-118.

21. Ralston, E. (1993) Changes in architecture of the Golgi complex and other subcellular organelles during myogenesis, *J Cell Biol 120*, 399-409.

22. Tassin, A. M., Paintrand, M., Berger, E. G., and Bornens, M. (1985) The Golgi apparatus remains associated with microtubule organizing centers during myogenesis, *J Cell Biol 101*, 630-638.

23. Towler, M. C., Kaufman, S. J., and Brodsky, F. M. (2004) Membrane traffic in skeletal muscle, *Traffic 5*, 129-139.

24. Flucher, B. E., Terasaki, M., Chin, H. M., Beeler, T. J., and Daniels, M. P. (1991) Biogenesis of transverse tubules in skeletal muscle in vitro, *Dev Biol 145*, 77-90.

25. Clark, K. A., McElhinny, A. S., Beckerle, M. C., and Gregorio, C. C. (2002) Striated muscle cytoarchitecture: an intricate web of form and function, *Annu Rev Cell Dev Biol 18*, 637-706.

26. Cao, J. X., Koop, B. F., and Upton, C. (1997) A human homolog of the vaccinia virus HindIII K4L gene is a member of the phospholipase D superfamily, *Virus Res 48*, 11-18.

27. Munck, A., Bohm, C., Seibel, N. M., Hashemol Hosseini, Z., and Hampe, W. (2005) Hu-K4 is a ubiquitously expressed type 2 transmembrane protein associated with the endoplasmic reticulum, *Febs J 272*, 1718-1726.

28. Pedersen, K. M., Finsen, B., Celis, J. E., and Jensen, N. A. (1998) Expression of a novel murine phospholipase D homolog coincides with late neuronal development in the forebrain, *J Biol Chem 273*, 31494-31504.

29. Tomczak, K. K., Marinescu, V. D., Ramoni, M. F., Sanoudou, D., Montanaro, F., Han, M., Kunkel, L. M., Kohane, I. S., and Beggs, A. H. (2004) Expression profiling and identification of novel genes involved in myogenic differentiation, *Faseb J 18*, 403-405.

30. Eckert, D., Williams, O., Meseda, C. A., and Merchlinsky, M. (2005) Vaccinia virus nicking-joining enzyme is encoded by K4L (VACWR035), *J Virol 79*, 15084-15090.

31. Blasco, R., and Moss, B. (1991) Extracellular vaccinia virus formation and cell-to-cell virus transmission are prevented by deletion of the gene encoding the 37,000-Dalton outer envelope protein, *J Virol 65*, 5910-5920.

32. Husain, M., and Moss, B. (2002) Similarities in the induction of post-Golgi vesicles by the vaccinia virus F13L protein and phospholipase D, *J Virol 76*, 7777-7789.

33. Roper, R. L., and Moss, B. (1999) Envelope formation is blocked by mutation of a sequence related to the HKD phospholipid metabolism motif in the vaccinia virus F13L protein, *J Virol 73*, 1108-1117.

34. Baek, S. H., Kwak, J. Y., Lee, S. H., Lee, T., Ryu, S. H., Uhlinger, D. J., and Lambeth, J. D. (1997) Lipase activities of p37, the major envelope protein of vaccinia virus, *J Biol Chem 272*, 32042-32049.

35. Kent, D. G., Copley, M. R., Benz, C., Wohrer, S., Dykstra, B. J., Ma, E., Cheyne, J., Zhao, Y., Bowie, M. B., Gasparetto, M., Delaney, A., Smith, C., Marra, M., and Eaves, C. J. (2009) Prospective isolation and molecular characterization of hematopoietic stem cells with durable self-renewal potential, *Blood 113*, 6342-6350.

36. Nagaoka-Yasuda, R., Matsuo, N., Perkins, B., Limbaeck-Stokin, K., and Mayford, M. (2007) An RNAi-based genetic screen for oxidative stress resistance reveals retinol saturase as a mediator of stress resistance, *Free Radic Biol Med 43*, 781-788.

37. Hansen, J. M., Klass, M., Harris, C., and Csete, M. (2007) A reducing redox environment promotes C2C12 myogenesis: implications for regeneration in aged muscle, *Cell Biol Int 31*, 546-553.

38. Morita, S., Kojima, T., and Kitamura, T. (2000) Plat-E: an efficient and stable system for transient packaging of retroviruses, *Gene Ther 7*, 1063-1066.

39. Lee, K., Tirasophon, W., Shen, X., Michalak, M., Prywes, R., Okada, T., Yoshida, H., Mori, K., and Kaufman, R. J. (2002) IRE1-mediated unconventional mRNA splicing and S2P-mediated ATF6 cleavage merge to regulate XBP1 in signaling the unfolded protein response, *Genes Dev 16*, 452-466.

40. Wang, Y., Shen, J., Arenzana, N., Tirasophon, W., Kaufman, R. J., and Prywes, R. (2000) Activation of ATF6 and an ATF6 DNA binding site by the endoplasmic reticulum stress response, *J Biol Chem 275*, 27013-27020.

41. Pajcini, K. V., Pomerantz, J. H., Alkan, O., Doyonnas, R., and Blau, H. M. (2008) Myoblasts and macrophages share molecular components that contribute to cell-cell fusion, *J Cell Biol 180*, 1005-1019.

42. Carozzi, A. J., Ikonen, E., Lindsay, M. R., and Parton, R. G. (2000) Role of cholesterol in developing T-tubules: analogous mechanisms for T-tubule and caveolae biogenesis, *Traffic 1*, 326-341.

43. Charlton, C. A., Mohler, W. A., Radice, G. L., Hynes, R. O., and Blau, H. M. (1997) Fusion competence of myoblasts rendered genetically null for N-cadherin in culture, *J Cell Biol 138*, 331-336.

44. Yang, J. T., Rando, T. A., Mohler, W. A., Rayburn, H., Blau, H. M., and Hynes, R. O. (1996) Genetic analysis of alpha 4 integrin functions in the development of mouse skeletal muscle, *J Cell Biol 135*, 829-835.

45. Rommel, C., Bodine, S. C., Clarke, B. A., Rossman, R., Nunez, L., Stitt, T. N., Yancopoulos, G. D., and Glass, D. J. (2001) Mediation of IGF-1-induced

skeletal myotube hypertrophy by PI(3)K/Akt/mTOR and PI(3)K/Akt/GSK3 pathways, *Nat Cell Biol 3*, 1009-1013.

46. Cooper, S. T., Maxwell, A. L., Kizana, E., Ghoddusi, M., Hardeman, E. C., Alexander, I. E., Allen, D. G., and North, K. N. (2004) C2C12 co-culture on a fibroblast substratum enables sustained survival of contractile, highly differentiated myotubes with peripheral nuclei and adult fast myosin expression, *Cell Motil Cytoskeleton 58*, 200-211.

47. Horsley, V., Jansen, K. M., Mills, S. T., and Pavlath, G. K. (2003) IL-4 acts as a myoblast recruitment factor during mammalian muscle growth, *Cell 113*, 483-494.

48. Nakanishi, K., Dohmae, N., and Morishima, N. (2007) Endoplasmic reticulum stress increases myofiber formation in vitro, *Faseb J 21*, 2994-3003.

49. Buckley, B. J., and Whorton, A. R. (1997) Tunicamycin increases intracellular calcium levels in bovine aortic endothelial cells, *Am J Physiol 273*, C1298-1305.

50. Li, M., Baumeister, P., Roy, B., Phan, T., Foti, D., Luo, S., and Lee, A. S. (2000) ATF6 as a transcription activator of the endoplasmic reticulum stress element: thapsigargin stress-induced changes and synergistic interactions with NF-Y and YY1, *Mol Cell Biol 20*, 5096-5106.

51. Nakanishi, K., Sudo, T., and Morishima, N. (2005) Endoplasmic reticulum stress signaling transmitted by ATF6 mediates apoptosis during muscle development, *J Cell Biol 169*, 555-560.

52. Basseri, S., Lhotak, S., Sharma, A. M., and Austin, R. C. (2009) The chemical chaperone 4-phenylbutyrate inhibits adipogenesis by modulating the unfolded protein response, *J Lipid Res 50*, 2486-2501.

53. Gass, J. N., Gunn, K. E., Sriburi, R., and Brewer, J. W. (2004) Stressed-out B cells? Plasma-cell differentiation and the unfolded protein response, *Trends Immunol 25*, 17-24.

54. Iwakoshi, N. N., Lee, A. H., and Glimcher, L. H. (2003) The X-box binding protein-1 transcription factor is required for plasma cell differentiation and the unfolded protein response, *Immunol Rev 194*, 29-38.

55. Iwakoshi, N. N., Lee, A. H., Vallabhajosyula, P., Otipoby, K. L., Rajewsky, K., and Glimcher, L. H. (2003) Plasma cell differentiation and the unfolded protein response intersect at the transcription factor XBP-1, *Nat Immunol 4*, 321-329.

56. Cho, Y. M., Jang, Y. S., Jang, Y. M., Chung, S. M., Kim, H. S., Lee, J. H., Jeong, S. W., Kim, I. K., Kim, J. J., Kim, K. S., and Kwon, O. J. (2009) Induction of unfolded protein response during neuronal induction of rat bone marrow stromal cells and mouse embryonic stem cells, *Exp Mol Med 41*, 440-452.

57. Hsieh, Y. H., Su, I. J., Lei, H. Y., Lai, M. D., Chang, W. W., and Huang, W. (2007) Differential endoplasmic reticulum stress signaling pathways mediated by iNOS, *Biochem Biophys Res Commun 359*, 643-648.

58. Haze, K., Yoshida, H., Yanagi, H., Yura, T., and Mori, K. (1999) Mammalian transcription factor ATF6 is synthesized as a transmembrane protein and activated by proteolysis in response to endoplasmic reticulum stress, *Mol Biol Cell 10*, 3787-3799.

59. Hamamura, K., Liu, Y., and Yokota, H. (2008) Microarray analysis of thapsigargin-induced stress to the endoplasmic reticulum of mouse osteoblasts, *J Bone Miner Metab 26*, 231-240.

60. Yip, K. H., Zheng, M. H., Steer, J. H., Giardina, T. M., Han, R., Lo, S. Z., Bakker, A. J., Cassady, A. I., Joyce, D. A., and Xu, J. (2005) Thapsigargin modulates osteoclastogenesis through the regulation of RANKL-induced signaling pathways and reactive oxygen species production, *J Bone Miner Res 20*, 1462-1471.

61. Kaufman, R. J. (1999) Stress signaling from the lumen of the endoplasmic reticulum: coordination of gene transcriptional and translational controls, *Genes Dev 13*, 1211-1233.

62. Sago, N., Omi, K., Tamura, Y., Kunugi, H., Toyo-oka, T., Tokunaga, K., and Hohjoh, H. (2004) RNAi induction and activation in mammalian muscle cells where Dicer and eIF2C translation initiation factors are barely expressed, *Biochem Biophys Res Commun 319*, 50-57.

63. Ear, P. H., and Michnick, S. W. (2009) A general life-death selection strategy for dissecting protein functions, *Nat Methods 6*, 813-816.

64. Ridley, A. J., Schwartz, M. A., Burridge, K., Firtel, R. A., Ginsberg, M. H., Borisy, G., Parsons, J. T., and Horwitz, A. R. (2003) Cell migration: integrating signals from front to back, *Science 302*, 1704-1709.

Appendix 1. Preliminary conditioned media mass spectrophotometry analysis

Protein Description	Total Of spectra	ER-mcherry spectra count	PLD3-myc spectra Count	PLD3-K418R-myc spectra count
FIBRONECTIN PRECURSOR.	158	59	20	79
COLLAGEN ALPHA-2(I) CHAIN PRECURSOR.	83	7	18	58
PIGMENT EPITHELIUM-DERIVED FACTOR PRECURSOR.	79	8	5	66
COLLAGEN ALPHA-1(III) CHAIN PRECURSOR.	70	2	13	55
ACTIN, ALPHA SKELETAL MUSCLE.	66	46	9	11
VIMENTIN.	57	32	6	19
ACTIN, CYTOPLASMIC 1.	42	29		13
ISOFORM 1 OF GELSOLIN PRECURSOR.	41	3	6	32
VINCULIN.	41	25	1	15
MYOSIN-9.	40	22		18
DECORIN PRECURSOR.	38		2	36
DESMIN.	37	26	3	8
ISOFORM PLEC-1I OF PLECTIN-1.	37	13		24
BASEMENT MEMBRANE-SPECIFIC HEPARAN SULFATE PROTEOGLYCAN CORE PROTEIN PRECURSOR.	32	20		12
ISOFORM 1 OF FILAMIN-A.	30	26		4
HEAT SHOCK PROTEIN 84B.	28	14	7	7
PEPTIDYL-PROLYL CIS-TRANS	28	15		13

ISOMERASE.				
ISOFORM 1 OF SULFHYDRYL OXIDASE 1 PRECURSOR.	27	14		13
72 KDA TYPE IV COLLAGENASE PRECURSOR.	26	1	3	22
TUBULIN ALPHA-1A CHAIN.	25	9		16
14-3-3 PROTEIN ZETA/DELTA.	25	11	4	10
MIMECAN PRECURSOR.	25	2	3	20
BIGLYCAN PRECURSOR.	25		5	20
ISOFORM 1 OF COLLAGEN ALPHA-1(I) CHAIN PRECURSOR.	22		3	19
ISOFORM N-CAM 180 OF NEURAL CELL ADHESION MOLECULE 1, 180 KDA ISOFORM PRECURSOR.	20	16		4
COLLAGEN ALPHA-1(VI) CHAIN PRECURSOR.	20		3	17
ISOFORM M2 OF PYRUVATE KINASE ISOZYMES M1/M2.	19	7	5	7
ALPHA-ENOLASE.	19	8		11
ISOFORM 1 OF FILAMIN-C.	19	12		7
CATHEPSIN D PRECURSOR.	18	7		11
ISOFORM 2 OF PERIOSTIN PRECURSOR.	18	15		3
ISOFORM 1 OF TROPOMYOSIN ALPHA-1 CHAIN.	18	10	4	4
FRUCTOSE-BISPHOSPHATE ALDOLASE A.	17	13		4
ISOFORM 1 OF NESTIN.	17	17		
TRIOSEPHOSPHATE ISOMERASE.	17	14		3
MOESIN.	16	5	1	10
H2A HISTONE FAMILY, MEMBER J.	16	8		8

ISOFORM 1 OF COLLAGEN ALPHA-1(XII) CHAIN PRECURSOR.	15			15
CYSTATIN-C PRECURSOR.	15	3	3	9
PHOSPHOLIPID TRANSFER PROTEIN PRECURSOR.	15	1	1	13
TUBULIN BETA-2B CHAIN.	14	10		4
COLLAGEN ALPHA-2(V) CHAIN PRECURSOR.	14	3	1	10
PREDICTED GENE, EG622339.	14	11	1	2
COLLAGEN ALPHA-1(V) CHAIN PRECURSOR.	14			14
OSTEOCLAST-LIKE CELL CDNA, RIKEN FULL-LENGTH ENRICHED LIBRARY, CLONE:I420039P15 PRODUCT:AE BINDING PROTEIN 1, FULL INSERT SEQUENCE.	14	2	3	9
ELONGATION FACTOR 1-ALPHA 1.	14	14		
TALIN-1.	14	14		
ALPHA-ACTININ-4.	13	1	2	10
ISOFORM 1 OF CORE HISTONE MACRO-H2A.1.	13	10		3
GLUCOSE-6-PHOSPHATE ISOMERASE.	13	3		10
PROTEIN DISULFIDE-ISOMERASE A3 PRECURSOR.	13	9		4
60S ACIDIC RIBOSOMAL PROTEIN P1.	12	5		7
HISTONE H2B TYPE 1-F/J/L.	12	1		11
ISOFORM 1 OF RAB GDP DISSOCIATION INHIBITOR BETA.	12			12
CHYMOTRYPSINOGEN B PRECURSOR.	12	11		1
78 KDA GLUCOSE-REGULATED	12	11		1

PROTEIN PRECURSOR.				
L-LACTATE DEHYDROGENASE A CHAIN.	12	4		8
RHO GDP-DISSOCIATION INHIBITOR 1.	12	4		8
ISOFORM 1 OF MACROPHAGE COLONY-STIMULATING FACTOR 1 PRECURSOR.	11	3		8
NUCLEOSIDE DIPHOSPHATE KINASE B.	11	6	1	4
NIDOGEN-2 PRECURSOR.	11			11
ALPHA-ACTININ-3.	11	6		5
ISOFORM C OF LAMIN-A/C.	11	4	5	2
PHOSPHOGLYCERATE KINASE 1.	11	3		8
INSULIN-LIKE GROWTH FACTOR-BINDING PROTEIN 6 PRECURSOR.	10			10
HEAT SHOCK COGNATE 71 KDA PROTEIN.	10	7		3
11 KDA PROTEIN.	10	6		4
COL6A3 PROTEIN.	10		1	9
FIBULIN 2 ISOFORM B.	10	5	1	4
ELONGATION FACTOR 1-ALPHA 2.	9	6	1	2
IMMUNOGLOBULIN SUPERFAMILY CONTAINING LEUCINE-RICH REPEAT PROTEIN PRECURSOR.	9	1		8
SPARC PRECURSOR.	9	2	2	5
ENDOPLASMIN PRECURSOR.	9	8		1
ADENYLYL CYCLASE-ASSOCIATED PROTEIN 1.	9			9
BIOTINIDASE.	9			9

MALATE DEHYDROGENASE, MITOCHONDRIAL PRECURSOR.	9			9
MYOSIN-3.	9	9		
PEROXIDASIN HOMOLOG PRECURSOR.	9	5		4
ISOFORM LONG OF EXTRACELLULAR MATRIX PROTEIN 1 PRECURSOR.	8		2	6
17 DAYS EMBRYO KIDNEY CDNA, RIKEN FULL-LENGTH ENRICHED LIBRARY, CLONE:I920160L24 PRODUCT:PROLYL 4-HYDROXYLASE, BETA POLYPEPTIDE, FULL INSERT SEQUENCE.	8	2		6
GLYPICAN-1 PRECURSOR.	8	4	1	3
CRL-1722 L5178Y-R CDNA, RIKEN FULL-LENGTH ENRICHED LIBRARY, CLONE:I730077L17 PRODUCT:THIOREDOXIN DOMAIN CONTAINING 7, FULL INSERT SEQUENCE.	8	8		
CALSEQUESTRIN 2.	8	8		
ISOFORM C2 OF LAMIN-A/C.	8	4	1	3
PROTEASOME SUBUNIT BETA TYPE-3.	8	5		3
PHOSPHOGLYCERATE MUTASE 1.	8	3		5
DYNACTIN SUBUNIT 2.	7	7		
PROCOLLAGEN C-ENDOPEPTIDASE ENHANCER 1 PRECURSOR.	7		2	5
FARNESYL PYROPHOSPHATE SYNTHETASE.	7	3		4
PEROXIREDOXIN-1.	7	4		3
ENOLASE.	7	4	1	2

LEGUMAIN PRECURSOR.	7			7
TRYPSINOGEN 7.	7	3	2	2
ALDOSE REDUCTASE.	7	3		4
PROFILIN-1.	7	3		4
BETA-ENOLASE.	7			7
ASPARTATE AMINOTRANSFERASE, CYTOPLASMIC.	7			7
COLLAGEN ALPHA-1(XV) CHAIN PRECURSOR.	7			7
ELONGATION FACTOR 2.	7	4	1	2
COLLAGEN ALPHA-2(VI) CHAIN PRECURSOR.	7		2	5
TRANSITIONAL ENDOPLASMIC RETICULUM ATPASE.	7	5		2
23 KDA PROTEIN.	6	3		3
SERPIN H1 PRECURSOR.	6	5		1
T-COMPLEX PROTEIN 1 SUBUNIT DELTA.	6	3		3
PEROXIREDOXIN-2.	6			6
THROMBOSPONDIN 1.	6	4		2
NUCLEOPHOSMIN.	6			6
CHLORIDE INTRACELLULAR CHANNEL PROTEIN 1.	6	3		3
SERUM ALBUMIN PRECURSOR.	6			6
HEAT SHOCK 70 KDA PROTEIN 1L.	6	2	3	1
FRUCTOSE-BISPHOSPHATE ALDOLASE.	6	4	2	

0 DAY NEONATE LUNG CDNA, RIKEN FULL-LENGTH ENRICHED LIBRARY, CLONE:E030024J03 PRODUCT:ISOCITRATE DEHYDROGENASE 1 (NADP+), SOLUBLE, FULL INSERT SEQUENCE.	6			6
CREATINE KINASE B-TYPE.	6	6		
HYPOTHETICAL PROTEIN LOC666586.	6	3	2	1
UBIQUITIN-CONJUGATING ENZYME E2 N.	6	4	1	1
ANNEXIN A1.	6	4		2
PROTEIN DISULFIDE ISOMERASE ASSOCIATED 4.	6	6		
OLFACTOMEDIN-LIKE PROTEIN 3 PRECURSOR.	6			6
PROTEIN-LYSINE 6-OXIDASE PRECURSOR.	6			6
IMPORTIN SUBUNIT BETA-1.	6	3		3
OLFACTOMEDIN-LIKE PROTEIN 2B PRECURSOR.	6			6
LYSYL OXIDASE HOMOLOG 1 PRECURSOR.	6	2		4
ALPHA-ACTININ-1.	6	5		1
ISOFORM 1 OF CALSYNTENIN-1 PRECURSOR (FRAGMENT).	6	1		5
ISOFORM 1 OF GLYOXALASE DOMAIN-CONTAINING PROTEIN 4.	5	5		
EXTRACELLULAR SUPEROXIDE DISMUTASE [CU-ZN] PRECURSOR.	5			5
EUKARYOTIC TRANSLATION ELONGATION FACTOR 1 DELTA ISOFORM A.	5	5		
DOUBLECORTIN-LIKE PROTEIN.	5			5

ISOFORM V0 OF VERSICAN CORE PROTEIN PRECURSOR.	5		1	4
HYPOXIA UP-REGULATED PROTEIN 1 PRECURSOR.	5	5		
CALRETICULIN PRECURSOR.	5	3		2
FOLLISTATIN-RELATED PROTEIN 1 PRECURSOR.	5		2	3
PROCOLLAGEN-LYSINE,2-OXOGLUTARATE 5-DIOXYGENASE 1 PRECURSOR.	5			5
PROTEASOME SUBUNIT BETA TYPE-4 PRECURSOR.	5			5
RAS-RELATED PROTEIN RAB-10.	5			5
60S RIBOSOMAL PROTEIN L8.	5	3		2
TALIN 2.	5	5		
ECTONUCLEOTIDE PYROPHOSPHATASE/PHOSPHODIESTERASE FAMILY MEMBER 2 PRECURSOR.	5			5
ANNEXIN A5.	5	3		2
COLLAGEN ALPHA-2(IV) CHAIN PRECURSOR.	5			5
NOD-DERIVED CD11C +VE DENDRITIC CELLS CDNA, RIKEN FULL-LENGTH ENRICHED LIBRARY, CLONE:F630118J10 PRODUCT:FIBRONECTIN 1, FULL INSERT SEQUENCE.	5			5
FASCIN.	5	3		2
ISOFORM SMOOTH MUSCLE OF MYOSIN LIGHT POLYPEPTIDE 6.	5			5
12 DAYS EMBRYO EMBRYONIC BODY BETWEEN DIAPHRAGM REGION AND NECK CDNA, RIKEN FULL-LENGTH ENRICHED LIBRARY, CLONE:9430060J01 PRODUCT:COFILIN 1, NON-MUSCLE HOMOLOG.	5	1		4

SIMILAR TO COFILIN-1 (COFILIN, NON-MUSCLE ISOFORM) ISOFORM 1.	5	4	1	
FILAMIN-B.	5	4		1
FIBRONECTIN TYPE III DOMAIN CONTAINING 1.	5	2		3
CATHEPSIN B PRECURSOR.	4	2	1	1
ALPHA-MANNOSIDASE 2.	4			4
ISOFORM 1 OF MYOSIN-11.	4	4		
MATRILIN-2 PRECURSOR.	4	1		3
14-3-3 PROTEIN EPSILON.	4	1		3
PROTEASOME SUBUNIT BETA TYPE-6 PRECURSOR.	4	4		
PROLIFERATION-ASSOCIATED PROTEIN 2G4.	4	4		
COATOMER SUBUNIT BETA.	4			4
ISOFORM 1 OF TROPOMYOSIN BETA CHAIN.	4	3		1
BETA-HEXOSAMINIDASE SUBUNIT ALPHA PRECURSOR.	4	3		1
CATHEPSIN L1 PRECURSOR.	4			4
PEPTIDYL-PROLYL CIS-TRANS ISOMERASE C.	4			4
ISOFORM 1 OF HETEROGENEOUS NUCLEAR RIBONUCLEOPROTEIN K.	4			4
GLUTATHIONE S-TRANSFERASE MU 1.	4			4
ISOFORM LONG OF 14-3-3 PROTEIN BETA/ALPHA.	4	4		
14-3-3 PROTEIN GAMMA.	4	4		
MYOSIN LIGHT CHAIN 6B.	4	1		3
HYPOTHETICAL PROTEIN	4	4		

ISOFORM 2.				
T-COMPLEX PROTEIN 1 SUBUNIT BETA.	4			4
SULFATED GLYCOPROTEIN 1 PRECURSOR.	4			4
ASPARTYL AMINOPEPTIDASE ISOFORM A.	4	2		2
RENIN RECEPTOR PRECURSOR.	4			4
PERLECAN.	4	3		1
AHNAK NUCLEOPROTEIN ISOFORM 1.	4	3		1
128 KDA PROTEIN.	4			4
ISOFORM 1 OF MACROPHAGE MANNOSE RECEPTOR 2 PRECURSOR.	4			4
ISOFORM 1 OF OBG-LIKE ATPASE 1.	3	3		
INSULIN-LIKE GROWTH FACTOR-BINDING PROTEIN 5 PRECURSOR.	3	3		
ISOFORM 1 OF MYC BOX-DEPENDENT-INTERACTING PROTEIN 1.	3	3		
ISOFORM APP770 OF AMYLOID BETA A4 PROTEIN PRECURSOR (FRAGMENT).	3	1		2
CALPONIN-2.	3			3
CERULOPLASMIN PRECURSOR.	3			3
MAMA PROTEIN.	3			3
FK506-BINDING PROTEIN 10 PRECURSOR.	3	1		2
KERATIN, TYPE I CYTOSKELETAL 25.	3			3
PROCOLLAGEN-LYSINE,2-OXOGLUTARATE 5-	3	3		

DIOXYGENASE 2 PRECURSOR.				
CYSTEINE AND GLYCINE-RICH PROTEIN 1.	3			3
ACID CERAMIDASE PRECURSOR.	3			3
SYNAPTIC VESICLE MEMBRANE PROTEIN VAT-1 HOMOLOG.	3	3		
60S RIBOSOMAL PROTEIN L10A.	3	3		
POLY(RC)-BINDING PROTEIN 1.	3			3
VITRONECTIN PRECURSOR.	3			3
TRANSLATIONALLY-CONTROLLED TUMOR PROTEIN.	3			3
ATP SYNTHASE SUBUNIT ALPHA, MITOCHONDRIAL PRECURSOR.	3	3		
TRIPEPTIDYL-PEPTIDASE 1 PRECURSOR.	3			3
ISOFORM LONG OF BETA-1,4-GALACTOSYLTRANSFERASE 1.	3	3		
ISOFORM 1 OF FIBULIN-2 PRECURSOR.	3	2		1
NUCLEOBINDIN-1 PRECURSOR.	3	1		2
40S RIBOSOMAL PROTEIN S21.	3	3		
PROTEIN CREG1 PRECURSOR.	3			3
CALUMENIN PRECURSOR.	3	3		
SIMILAR TO GLYCERALDEHYDE-3-PHOSPHATE DEHYDROGENASE (GAPDH) ISOFORM 1.	3		2	1
40S RIBOSOMAL PROTEIN S7.	3			3
CARBONIC ANHYDRASE 3.	3			3
ISOFORM 2 OF PRE-MRNA-PROCESSING FACTOR 19.	3	3		

ACETYL-COA ACETYLTRANSFERASE, CYTOSOLIC.	3			3
PHOSPHOGLYCERATE MUTASE 2.	3	1		2
SIMILAR TO RIBOSOMAL PROTEIN.	3	3		
RTN4.	3	3		
SPONDIN-2 PRECURSOR.	3			3
ISOFORM 1 OF FOUR AND A HALF LIM DOMAINS PROTEIN 1.	3	3		
ANNEXIN A6 ISOFORM B.	3	3		
LUMICAN PRECURSOR.	3			3
60S ACIDIC RIBOSOMAL PROTEIN P0.	3	3		
10, 11 DAYS EMBRYO WHOLE BODY CDNA, RIKEN FULL-LENGTH ENRICHED LIBRARY, CLONE:2810417B17 PRODUCT:MYOSIN LIGHT CHAIN, ALKALI, CARDIAC ATRIA, FULL INSERT SEQUENCE.	3	3		
ELONGATION FACTOR 1-BETA.	3			3
IGFBP7 PROTEIN (FRAGMENT).	3	3		
MYB-BINDING PROTEIN 1A.	3	3		
HEAT SHOCK 70 KDA PROTEIN 4.	3			3
LYSOSOMAL ALPHA-MANNOSIDASE PRECURSOR.	3			3
ISOFORM 1 OF TENASCIN PRECURSOR.	3	3		
IQ MOTIF CONTAINING GTPASE ACTIVATING PROTEIN 2.	3	3		
ISOFORM 1 OF 14-3-3 PROTEIN THETA.	3	1		2
TROPOMYOSIN ALPHA-4 CHAIN.	3	2	1	

PROTEIN FAM3C PRECURSOR.	3			3
RPL12 PROTEIN (FRAGMENT).	3		3	
THREONYL-TRNA SYNTHETASE, CYTOPLASMIC.	3	3		
COMPLEMENT C1S-B SUBCOMPONENT PRECURSOR.	3			3
13 DAYS EMBRYO MALE TESTIS CDNA, RIKEN FULL-LENGTH ENRICHED LIBRARY, CLONE:6030458D19 PRODUCT:MANNAN-BINDING LECTIN SERINE PROTEASE 1, FULL INSERT SEQUENCE.	3			3
PEROXIREDOXIN-6.	3	3		
CADHERIN-15 PRECURSOR.	2	2		
ISOFORM 1 OF PROTEIN SET.	2	2		
PROTEASOME SUBUNIT BETA TYPE-1 PRECURSOR.	2			2
INOSITOL MONOPHOSPHATASE.	2	2		
13 DAYS EMBRYO LIVER CDNA, RIKEN FULL-LENGTH ENRICHED LIBRARY, CLONE:I920006B08 PRODUCT:PLASTIN 3 (T-ISOFORM), FULL INSERT SEQUENCE.	2	2		
T-COMPLEX PROTEIN 1 SUBUNIT ZETA.	2			2
EUKARYOTIC TRANSLATION INITIATION FACTOR 2 SUBUNIT 2.	2	2		
RNA-BINDING PROTEIN FUS.	2		2	
EUKARYOTIC INITIATION FACTOR 4A-I.	2			2
CARBOXYPEPTIDASE E PRECURSOR.	2			2
INOSITOL-3-PHOSPHATE SYNTHASE.	2			2

BETA-GALACTOSIDE-BINDING LECTIN (FRAGMENT).	2	2		
FIBROMODULIN PRECURSOR.	2			2
ISOFORM 2 OF SPECTRIN BETA CHAIN, BRAIN 1.	2	2		
PROLARGIN PRECURSOR.	2			2
DIHYDROPYRIMIDINASE-RELATED PROTEIN 3.	2	2		
60S RIBOSOMAL PROTEIN L27.	2	2		
UBIQUITIN-LIKE MODIFIER-ACTIVATING ENZYME 1 X.	2	1		1
40S RIBOSOMAL PROTEIN SA.	2	2		
ISOFORM HSP105-ALPHA OF HEAT SHOCK PROTEIN 105 KDA.	2	2		
ISOFORM A OF HEAT SHOCK PROTEIN BETA-1.	2	2		
EUKARYOTIC TRANSLATION INITIATION FACTOR 3 SUBUNIT A.	2	2		
ISOFORM 5G OF PERIPHERIN.	2	2		
ISOFORM PBX3A OF PRE-B-CELL LEUKEMIA TRANSCRIPTION FACTOR 3.	2	2		
COMPLEMENT COMPONENT FACTOR H.	2			2
IMPORTIN-9.	2			2
PHOSPHOLIPASE D3.	2	2		
BONE MARROW MACROPHAGE CDNA, RIKEN FULL-LENGTH ENRICHED LIBRARY, CLONE:I830057G04 PRODUCT:PROTEASOME (PROSOME, MACROPAIN) 26S SUBUNIT, NON-ATPASE, 12, FULL INSERT SEQUENCE.	2			2
26S PROTEASE REGULATORY	2	2		

SUBUNIT 6A.				
PYRUVATE KINASE ISOZYMES R/L.	2	2		
MATRIX METALLOPROTEINASE-14 PRECURSOR.	2			2
PROTEIN CANOPY HOMOLOG 2 PRECURSOR.	2			2
EUKARYOTIC TRANSLATION INITIATION FACTOR 5.	2			2
TROPONIN I, FAST SKELETAL MUSCLE.	2	2		
ISOFORM C OF ARSENITE-RESISTANCE PROTEIN 2.	2	2		
THIOREDOXIN.	2	1		1
ISOFORM 2 OF HETEROGENEOUS NUCLEAR RIBONUCLEOPROTEIN D0.	2	2		
HISTONE H2A.X.	2	2		
HISTONE H3.2.	2	2		
PROTEASOME SUBUNIT ALPHA TYPE-1.	2	2		
ALPHA-N-ACETYLGLUCOSAMINIDASE.	2			2
TORSIN FAMILY 1, MEMBER B.	2			2
KERATIN KB40.	2			2
UTROPHIN.	2			2
ISOFORM 1 OF SEPTIN-9.	2	2		
MULTIPLE INOSITOL POLYPHOSPHATE PHOSPHATASE 1 PRECURSOR.	2			2
PLATELET-DERIVED GROWTH FACTOR RECEPTOR-LIKE PROTEIN PRECURSOR.	2			2
ATP SYNTHASE SUBUNIT BETA,	2	2		

MITOCHONDRIAL PRECURSOR.				
ISOFORM 2 OF THIOREDOXIN REDUCTASE 1, CYTOPLASMIC.	2			2
T-COMPLEX PROTEIN 1 SUBUNIT THETA.	2	2		
EUKARYOTIC TRANSLATION INITIATION FACTOR 2 SUBUNIT 1.	2	2		
TITIN ISOFORM N2-A.	2	2		
ISOFORM 1 OF IMPORTIN SUBUNIT BETA-3.	2			2
SIMILAR TO PERLECAN.	2	2		
COLLAGEN ALPHA3(VI) PRECURSOR (FRAGMENT).	2			2
ISOFORM D OF LEUKOCYTE TYROSINE KINASE RECEPTOR PRECURSOR.	1	1		
EUKARYOTIC TRANSLATION INITIATION FACTOR 5A-1.	1			1
SIMILAR TO SMT3B PROTEIN ISOFORM 3.	1			1
MYOSIN LIGHT CHAIN, REGULATORY B-LIKE.	1			1
BETA-2-MICROGLOBULIN PRECURSOR.	1			1
F-ACTIN-CAPPING PROTEIN SUBUNIT ALPHA-2.	1			1
CTP SYNTHASE 1.	1	1		
LIM DOMAIN AND ACTIN BINDING 1 ISOFORM A.	1	1		
SIMILAR TO 40S RIBOSOMAL PROTEIN S14 ISOFORM 1.	1	1		
FATTY ACID SYNTHASE.	1	1		
METALLOPROTEINASE INHIBITOR 1 PRECURSOR.	1			1

BETA-HEXOSAMINIDASE SUBUNIT BETA PRECURSOR.	1			1
ACTIN-RELATED PROTEIN 3.	1	1		
ISOFORM 2 OF NEUTRAL ALPHA-GLUCOSIDASE AB PRECURSOR.	1			1
ISOFORM 1 OF GLUCOSIDASE 2 SUBUNIT BETA PRECURSOR.	1	1		
SERINE (OR CYSTEINE) PROTEINASE INHIBITOR, CLADE B, MEMBER 9.	1			1
ISOFORM CW17 OF SPLICING FACTOR 1.	1	1		
HSC70-INTERACTING PROTEIN.	1	1		
AP-2 COMPLEX SUBUNIT MU-1.	1	1		
CAMP-DEPENDENT PROTEIN KINASE TYPE II-ALPHA REGULATORY SUBUNIT.	1			1
G PROTEIN PATHWAY SUPPRESSOR 1.	1	1		
TUBULIN ALPHA-1B CHAIN.	1			1
T-COMPLEX PROTEIN 1 SUBUNIT ALPHA A.	1	1		
CYTOPLASMIC DYNEIN 1 HEAVY CHAIN 1.	1	1		
33 KDA PROTEIN.	1	1		
MAJOR PRION PROTEIN PRECURSOR.	1	1		
COMPLEMENT FACTOR H-RELATED PROTEIN.	1			1
CYSTEINE-RICH PROTEIN 2.	1	1		
SERPIN B6.	1			1
DYNEIN LIGHT CHAIN 1, CYTOPLASMIC.	1			1
TAR DNA-BINDING PROTEIN 43.	1	1		

FIBRILLIN-1 PRECURSOR.	1			1
KERATIN, TYPE II CYTOSKELETAL 79.	1			1
TRANSALDOLASE.	1	1		
EXOSTOSIN-1.	1			1
NEURONAL PENTRAXIN-1 PRECURSOR.	1			1
ISOFORM 1 OF PLASMA GLUTAMATE CARBOXYPEPTIDASE PRECURSOR.	1			1
GTP-BINDING NUCLEAR PROTEIN RAN, TESTIS-SPECIFIC ISOFORM.	1	1		
ISOFORM ALPHA OF LAMINA-ASSOCIATED POLYPEPTIDE 2 ISOFORMS ALPHA/ZETA.	1	1		
ISOFORM 1 OF VASCULAR CELL ADHESION PROTEIN 1 PRECURSOR.	1			1
OSTEOCLAST-LIKE CELL CDNA, RIKEN FULL-LENGTH ENRICHED LIBRARY, CLONE:I420023N04 PRODUCT:CGI-27 PROTEIN (C21ORF19-LIKE PROTEIN), FULL INSERT SEQUENCE.	1			1
SH3 DOMAIN-BINDING GLUTAMIC ACID-RICH-LIKE PROTEIN 3.	1	1		
OSTEOMODULIN PRECURSOR.	1			1
FRACTALKINE PRECURSOR.	1			1
TRYPSIN 4.	1		1	
PROTOCADHERIN-21 PRECURSOR.	1			1
NADP-DEPENDENT MALIC ENZYME.	1			1
TRANSCRIPTIONAL ACTIVATOR	1	1		

PROTEIN PUR-BETA.				
SPLICING FACTOR, PROLINE-AND GLUTAMINE-RICH.	1			1
APOPTOSIS-INDUCING FACTOR 1, MITOCHONDRIAL PRECURSOR.	1	1		
MICROTUBULE-ASSOCIATED PROTEIN 1B.	1	1		
KERATIN, TYPE II CYTOSKELETAL 6B.	1			1
PROTEASOME SUBUNIT ALPHA TYPE-6.	1			1
ADAM 10 PRECURSOR.	1			1
S-METHYL-5'-THIOADENOSINE PHOSPHORYLASE.	1			1
MANNOSYL-OLIGOSACCHARIDE 1,2-ALPHA-MANNOSIDASE IA.	1			1
40 KDA PEPTIDYL-PROLYL CIS-TRANS ISOMERASE.	1	1		
MITOGEN-ACTIVATED PROTEIN KINASE KINASE 1-INTERACTING PROTEIN 1.	1			1
PUTATIVE ATP-DEPENDENT RNA HELICASE PL10.	1			1
STRESS-70 PROTEIN, MITOCHONDRIAL PRECURSOR.	1	1		
ISOFORM 1 OF MYOSIN-IXB.	1	1		
PROTEASOME SUBUNIT BETA TYPE-7 PRECURSOR.	1	1		
TRANSCOBALAMIN-2 PRECURSOR.	1			1
LYSOSOMAL PROTECTIVE PROTEIN PRECURSOR.	1			1
PHOSPHATIDYLETHANOLAMINE -BINDING PROTEIN 1.	1			1

40S RIBOSOMAL PROTEIN S28.	1			1
INSULIN-LIKE GROWTH FACTOR II PRECURSOR.	1			1
60S ACIDIC RIBOSOMAL PROTEIN P2.	1	1		
DENTIN MATRIX PROTEIN 4 PRECURSOR.	1			1
ACTIN-RELATED PROTEIN 2.	1	1		
ZINC FINGER PROTEIN 787.	1	1		
CYTOCHROME C, SOMATIC.	1	1		
ISOFORM 1 OF STRESS 70 PROTEIN CHAPERONE MICROSOME-ASSOCIATED 60 KDA PROTEIN PRECURSOR.	1			1
TUBULIN-SPECIFIC CHAPERONE A.	1	1		
CD44 ANTIGEN ISOFORM C.	1	1		
ISOFORM 1 OF N-ACETYLLACTOSAMINIDE BETA-1,3-N-ACETYLGLUCOSAMINYLTRANSFERASE.	1			1
TRANSGELIN.	1	1		
KERATIN, TYPE I CYTOSKELETAL 14.	1			1
ZYXIN.	1	1		
MYRISTOYLATED ALANINE-RICH C-KINASE SUBSTRATE.	1			1
ISOFORM 3 OF MICROTUBULE-ACTIN CROSS-LINKING FACTOR 1.	1			1
MUSCLEBLIND-LIKE PROTEIN 3.	1	1		
COFILIN-2.	1			1
ISOFORM 2 OF RETICULON-4.	1	1		

SIMILAR TO RIBOSOMAL PROTEIN S8 ISOFORM 1.	1	1		
HYPOXANTHINE-GUANINE PHOSPHORIBOSYLTRANSFERASE.	1			1
ISOFORM 1 OF 60 KDA HEAT SHOCK PROTEIN, MITOCHONDRIAL PRECURSOR.	1			1
LAMININ SUBUNIT ALPHA-2 PRECURSOR.	1	1		
N-ACETYLGALACTOSAMINE-6-SULFATASE PRECURSOR.	1			1
TYROSINE-PROTEIN KINASE RECEPTOR UFO PRECURSOR.	1			1
WD REPEAT-CONTAINING PROTEIN 1.	1	1		
ARGININOSUCCINATE LYASE.	1	1		
POLYPEPTIDE N-ACETYLGALACTOSAMINYLTRANSFERASE 10.	1			1
NUCLEOLIN.	1		1	
EH-DOMAIN CONTAINING 4-KJR (FRAGMENT).	1		1	
NOVEL HISTONE H2A FAMILY MEMBER.	1	1		
TETRANECTIN PRECURSOR.	1			1
IMMUNOGLOBULIN SUPERFAMILY MEMBER 8 PRECURSOR.	1			1
UBIQUITIN-CONJUGATING ENZYME E2 K.	1	1		
TRANSCRIPTIONAL REGULATOR ATRX.	1		1	
FIBULIN-5 PRECURSOR.	1			1
CADHERIN-2 PRECURSOR.	1	1		

RAB GDP DISSOCIATION INHIBITOR ALPHA.	1	1		
ISOFORM 3 OF PROGRAMMED CELL DEATH 6-INTERACTING PROTEIN.	1	1		
PEPTIDYL-GLYCINE ALPHA-AMIDATING MONOOXYGENASE PRECURSOR.	1			1
10 DAYS EMBRYO WHOLE BODY CDNA, RIKEN FULL-LENGTH ENRICHED LIBRARY, CLONE:2610201K07 PRODUCT:RAS SUPPRESSOR PROTEIN 1, FULL INSERT SEQUENCE.	1	1		
SIMILAR TO RIBOSOMAL PROTEIN L12.	1		1	
ISOFORM 1 OF MSX2-INTERACTING PROTEIN.	1	1		
AGRIN.	1			1
TRY10-LIKE TRYPSINOGEN.	1		1	
26S PROTEASOME NON-ATPASE REGULATORY SUBUNIT 8.	1			1
COMPLEMENT C1R-A SUBCOMPONENT PRECURSOR.	1			1
TBP-INTERACTING PROTEIN ISOFORM 1.	1			1
CATHEPSIN O PRECURSOR.	1			1
52 KDA PROTEIN.	1	1		
SIMILAR TO GLYCERALDEHYDE-3-PHOSPHATE DEHYDROGENASE.	1			1
SEMAPHORIN-4B PRECURSOR.	1	1		
ISOFORM 1 OF MYOFERLIN.	1	1		
6-PHOSPHOGLUCONATE DEHYDROGENASE, DECARBOXYLATING.	1			1

ANNEXIN A2.	1	1		
PHOSPHOGLYCERATE KINASE 2.	1			1
ISOFORM 2 OF UBIQUITIN CARBOXYL-TERMINAL HYDROLASE 34.	1	1		
COMPLEMENT COMPONENT 1, S SUBCOMPONENT.	1			1
ISOFORM 2 OF NGFI-A-BINDING PROTEIN 2.	1	1		
OSTEOCLAST-LIKE CELL CDNA, RIKEN FULL-LENGTH ENRICHED LIBRARY, CLONE:I420016I18 PRODUCT:EXTRACELLULAR MATRIX PROTEIN 1, FULL INSERT SEQUENCE.	1			1

Appendix 2. Secondary condition media mass spectrophotometry analysis

Protein Description	Total of spectra count	ER-mcherry spectra count	PLD3-K418R-myc spectra count	PLD3-myc spectra count
Tnnt2 Isoform A3B of Troponin T, cardiac muscle	12	4	5	3
Actn3 Alpha-actinin-3	19	x	12	7
Prdx6 Peroxiredoxin 6	6	1	4	1
Ppia Peptidyl-prolyl cis-trans isomerase	67	30	15	22
S100a6 Protein S100-A6	5	1	1	3
Ak1 Isoform 1 of Adenylate kinase isoenzyme 1	4	1	x	3
Actg2 Actin, gamma-enteric smooth muscle	12	6	3	3
Eif3a Eukaryotic translation initiation factor 3 subunit A	5	x	4	x
Htra1 Serine protease HTRA1 precursor	9	6	3	x
Msn Moesin	81	15	41	25
Akr1b3 Aldose reductase	11	5	4	2
Eif3b Eif3b protein	7	2	4	1
Tpm2 Isoform 1 of Tropomyosin beta chain	49	20	10	19
Pa2g4 Proliferation-associated protein 2G4	7	1	2	4
Hnrpab Hnrpab protein	9	1	3	5
Tars Threonyl-tRNA synthetase, cytoplasmic	4	x	4	x
Eif4b Eukaryotic translation initiation factor 4B	28	7	11	10

Rpl12 60S ribosomal protein L12	7	2	3	2
Hdgfrp2 Isoform 3 of Hepatoma-derived growth factor-related protein 2	4	x	3	1
Rpl18 60S ribosomal protein L18	4	x	4	x
Tagln2 transgelin 2	6	x	4	2
Gsn Isoform 2 of Gelsolin precursor	36	31	3	2
Ppib peptidylprolyl isomerase B	11	1	7	3
Capg Macrophage-capping protein	12	1	10	1
Lgals1 Galectin-1	6	x	x	6
Ywhae 14-3-3 protein epsilon	24	x	16	8
Thbs1 Thrombospondin 1	18	x	13	5
Gdi2 Isoform 1 of Rab GDP dissociation inhibitor beta	29	11	8	10
Kif5b Kinesin-1 heavy chain	7	x	4	3
Myl4 10, 11 days embryo whole body cDNA, RIKEN full-length enriched library, clone:2810417B17 product:myosin light chain, alkali, cardiac atria, full insert sequence	3	x	3	x
Rps25 40S ribosomal protein S25	3	x	3	x
Actn1 Alpha-actinin-1	68	7	39	22
Fhl1 Isoform 1 of Four and a half LIM domains protein 1	4	x	4	x
Ccdc80 Coiled-coil domain-containing protein 80 precursor	6	x	4	2
Cfl1 Cofilin-1	14	4	4	6
Cdh2 Cadherin-2 precursor	5	3	x	2
S100a4 Protein S100-A4	10	2	4	4
Hpx hemopexin	17	3	x	3
Tpm4 Tropomyosin alpha-4 chain	42	15	19	8

Cd44 Isoform 7 of CD44 antigen precursor	5	x	5	x
Col6a1 Collagen alpha-1(VI) chain precursor	23	23	x	x
Col6a3 Col6a3 protein	18	18	x	x
Fdps Farnesyl pyrophosphate synthetase	9	5	x	4
App Isoform APP695 of Amyloid beta A4 protein precursor (Fragment)	17	4	6	7
Purb Transcriptional activator protein Pur-beta	23	3	10	10
Gpi1 Glucose-6-phosphate isomerase	37	13	14	10
Sod3 Extracellular superoxide dismutase [Cu-Zn] precursor	6	5	1	x
Glo1 Lactoylglutathione lyase	12	1	10	1
Ldha L-lactate dehydrogenase A chain	25	9	10	6
Pgam1 Phosphoglycerate mutase 1	29	10	12	7
Timp1 Metalloproteinase inhibitor 1 precursor	9	2	1	6
Csrp1 Cysteine and glycine-rich protein 1	9	3	3	3
Tnni1 Troponin I, slow skeletal muscle	5	4	1	x
Ppic Peptidyl-prolyl cis-trans isomerase C	10	7	x	3
Bgn Biglycan precursor	46	40	5	1
Vim Vimentin	157	31	64	54
Cd200 Cd200 antigen	2	x	2	x
Hist1h2af Histone H2A type 1-F	24	5	11	8
Actn4 Alpha-actinin-4	8	5	2	1
Rps28;LOC100048156;LOC100043527 40S ribosomal protein S28	9	2	4	3

Anxa1 Annexin A1	71	16	37	18
Ubb;Rps27a;Gm1821;Ubc ubiquitin C	207	9	10	4
Ctrb1 Chymotrypsinogen B precursor	3	x	3	x
Qsox1 Isoform 2 of Sulfhydryl oxidase 1 precursor	44	33	9	2
Atp6ap2 Renin receptor precursor	8	6	x	2
Bin1 Isoform 1 of Myc box-dependent-interacting protein 1	20	3	14	3
Ctsd B6-derived CD11 +ve dendritic cells cDNA, RIKEN full-length enriched library, clone:F730002E02 product:cathepsin D, full insert sequence	8	5	2	1
Spna2 Isoform 2 of Spectrin alpha chain, brain	11	x	7	4
Pgcp Isoform 2 of Plasma glutamate carboxypeptidase precursor	18	18	x	x
Ncl Nucleolin	18	7	3	8
Hsp90aa1 Heat shock protein HSP 90-alpha	29	11	14	4
H2afv Histone H2AV	20	3	12	5
Npm1 Nucleophosmin	5	x	5	x
Hist1h1c Histone H1.2	5	x	4	1
Timp2 TIMP metallopeptidase inhibitor 2	7	2	3	2
Fndc1 fibronectin type III domain containing 1	26	7	13	6
Hsp90b1 Endoplasmin precursor	51	4	22	25
Rpl5;LOC100043295 60S ribosomal protein L5	12	x	9	3
Dag1 Dystroglycan precursor	9	5	x	4
Vcl Vinculin	145	26	73	46

Rtn4 Isoform 1 of Reticulon-4	2	x	2	x
Nid2 nidogen 2	17	17	x	x
Rpl10a 60S ribosomal protein L10a	5	x	3	2
Cdh15 Cadherin-15 precursor	74	26	32	16
Zyx Zyx protein	5	3	1	1
Rdx radixin isoform a	4	x	3	1
Matr3 Matrin-3	3	x	3	x
Tubb6 Tubulin beta-6 chain	7	2	4	1
Serpinh1 serine (or cysteine) proteinase inhibitor, clade H, member 1	23	1	15	7
Dstn Destrin	7	x	5	2
Basp1 Brain acid soluble protein 1	42	4	20	18
sp|Q8IV08|PLD3_HUMAN Phospholipase D3 OS=Homo sapiens GN=PLD3 PE=1 SV=1	3	x	3	x
Tpm1 Isoform 1 of Tropomyosin alpha-1 chain	99	24	46	29
Rps19 Rps19 protein	8	x	5	3
Tagln Transgelin	27	x	17	10
Ckm Creatine kinase M-type	4	x	4	x
Vcp Transitional endoplasmic reticulum ATPase	17	7	3	7
Actb Actin, cytoplasmic 1	131	31	56	44
Plau Urokinase-type plasminogen activator precursor	12	x	6	6
Rplp2 60S acidic ribosomal protein P2	25	11	12	2
Mgp Matrix Gla protein precursor	10	10	x	x
Ywhag 14-3-3 protein gamma	32	17	5	10
Ncam1 neural cell adhesion molecule 1 isoform 2	25	7	9	9

Hnrpk Isoform 3 of Heterogeneous nuclear ribonucleoprotein K	7	x	4	3
Sparc SPARC precursor	56	13	27	16
Calu Calumenin precursor	18	8	8	2
Aebp1 AE binding protein 1	16	14	2	x
Pltp Phospholipid transfer protein precursor	3	3	x	x
Myh6 Myosin-6	6	x	4	2
Cdv3 Isoform 1 of Protein CDV3	16	4	6	6
Col6a2 Collagen alpha-2(VI) chain precursor	23	23	x	x
Serbp1 Isoform 1 of Plasminogen activator inhibitor 1 RNA-binding protein	28	10	8	10
Mtap4 Isoform 1 of Microtubule-associated protein 4	12	2	6	4
2900073G15Rik myosin light chain, regulatory B-like	12	1	6	5
Col5a1 Collagen alpha-1(V) chain precursor	49	26	12	11
Capzb Isoform 1 of F-actin-capping protein subunit beta	2	x	2	x
Igfbp3 Insulin-like growth factor-binding protein 3 precursor	7	7	x	x
Hsp90ab1 Heat shock protein 84b	110	38	42	30
Col5a2 Collagen alpha-2(V) chain precursor	21	13	6	2
EG317677 Complement C1s-B subcomponent precursor	10	10	x	x
Hspa5 78 kDa glucose-regulated protein precursor	77	18	37	22
Spp1 Mammary gland RCB-0527 Jyg-MC	2	2	x	x
Tuba1c Tubulin alpha-1C chain	58	15	28	15

Eef1g Elongation factor 1-gamma	4	x	4	x
Igfbp5 Insulin-like growth factor-binding protein 5 precursor	28	3	14	11
Pebp1 Phosphatidylethanolamine-binding protein 1	8	x	8	x
Eef2 Elongation factor 2	76	9	45	22
Mmp2 72 kDa type IV collagenase precursor	18	16	2	x
Ywhah 14-3-3 protein eta	5	1	4	x
Mdh1 Malate dehydrogenase, cytoplasmic	9	x	6	3
Nme2 Nucleoside diphosphate kinase B	25	12	11	2
Pdia3 Protein disulfide-isomerase A3 precursor	70	14	24	32
Atp5b ATP synthase subunit beta, mitochondrial precursor	4	x	4	x
Serpinf1 Pigment epithelium-derived factor precursor	80	47	18	15
Myh3 Myosin-3	162	x	106	56
Tnnc1 Troponin C, slow skeletal and cardiac muscles	10	2	5	3
Fn1 NOD-derived CD11c +ve dendritic cells cDNA, RIKEN full-length enriched library, clone:F630118J10 product:fibronectin 1, full insert sequence	15	12	3	x
Fn1 cDNA, RIKEN full-length enriched library, clone:M5C1012H16 product:fibronectin 1, full insert sequence	385	171	128	86
Crip2 Cysteine-rich protein 2	11	3	3	5
Hspa8 Heat shock cognate 71 kDa protein	153	52	53	48
Hist1h2bp Isoform 1 of Histone H2B	34	4	14	16

type 1-P				
Cfl2 Cofilin-2	22	5	11	6
Pfn1 Profilin 1	23	3	6	14
Pxdn Peroxidasin homolog precursor	6	5	1	x
Rps23;LOC100038875;LOC100046668 11 days embryo whole body cDNA, RIKEN full-length enriched library, clone:2700086E01 product:ribosomal protein S23, full insert sequence	5	x	4	1
Eef1a1 Elongation factor 1-alpha 1	26	7	11	8
Tln1 Talin-1	53	x	35	18
LOC100045332;Rpsa 40S ribosomal protein SA	5	x	2	3
Flna Isoform 1 of Filamin-A	140	22	69	49
Tmpo Isoform Beta of Lamina-associated polypeptide 2 isoforms beta/delta/epsilon/gamma	9	x	7	2
Ltf Lactotransferrin precursor	11	6	3	x
Col3a1 Collagen alpha-1(III) chain precursor	205	166	20	19
Lmna Isoform C of Lamin-A/C	89	9	43	37
Col4a2 Collagen alpha-2(IV) chain precursor	5	x	4	1
Rps18 40S ribosomal protein S18	5	x	2	3
Tpi1 Triosephosphate isomerase	29	7	15	7
Mdh2 Malate dehydrogenase, mitochondrial precursor	21	3	12	6
Tnc Isoform 1 of Tenascin precursor	72	27	22	23

Hspg2 Basement membrane-specific heparan sulfate proteoglycan core protein precursor	7	3	3	1
Plec1 Isoform PLEC-1B of Plectin-1	58	11	31	16
Postn Isoform 5 of Periostin precursor	37	2	27	8
Ogn Mimecan precursor	28	24	2	2
Marcks Myristoylated alanine-rich C-kinase substrate	11	1	5	5
Tubb5 Tubulin beta-5 chain	40	14	18	8
Col4a1 Collagen alpha-1(IV) chain precursor	4	4	x	x
Plod1 Procollagen-lysine,2-oxoglutarate 5-dioxygenase 1 precursor	2	2	x	x
Enah enabled homolog isoform 1	6	x	3	3
St13 Hsc70-interacting protein	6	3	x	3
Pkm2 Isoform M2 of Pyruvate kinase isozymes M1/M2	86	32	32	22
Got1 glutamate oxaloacetate transaminase 1, soluble	14	3	5	6
Eno1;EG433182;LOC100044223 Alpha-enolase	96	27	40	29
Cltc Clathrin, heavy polypeptide	7	x	5	2
Hnrnpu Osteoclast-like cell cDNA, RIKEN full-length enriched library, clone:I420039N16 product:heterogeneous nuclear ribonucleoprotein U, full insert sequence	4	x	2	2
Fbln2 fibulin 2 isoform b	24	9	8	7
Ptms Ptms protein	27	8	8	11
Nes Isoform 1 of Nestin	81	8	34	24
Cilp cartilage intermediate layer protein, nucleotide	2	2	x	x

pyrophosphohydrolase				
Nucb1 Nucleobindin-1 precursor	14	7	4	3
P4hb 17 days embryo kidney cDNA, RIKEN full-length enriched library, clone:I920160L24 product:prolyl 4-hydroxylase, beta polypeptide, full insert sequence	23	8	3	12
Fkbp1a FK506-binding protein 1A	5	1	1	3
Pgk1 Phosphoglycerate kinase 1	64	18	27	19
Naca Nascent polypeptide-associated complex subunit alpha, muscle-specific form	6	2	3	1
Clic1 Chloride intracellular channel protein 1	10	1	6	3
Rps3a 40S ribosomal protein S3a	5	x	5	x
Hspa4 Heat shock 70 kDa protein 4	40	9	15	16
Pdia6 CRL-1722 L5178Y-R cDNA, RIKEN full-length enriched library, clone:I730077L17 product:thioredoxin domain containing 7, full insert sequence	12	x	7	5
Psma7 Proteasome subunit alpha type-7	5	4	1	x
Calr Calreticulin precursor	51	13	26	12
Eef1b2 Elongation factor 1-beta	7	1	x	6
Ctsz Cathepsin Z	6	3	3	x
Spnb2 Isoform 2 of Spectrin beta chain, brain 1	8	1	5	2
Eno3 Beta-enolase	33	15	15	3
Psat1 Phosphoserine aminotransferase	9	9	x	x
Gpc1 Glypican-1 precursor	25	1	16	8
Coro1c Coronin-1C	9	x	5	4

Col1a2 Collagen alpha-2(I) chain precursor	174	98	31	45
Dcn Decorin precursor	39	39	x	x
Flnb Filamin-B	26	x	13	13
Palld Isoform 4 of Palladin	2	x	2	x
Cct2 Brain cDNA, clone MNCb-1272, similar to Mus musculus chaperonin subunit 2 (beta) (Cct2), mRNA	6	x	5	1
Casq2 calsequestrin 2	13	x	11	2
Des Desmin	212	32	95	85
Lmnb1 Lamin-B1	9	x	x	9
Pgm2;Pgm1 Phosphoglucomutase-1	7	3	x	4
Ppt1 Palmitoyl-protein thioesterase	2	2	x	x
Spon2 Spondin-2 precursor	6	6	x	x
Cst3 Cystatin-C precursor	26	20	4	2
Park7 Protein DJ-1	7	x	6	1
Sh3bgrl SH3 domain-binding glutamic acid-rich-like protein	4	x	x	4
Igfbp2 Insulin-like growth factor binding protein 2	15	x	8	7
Prdx1 Peroxiredoxin-1	14	2	5	7
Ywhaz 14-3-3 protein zeta/delta	35	8	15	12
Flnc Isoform 2 of Filamin-C	142	15	77	50
Arhgdia Rho GDP-dissociation inhibitor 1	26	8	10	8
Ecm1 Isoform Long of Extracellular matrix protein 1 precursor	14	10	2	2
Wdr1 WD repeat-containing protein 1	11	1	x	10
Txnrd1 Isoform 2 of Thioredoxin reductase 1, cytoplasmic	5	x	4	1

Ctsb Cathepsin B precursor	14	8	3	3
Ctsl Cathepsin L1 precursor	16	10	3	3
Clta clathrin, light polypeptide (Lca) isoform a	4	x	2	2
Prdx2 Peroxiredoxin-2	19	7	7	5
Rps8;LOC100040298 40S ribosomal protein S8	3	x	3	x
Eprs Bifunctional aminoacyl-tRNA synthetase	9	x	6	3
Stip1 Stress-induced-phosphoprotein 1	18	1	14	3
Col1a1 Isoform 1 of Collagen alpha-1(I) chain precursor	107	95	7	5
Col12a1 Isoform 1 of Collagen alpha-1(XII) chain precursor	34	34	x	x
Hspb1 Isoform A of Heat shock protein beta-1	35	3	21	11
Clu Clusterin precursor	21	x	15	6
Csf1 Isoform 1 of Macrophage colony-stimulating factor 1 precursor	8	8	x	x
Anxa2 Annexin A2	8	4	2	2
Tpm3 29 kDa protein	5	x	5	x
B2m Beta-2-microglobulin precursor	9	1	5	3
Ttn Isoform 1 of Titin	6	x	6	x
Rsu1 Ras suppressor protein 1	4	x	2	2
Myh9 15 days pregnant adult female amnion cDNA, RIKEN full-length enriched library, clone:M421002E03 product:myosin heavy chain IX, full insert sequence	188	23	93	72
Aldoa Fructose-bisphosphate aldolase	53	12	22	19
Macf1 Microtubule-actin crosslinking factor 1	4	x	4	x

Ltbp1 latent transforming growth factor beta binding protein 1 isoform LTBP-1L	16	5	8	3
Fstl1 34 kDa protein	48	24	14	10
Pcolce 53 kDa protein	33	19	7	7
- 11 kDa protein	29	4	11	14
Cald1 62 kDa protein	13	5	3	5
LOC675192;EG668182 hypothetical protein	3	x	x	3
Clstn1 115 kDa protein	4	3	1	x
- 14 kDa protein	40	6	22	12
LOC674419 hypothetical protein	9	1	5	3
- 23 kDa protein	7	x	6	1
LOC100040109 similar to Glyceraldehyde-3-phosphate dehydrogenase isoform 1	35	3	20	12
Vcan versican	20	20	x	x
C1qtnf3 35 kDa protein	18	13	3	2
EG433297 similar to MYL6 protein	16	x	7	9
Ywhaq 34 kDa protein	10	3	4	3
Tpt1 17 kDa protein	23	7	12	4
LOC100045189 similar to transcription factor EF1	37	6	17	14
LOC100045191 similar to heterogeneous nuclear ribonucleoprotein A2/B1	14	3	8	3
LOC670717;LOC100045925 similar to cytochrome c	10	x	7	3
LOC100047061 similar to perlecan	75	27	31	8
EG620213 similar to ribosomal protein L6	7	x	6	1

EG665509 similar to endothelial monocyte-activating polypeptide	6	x	3	3
EG544973 hypothetical protein isoform 1	6	1	3	2
EG667618 similar to Acidic ribosomal phosphoprotein P0	9	4	1	4